Preface

This thesis constitutes the final part of a "Sivilingeniør" (M.Sc.) degree in Physics and Mathematics at the Norwegian University of Science and Technology. It was written during the spring of 2022, after a five-year study program. All notes, Mathematica programs, figures, and other files may be found at GiHub: https://github.com/Northo/MasterThesis.[1]

I would like to thank my supervisor, Alireza Qaiumzadeh, for excellent guidance throughout this last year. This has been a novel topic for both of us, and our weekly meetings have been filled with interesting discussions and conversations. Thank you for being a guiding lantern through an overwhelming maze of information, letting me see what is relevant and what is not.

Furthermore, I want to thank María A. H. Vozmediano[2] and Alberto Cortijo[1] for excellent discussions during the finalization of the thesis. Through our meetings, the significance and interpretation of the results were made more clear, and interesting questions and continuations discussed. It was also reassuring to hear that you had struggled with some of the same issues that we have faced.

The work presented in this thesis is currently being worked into a manuscript written primarily by me and Alireza, in collaboration with Maria and Alberto.

`This document has been typeset with the intention of printing on B5 paper. Consequently, the text and figures will look too large when printed on A4 paper.`

---

[1] Which will be made public *after* grading of the thesis, due to plagiarism concerns.

[2] Materials Science Factory, Instituto de Ciencia de Materiales de Madrid, CSIC, Cantoblanco, 28049 Madrid, Spain.

Summary

Emergent Dirac equations in topological condensed matter physics may, as opposed to their high energy physics equivalents, have Lorentz-breaking terms. Several such systems have been discovered both theoretically and experimentally, among them the tilted Dirac and Weyl semimetals. Non-tilted Dirac and Weyl semimetals have previously been shown to house a transverse thermoelectric effect, a Nernst contribution. The origin of the effect is the conformal anomaly, a quantum anomaly related to non-flat spacetime. The effect, importantly, is finite even for zero chemical potential and temperature. Using the Kubo formalism, we have extended the calculation to find the response function for a system with tilt.

Using Luttinger's relation, we introduce an effective gravitational field from a thermal gradient, which couples to the energy density. By employing the conservation of energy, we then reformulate the response as a response to the derivatives of off-diagonal elements of the energy-momentum tensor.

We find the effect to be tunable by the direction and magnitude of the tilt with respect to the magnetic field. Several possible candidates for experimental signatures are presented. This work thus enables further experimental and theoretical investigation into the effect. Furthermore, we show the importance of the specific choice of the energy-momentum tensor, which for non-zero tilt directly affects the computed response. The ambiguity of the energy-momentum tensor is well known, however, our results show explicitly that in these types of systems, the choice is not only a conceptual formality but has qualitative consequences.

Summary

Non-tilted Dirac and Weyl semimetals have previously been shown to house a transverse thermoelectric effect, a Nernst contribution. The origin of the effect is the conformal anomaly, a quantum anomaly related to non-flat spacetime. The effect, importantly, is finite even for zero chemical potential and temperature. Using the Kubo formalism, we have extended the calculation to find the response function of tilted Dirac and Weyl semimetals.

Using Luttinger's relation, we introduce an effective gravitational field from a thermal gradient, which couples to the energy density. By employing the conservation of energy, we then reformulate the response as a response to the derivatives of off-diagonal elements of the energy-momentum tensor.

We find the effect to be tunable by the direction and magnitude of the tilt with respect to the magnetic field. Several possible candidates for experimental signatures are presented. This work thus enables further experimental and theoretical investigation into the effect. Furthermore, we show the importance of the specific choice of the energy-momentum tensor, which for non-zero tilt directly affects the computed response. The ambiguity of the energy-momentum tensor is well known, however, our results show explicitly that in these types of systems, the choice is not only a conceptual formality but has qualitative consequences.

Oppsummering

Effektive Dirac likninger i topologisk faststoff-fysikk kan, i motsetning til høy-energi ekvivalentene, ha ledd som bryter Lorentz invarianse. Flere slike systemer har blitt oppdaget, både teoretisk og eksperimentelt, deriblant skråstilte Dirac og Weyl semimetaller. Det har tidligere blitt vist at ikke-skråstilte Dirac og Weyl semimetaller gir opphave til en transversal termoelektrisk effekt, et bidrag til Nernst effekten. Effektens opphav er den konforme anomaliteten, en kvante-anomalitet relatert kurvet romtid. Effekten består, viktig nok, også ved null kjemisk potensiale og temperatur. Vi har generalisert utregningen til skråstilte systemer, ved hjelp av Kubo-formalismen.

Gjennom Luttingers relasjon introduserer vi et effektivt gravitasjonsfelt fra en termiske gradient, som vekselvirker med energitettheten. Ved bevaringsloven for energi, kan dette omformuleres som en respons på den deriverte til ikke-diagonale elementer av energi-impuls-tensoren.

Vi ser at effekten er justerbar ved retning og størrelse på skråstillingen i forhold til magnetfeltet. Flere kandidater til eksperimentell signatur presenteres, og dette kan dermed være en mulighet for videre eksperimentell utforsking av effekten. Videre viser vi viktigheten av valg av energi-impuls-tensoren, som for skråstilte systemer påvirker resultatet av beregningen. Tvetydigheten rundt definisjonen av tensoren er vellkjent, men vårt resultat viser eksplisit at i denne typen systemer, så har valget ikke bare konseptuell betydning, men direkte kvalitative effekt.

Conventions and Symbols

- e is the fundamental charge, i.e. $e = |e|$.
- l_B is the characteristic length of a B-field, given as $l_B = \sqrt{\hbar/eB}$, with e the fundamental charge defined above.
- The signature of the Monegasque metric is taken to be -2, i.e. the metric tensor $\eta_{\mu\nu} = \text{diag}(+1, -1, -1, -1)$.
- For a $3+1$ dimensional case ($\boldsymbol{q}$ three-dimensional), the Fourier transform is defined as

$$\begin{aligned} A(\boldsymbol{q}, \omega) &= \iint \mathrm{d}t\mathrm{d}\boldsymbol{r} e^{i(\omega t - \boldsymbol{q}\boldsymbol{r})} A(\boldsymbol{r}, t), \\ A(\boldsymbol{r}, t) &= \iint \frac{\mathrm{d}\omega \mathrm{d}\boldsymbol{q}}{(2\pi)^4} e^{-i(\omega t - \boldsymbol{q}\boldsymbol{r})} A(\boldsymbol{q}, \omega). \end{aligned} \tag{1}$$

  For other dimensionalities, the exponent of the 2π factor must be chosen accordingly.
- Vectors will be written in bold font, $\boldsymbol{v} = (v_1, v_2, v_3)$, and with Roman indices, i, j, k, for two and three-dimensional vectors. Four dimensional vectors will be typed in normal weight, v, with Greek indices, μ, ν, λ, and upper and lower indices indicating contravariant and covariant quantities
- Natural units $\hbar = c = 1$ will be used in parts of the thesis, for more clear notation and in order to make it easier for the reader to recognize the similarities with high energy physics literature.
- For spin degrees of freedom, the Pauli matrices will be denoted by σ for real spin and τ for pseudo-spin.
- Operators will in general be typed with as normal quantities: O for scalar operators and $\boldsymbol{O}$ or O for vector operators, depending on their dimensions. The hat symbol, $\hat{O}$, will not be used unless not including a hat will be confusing.
- In Chapter 4, we will use capital letters M, N to indicate the absolute value of the corresponding quantity, $M = |m|$.

Contents

Introduction

Topological materials have been of central interest in contemporary condensed matter physics [FC13], with the first topological phases arising in the context of integer quantum Hall effect [KDP80; as cited in FC13]. A solid understanding of the topological theory behind this has been developed during the last decade and a half [BH13; FC13], with the Nobel Prize in Physics 2016 awarded for theoretical work on topological matter [Sci16]. Two excellent reviews of topological materials are [FC13] and, most directly relevant for this thesis, [AMV18].

One interesting phenomenon in topological materials is the emergence of quantum anomalies and the emergent particles' analogy to fundamental particles of QFT (quantum field theory). Noether's theorem says that for any continuous symmetry of the action of a system, there is an accompanying conserved current. This explains, for example, the conservation of momentum and energy as a result of the position and time independence of our universe. In a quantum mechanical treatment, however, the symmetry of the classical theory may be broken, which gives rise to an *anomaly*. The chiral anomaly, for example, has been of great interest in condensed matter research in recent years [ACV19]. The chiral anomaly explains the non-conservation of the axial current [Zee10], and gives rise to exotic transport phenomena in condensed matter systems [Bur15; Bur16; WBB14]. A less investigated anomaly is the conformal anomaly, the appearance of a non-vanishing trace of the energy-momentum tensor in a conformally scaled metric. Transport from the conformal anomaly has recently been investigated and shown in Weyl and Dirac semimetals [ACV19; Arj19; CCV18; Che16].

Arjona, Chernodub, and Vozmediano [ACV19] derived, using the Kubo formalism, the charge current response to thermal perturbations in Weyl and Dirac semimetals. This response, a contribution to the Nernst current, has its origin in the conformal anomaly. In this thesis, we extend the calculation *tilted* Dirac and Weyl semimetals – Lorentz breaking extensions of the Dirac equation. The work combines important theory and concepts from both high-energy and condensed matter physics.

The thesis consists of four chapters; the three first chapters introduce concepts central to the main derivation of the thesis, while the fourth chapter represents the bulk work of the thesis, namely the derivation itself. Note that some sections of the first and second chapter, and most of the third chapter, started as parts of a specialization project report written in the fall of 2021.

The first chapter gives an overview of concepts important to topological materials, starting with symmetries and ending with a more in-depth discussion of Weyl and Dirac semimetals, with a special focus on the tilted type. In the second chapter, linear responses theory is introduced in light of the Kubo formalism and the Luttinger formalism of thermal transport. In chapter three, we introduce anomalies of QFT in the context of high-energy physics. The thesis also contains three appendices; Appendix A contains long expressions not included in the main text, Appendix B contains a lengthy calculation that runs somewhat in parallel to the main text, for an alternative choice of the energy-momentum tensor (details discussed in the main text), and lastly, Appendix C contains several minor results the author finds interesting, that are only tangentially relevant to the main work.

1 Topological Materials

In this chapter, we consider various concepts from physics that are relevant in the context of topological materials. Firstly, the symmetry-related concepts of parity, time-reversal, Kramer's degeneracy, and accidental degeneracy are explained. Then follows a quick summary of spin-orbit interactions. Lastly, Weyl and Dirac cones are discussed, with particular focus on *tilted* cones. The chapter is intended as a quick introduction to the vast field of topological materials for someone who is not familiar with these concepts.

Some topics discussed are directly applicable to the thesis, while others are included both in order to put the concepts of the thesis in a greater context, and also with regard to further continuation of this work.

1.1. Parity

We consider now the discrete transformation of space inversion, or *parity*. Firstly, basic properties of the transformation will be presented and discussed. Its effect on the position, momentum, and angular momentum operators will be discussed, before a more general discussion on how it transforms proper- and pseudo-tensors.

Let the parity operator P be a unitary operator

$$P: \quad |a\rangle \to P\,|a\rangle\,. \tag{1.1}$$

By definition, we require

$$P^\dagger x P = -x, \tag{1.2}$$

$$P^\dagger p P = -p, \tag{1.3}$$

where x, p are the position and momentum operators. By the unitarity of P, which means that $P^\dagger P = I$,

$$xP = -Px.$$

We now use this anticommutation to find an explicit form of the transformation in the position representation. By noting that, given the position eigenstate $|x_1\rangle$,

$$xP\,|x_1\rangle = -Px_1\,|x_1\rangle = -x_1 P\,|x_1\rangle\,, \tag{1.4}$$

with x_1 the eigenvalue of the state, we may conclude

$$P\left|x_1\right\rangle = \left|-x_1\right\rangle$$

up to some arbitrary phase. We chose this phase to be unity. Then

$$P^2\left|x_1\right\rangle = \left|x_1\right\rangle \tag{1.5}$$

for any position eigenstate, which gives the operator relation $P^2 = 1 \implies P = \pm 1$. This also means that P is Hermitian,

$$P = P^{-1} = P^\dagger.$$

The treatment of angular momentum is somewhat more involved. Some sources simply state that as the orbital angular momentum

$$L = x \times p$$

is a product of two odd quantities, it must be even under parity. This, of course, is a gross over simplification, as extra care must be taken when considering the spin angular momentum S contributing to the total angular momentum

$$J = L + S.$$

The angular momentum operator is the generator of rotations

$$R = e^{-i\epsilon J\cdot n} \approx 1 - i\epsilon J \cdot n$$

where we expanded the operator under the assumption of a small angle, $\epsilon \ll 1$. As rotations are invariant during space inversion,

$$P^\dagger R P = R \tag{1.6}$$

$$\implies P^\dagger J\cdot n P = J \cdot n \tag{1.7}$$

from which it follows that

$$P^\dagger J P = J, \tag{1.8}$$

as the parity operator obviously does not act on the normal vector n. Thus, the angular momentum operator, unlike the linear momentum operator, is even under parity.

For a general vector-like[1] quantity V, we will consider how it transforms during space inversion. If the quantity "flips" during space inversion, $P^\dagger V P =$

[1] We use the term *vector-like* instead of vector, as the term vector is defined as something that is odd under parity, as opposed to for example a pseudo vector, even though they naively "look" like vectors. This can be compared to tensors. The definition of a tensor is something that transforms like a tensor under a Lorentz transformation, so we may have matrix objects that "look" like tensors, but transforms differently.

$-V$, we say simply that it is a vector, also sometimes known as a polar vector. Quantities that do not "flip", so that they turn into their opposites in the flipped image, we denote pseudo vectors. Thus, depending on whether the eigenvalue of an operator under space inversion is $+1$ or -1 we say that it is either a pseudo-vector or vector, respectively. Position and momentum are examples of vectors, while angular momentum and the magnetic field are examples of pseudo-vectors. An illustrative explanation of this is shown in Fig. 1.1, which explains both angular momentum and magnetic fields.

Remark about dimensionality: The above discussion about parity, which is the standard way to present parity in condensed matter physics, is valid for three dimensions. In two dimensions, however, one must separate *parity* and *space inversion*. The former takes a right-handed system to a left-handed system [SN17], while the latter inverts space, $x \to -x$. In odd dimensions, this is the same, while in even dimensions they differ. In even dimensions, inversion corresponds to a rotation, while a parity transform is different from any rotation. In more formal terms, inversion is part of the group of proper rotations $SO(n)$ for even dimensions, as the determinant is $+1$, the definition of a proper rotation. Parity should in general be taken to be the operation P such that the group of all rotations $O(n) = SO(n) \times \{E, P\}$, with E the identity transformation. This will not be of direct importance here, but it is an important detail to note.

1.2. Time-reversal

We will now consider the time-reversal operator $\mathcal{T}$. Firstly we will show that it must be antiunitary, then we will show $\mathcal{T}^2 = \pm 1$, and find a more specific form of $\mathcal{T}$ for half-integer spin systems.

The time-reversal operator by definition will invert the value of the time

$$\mathcal{T} : t \to -t$$

while leaving space unchanged. The invariance of space is summaries by the operator relation,

$$\mathcal{T} x \mathcal{T}^{-1} = x, \tag{1.9}$$

where x is understood as the position operator. The momentum operator, however, is flipped due to its time dependence

$$\mathcal{T} p \mathcal{T}^{-1} = -p. \tag{1.10}$$

A schematic representation of inversion symmetry and time-reversal symmetry is given in Fig. 1.2.

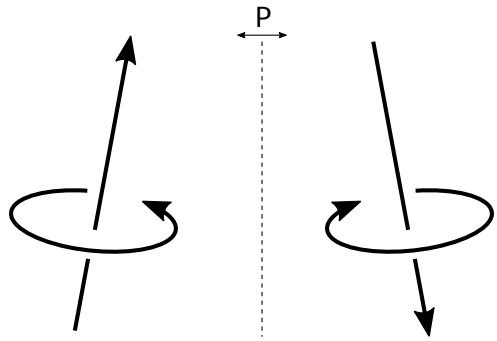

Figure 1.1.: Schematic illustration of vectors and pseudovectors. A vector field with curl, which may be taken to be either momentum or current, is shown as a rotating arrow. The curl of this field, which will respectively be the angular momentum or B-field, is shown as a straight arrow. Under inversion, shown as a mirror operation, the curl generated by the field is inverted in addition to the mirroring, i.e. rotated. This non-formal illustration gives an intuitive explanation of the concepts vector and pseudovector. Note that as the example is two-dimensional, mirror symmetry here the same as parity, and not inversion. See main text for details.

We are now in a position to show that $\mathcal{T}$ must be antiunitary by requiring the invariance of the commutation relation between momentum and position, $[x, p] = i\hbar$.

$$\mathcal{T}[x,p]\mathcal{T}^{-1} = \mathcal{T}i\hbar\mathcal{T}^{-1} = -[x,p] = -i\hbar. \tag{1.11}$$

In the first equality, the commutation relation was used directly. In the second equality, Eqs. (1.9) and (1.10) were used to gain a minus sign. This all leads to the relation

$$\mathcal{T}i\mathcal{T}^{-1} = -i. \tag{1.12}$$

From this, we gather that the time-reversal operator must be antiunitary. An antiunitary transformation O is a transformation

$$|a\rangle \to |\tilde{a}\rangle = O\,|a\rangle\,, \quad |b\rangle \to |\tilde{b}\rangle = O\,|b\rangle\,,$$

such that

$$\langle\tilde{b}|\tilde{a}\rangle = \langle b|a\rangle^*\,, \tag{1.13}$$

$$O\left(c_1\,|a\rangle + c_2\,|b\rangle\right) = c_1^* O\,|a\rangle + c_2^* O\,|b\rangle\,. \tag{1.14}$$

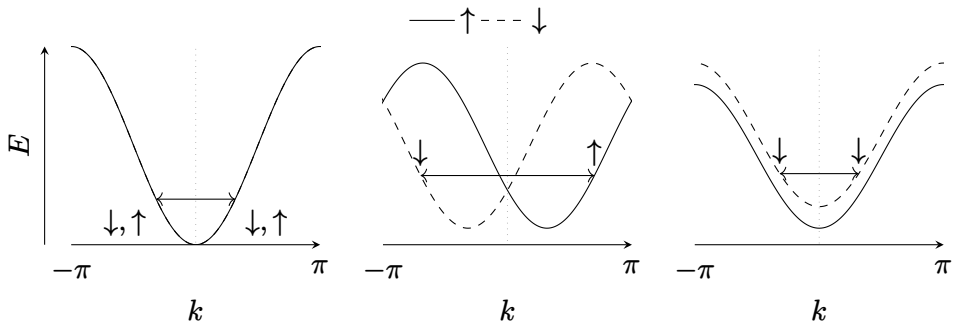

Figure 1.2.: Schematic illustration of time and inversion breaking of degenerate energy bands of a two-level system. The two levels are denoted ↑ and ↓. **(Left:)** Both time-reversal and inversion symmetry present, with the two energy bands being degenerate at all momenta. **(Center:)** Inversion symmetry is broken. Notice how at the TRIM (time-reversal independent momenta) points, $-\pi, 0, \pi$, the two energy levels are degenerate, as, by definition, we have $\boldsymbol{k} = -\boldsymbol{k}$. **(Right:)** Time-reversal symmetry is broken. Notice how in the time-reversal symmetric case Kramer's doublet is present, as for any state at k, the state at $-k$ is degenerate in energy and has opposite spin. This is not the case when time-reversal symmetry is broken, as the spin at $-k$ has the same spin. (Kramer's doubled discussed more in Section 1.3.) Figure inspired by Ramazashvili [Ram19].

A note of caution: the Dirac bra-ket notation was originally designed to handle linear operators, where it excels. For anti-linear operators, which antiunitary operators are, the bra-ket notation can be deceiving. We will always take anti-linear operators to work on kets, never on bras from the right. So, for example,

$$\langle a|O|b\rangle$$

should be understood as

$$\langle a|\left(|O|b\rangle\right)$$

and *never*

$$\left(\langle a|O|\right)|b\rangle\,.$$

The right operation of an anti-linear operator on a bra, $\langle a|\,O$, will not be defined [discussion based on SN17, Ch. 4.4].

We will in general write

$$\mathcal{T} = UK \tag{1.15}$$

where U is a unitary transformation and K is the complex conjugation. Now, we will show that $\mathcal{T}^2 = \pm 1$, by an elegant method inspired by Bernevig and Hughes [BH13]. Consider

$$\mathcal{T}^2 = UKUK = UU^* = U(U^T)^{-1} \equiv \phi, \tag{1.16}$$

where we in the second last equality used the unitarity of U. As applying the time-reversal operator twice must result in the original state, up to some phase, ϕ must surely be diagonal. From Eq. (1.16) it follows

$$U = \phi U^T, \quad U^T = U\phi \tag{1.17}$$

where the fact that $\phi^T = \phi$ for any diagonal matrix was used. From this follows that

$$U = \phi U \phi \Rightarrow U\phi^{-1} = \phi U. \tag{1.18}$$

This holds in general only for $\phi = \pm 1$, and thus $\mathcal{T}^2 = \pm 1$. Furthermore, we will in the next section show that for integer spin particles $\mathcal{T}^2 = 1$ while for half-integer spin particles $\mathcal{T}^2 = -1$.

1.2.1. Time-reversal operator on spinful particles

When considering spinful particles, we must enforce yet another property on the time-reversal operator. As spin is odd under time-reversal one must have

$$\mathcal{T} S \mathcal{T}^{-1} = -S. \tag{1.19}$$

Consider now specifically a spin-s state, with the basis $|s, m\rangle$, being an eigenstate of S_z, S^2, with eigenvalues $m\hbar$, $s(s+1)\hbar^2$ respectively. By Eq. (1.19) it follows that $\mathcal{T}|s, m\rangle$ is also an eigenstate of S_z, with eigenvalue $-m\hbar$, since

$$S_z \mathcal{T}|s, m\rangle = -\mathcal{T} S_z |s, m\rangle = -m\hbar \mathcal{T}|s, m\rangle . \tag{1.20}$$

Let

$$\mathcal{T}|s, m\rangle = \eta |s, -m\rangle ,$$

where η is some phase. Consider now the commutation of the ladder operators $J_\pm = S_x \pm iS_y$ with the time-reversal operator.

$$\begin{aligned} \underbrace{[S_x \pm iS_y]}_{S_\pm} \mathcal{T} &= -\mathcal{T} S_x \mp i\mathcal{T} S_y \\ &= -\mathcal{T} \underbrace{[S_x \mp iS_y]}_{S_\mp}, \end{aligned} \tag{1.21}$$

where the anti-linearity of $\mathcal{T}$ is emphasized. Thus, operating with S_+ on $\mathcal{T}|s,m\rangle$ gives

$$\begin{aligned} S_+\mathcal{T}|s,m\rangle &= \eta_{sm} S_+ |s,-m\rangle \\ &= \eta_{sm}\hbar\sqrt{(s+m)(s-m+1)}\,|s,-m+1\rangle\,. \end{aligned} \tag{1.22}$$

On the other hand, commuting the two operators first gives

$$\begin{aligned} S_+\mathcal{T}|s,m\rangle &= -\mathcal{T}S_-|s,m\rangle \\ &= -\mathcal{T}\hbar\sqrt{(s+m)(s-m+1)}\,|s,m-1\rangle \\ &= -\hbar\sqrt{(s+m)(s-m+1)}\eta_{s,m-1}\,|s,-m+1\rangle\,. \end{aligned} \tag{1.23}$$

By comparison, $\eta_{sm} = -\eta_{s,m-1}$; η_{sm} has a flip of its sign under increments of m. The m dependence should therefore be $(-1)^m$. For later convenience, we will choose to also include an s-term in the exponent, so that the exponent is integer also for half-integer systems, resulting in

$$\eta_{sm} = (-1)^{s-m} f(s), \tag{1.24}$$

where $f(s)$ is some phase that does not depend on m. We are now in a position where we may find $\mathcal{T}^2$, by acting on a general spin s system.

$$\begin{aligned} \mathcal{T}^2 \sum_{m=-s}^{s} a_m |s,m\rangle &= \mathcal{T}\sum_m a_m^* f(s)(-1)^{s-m}|s,-m\rangle \\ &= \sum_m a_m f^*(s)(-1)^{s-m}\mathcal{T}|s,-m\rangle \\ &= \sum_m a_m |f(s)|^2(-1)^{2s}|s,m\rangle\,. \end{aligned} \tag{1.25}$$

Note that it was important that $(-1)^{s-m}$ was real, which is taken care of by the s-term. As $f(s)$ is only a phase, this gives

$$\mathcal{T}^2 = (-1)^{2s}, \tag{1.26}$$

for any spin s system. Thus, for half integer spin, $\frac{1}{2}, \frac{3}{2}, \ldots$, $\mathcal{T}^2 = -1$, while for integer spin $\mathcal{T}^2 = +1$.

1.3. Kramer's degeneracy

Kramer's degeneracy states that for any half-integer system that is time-reversal symmetric, energy levels are at least two-fold degenerate. The proof

of this is simple, and uses the fact that for any half-integer spin system, $\mathcal{T}^2 = -1$. A heuristic way to see this is the fact that spin is odd under time-reversal, and for half-integer systems there is no zero-spin state, so reversing the spin cannot result in the same state.

Proof: Assume

$$[H, \mathcal{T}] = 0$$

and that $|n\rangle$ is an eigenstate of the system

$$H|n\rangle = E_n|n\rangle .$$

Then

$$H\mathcal{T}|n\rangle = \mathcal{T}H|n\rangle = \mathcal{T}E_n|n\rangle = E_n\mathcal{T}|n\rangle$$

and so $\mathcal{T}|n\rangle$ is also an eigenstate with the eigenvalue E_n. To assert that the eigenvalue is in fact degenerate, one must also show that the two states are not the same ray. That is $\mathcal{T}|n\rangle \neq e^{i\delta}|n\rangle$, where δ is some phase. Suppose that the above is *not* true, $\mathcal{T}|n\rangle = e^{i\delta}|n\rangle$. Then,

$$\mathcal{T}^2|n\rangle = \mathcal{T}e^{i\delta}|n\rangle = e^{-i\delta}\mathcal{T}|n\rangle = +|n\rangle .$$

However, as was stated above, $\mathcal{T}^2 = -1$ for all half-integer systems. The assumption must therefore be wrong, and the eigenvalue is degenerate. □

The two states, $|n\rangle$ and $\mathcal{T}|n\rangle$, are often referred to as Kramer's doublet. Note that the two states have opposite spin.

1.3.1. Generalization to time and parity symmetry

Consider now a time-reversal and parity symmetric system, $[H, P\mathcal{T}] = 0$. This will, similar to the case for time-reversal, make the energy levels at least two-fold degenerate.

Proof: Assume

$$[H, P\mathcal{T}] = 0$$

and that $|n\rangle$ is an eigenstate of the system

$$H|n\rangle = E_n|n\rangle .$$

Then

$$HP\mathcal{T}|n\rangle = P\mathcal{T}H|n\rangle = P\mathcal{T}E_n|n\rangle = E_nP\mathcal{T}|n\rangle .$$

Assume now that $P\mathcal{T}|n\rangle = e^{i\delta}|n\rangle$, which we will prove to be false. That would lead to

$$(P\mathcal{T})^2|n\rangle = P\mathcal{T}e^{i\delta}|n\rangle = |n\rangle\,.$$

However, as $[P,\mathcal{T}]=0$, we have

$$(P\mathcal{T})^2 = P\mathcal{T}P\mathcal{T} = P\mathcal{T}^2P = -1$$

as $P^2 = 1$. As above, the states are thus different, and the eigenvalue is degenerate. □

1.4. Accidental degeneracy

In general, for a two-level system depending on some parameter set, the energy levels of the two levels will not cross, i.e. be degenerate, unless there are symmetries in the system forcing them to be degenerate, as is the case in for example Kramer's degeneracy. However, even without any symmetries[2] there will be so-called *accidental degeneracies* if the parameter space is sufficiently large. Consider a general two-level Hamiltonian

$$H = f_1\sigma_x + f_2\sigma_y + f_3\sigma_z, \tag{1.27}$$

which will have an energy splitting between the two levels

$$\Delta E = 2\sqrt{f_1^2 + f_2^2 + f_3^2}. \tag{1.28}$$

In general, we may solve $\Delta E = 0$ by tuning the three parameters simultaneously, and thus there must be degenerate points – accidental degeneracies. Supposing that the parameters f_i can be expressed as functions of the momentum components, $f_i = f_i(p_i)$, this will correspond to degenerate points in momentum space.

If there are in addition some symmetry constraints on the system, the space of degenerate points may increase. Suppose, for example, the system is time-reversal symmetric. Recalling the time-reversal operator defined in Eq. (1.15)

$$\mathcal{T} = UK,$$

with U being a unitary operator and K the complex conjugate, the imaginary Pauli matrix σ_y must be excluded from the Hamiltonian, $f_2 = 0$. Thus, the solution to the closing of the band gap has a free parameter, and the degenerate space has dimension one.

[2] There will always, for a degenerate system, be some symmetry, although it might be a *hidden* symmetry. We here mean no a priori apparent symmetry.

1.5. Spin-orbit interaction

Spin-orbit interactions are not used directly in this thesis. It is, however, relevant to include some superficial introduction to the subject, both in order to conclude that spin-orbit interactions are not something one has to consider in later derivations of this thesis, and also that it might prove useful in future applications of the ideas and theory discussed in the thesis.

Spin-1/2 particles are in general governed by the Dirac equation. In the non-relativistic regime, as is the case in condensed matter physics, we may reduce the equation to the Pauli equation. This equation contains as a relativistic correction the spin orbit coupling term [ERH07]

$$H_{SO} = \lambda_{\text{vac}} \boldsymbol{\sigma} \cdot (\boldsymbol{k} \times \nabla \tilde{V}), \tag{1.29}$$

where λ_{vac} is a constant with dimension length squared, $\boldsymbol{\sigma}$ are the Pauli matrices representing spin, and $\tilde{V}$ is the total potential in the system. In preparation of the considerations to come, split up the potential in the periodic crystal potential V_{cr} and the remaining potential V from impurities

$$\tilde{V} = V_{\text{cr}} + V. \tag{1.30}$$

Changing basis to a quasi-particle picture of free particles, thus eliminating V_{cr} from the equation, one gets the effective Hamiltonian [ERH07]

$$H_{\text{eff}} = \epsilon_k + V + H_{\text{int}} + H_{\text{ext}}, \tag{1.31}$$

$$H_{\text{int}} = -\frac{1}{2} \boldsymbol{b}(\boldsymbol{k}) \cdot \boldsymbol{\sigma}, \tag{1.32}$$

$$H_{\text{ext}} = \lambda \boldsymbol{\sigma} \cdot (\boldsymbol{k} \times \nabla V). \tag{1.33}$$

Here, the subscripts denote the effective Hamiltonian H_{eff}, consisting of an intrinsic part, H_{int}, and an extrinsic part, H_{ext}. $\boldsymbol{b}(\boldsymbol{k})$ is the intrinsic spin-orbit field, the part of the crystal potential V_{cr} that is not eliminated by our change of basis. As the intrinsic spin-orbit interaction should be time-reversal invariant, we can argue that $\boldsymbol{b}$ must be an odd function.

$$\mathcal{T} H_{\text{int}} \mathcal{T}^{-1} = H_{\text{int}} \implies \boldsymbol{b}(\boldsymbol{k}) \cdot \boldsymbol{\sigma} = -\boldsymbol{b}(-\boldsymbol{k}) \cdot \boldsymbol{\sigma}, \tag{1.34}$$

where the well known effects of the time-reversal operator was applied to the momentum and spin, as $\mathcal{T} \boldsymbol{k} \mathcal{T}^{-1} = -\boldsymbol{k}$ and $\mathcal{T} \boldsymbol{\sigma} \mathcal{T}^{-1} = -\boldsymbol{\sigma}$. Obviously, this means that inversion symmetry must be broken for the intrinsic interaction term to be finite. This is easily seen as, with P being the parity operator,

$$P H_{\text{int}} P^{-1} = H_{\text{int}} \Rightarrow \boldsymbol{b}(-\boldsymbol{k}) = \boldsymbol{b}(\boldsymbol{k}), \tag{1.35}$$

since spin is invariant under inversion.

The external contribution to the spin-orbit interaction is contained in H_{ext}, which does not require any particular symmetry to be present. A Zeeman term, where time-reversal is broken, would be represented in the external part of the Hamiltonian.

The spin-orbit field $\boldsymbol{b}(\boldsymbol{k})$ may take many forms depending on the specifics of the system at hand. The Dresselhaus term

$$H_D = \alpha p_x (p_y^2 - p_z^2)\sigma_x + \text{c.p.} \tag{1.36}$$

where c.p. denotes terms of circular permutation of the indices, [Man+15] and the Rashba term [Wu+20]

$$H_R = \alpha(p_y\sigma_x - p_x\sigma_y), \tag{1.37}$$

are arguably the most well-known models.

We immediately see that the Rashba Hamiltonian 1.37 does not break time-reversal invariance, as both momentum and spin are odd under time-reversal. It is however odd under inversion. This is of course exactly opposite of a Zeeman term, where we introduce an external magnetic field, thus breaking time-reversal symmetry. Consider a free electron model where we add a Rashba term

$$H = \frac{p^2}{2m} + \alpha(p_y\sigma_x - p_x\sigma_y). \tag{1.38}$$

The Hamiltonian commutes with the momentum operator, so we may replace the momentum operator with its eigenvalue $\hbar\boldsymbol{k}$. Solving for the eigenvalue is straight forward, and gives

$$E_\pm = \frac{\hbar k^2}{2m} \pm \alpha k, \tag{1.39}$$

where $k = |\boldsymbol{k}|$. We expect the eigenvalues to be linear combinations of spin up and spin down states, and also that the coefficients depend on k, as the Rashba term has coupled spin and momentum. Take

$$\psi_\pm = \frac{e^{i\boldsymbol{k}\boldsymbol{r}}}{\sqrt{2}}\left(|\uparrow\rangle + a\,|\downarrow\rangle\right), \tag{1.40}$$

where a is some phase we must find. By inserting into the time-independent Schrödinger equation, we find $a = \mp i(k_x + k_y)/k$, which is obviously $a = \mp i\exp(i\theta)$, where θ is the angle of the momentum, $\boldsymbol{k} = (k\cos\theta, k\sin\theta)$. Using

the matrix representation $|\uparrow\rangle = (1,0)^T, |\downarrow\rangle = (0,1)^T$, the eigenvalues are given as

$$\psi_\pm = \frac{e^{ikr}}{\sqrt{2}} \begin{pmatrix} 1 \\ \mp i e^{i\theta} \end{pmatrix}. \tag{1.41}$$

These states have interesting spin expectation values

$$\langle \psi_\pm | \boldsymbol{\sigma} | \psi_\pm \rangle = \pm \left[\sin\theta \hat{x} - \cos\theta \hat{y} \right]. \tag{1.42}$$

The spin is orthogonal to the momentum, making a circular pattern around the origin. The direction of the rotation defines the chirality of the state. The spin together with the energy solutions are shown in Fig. 1.3.

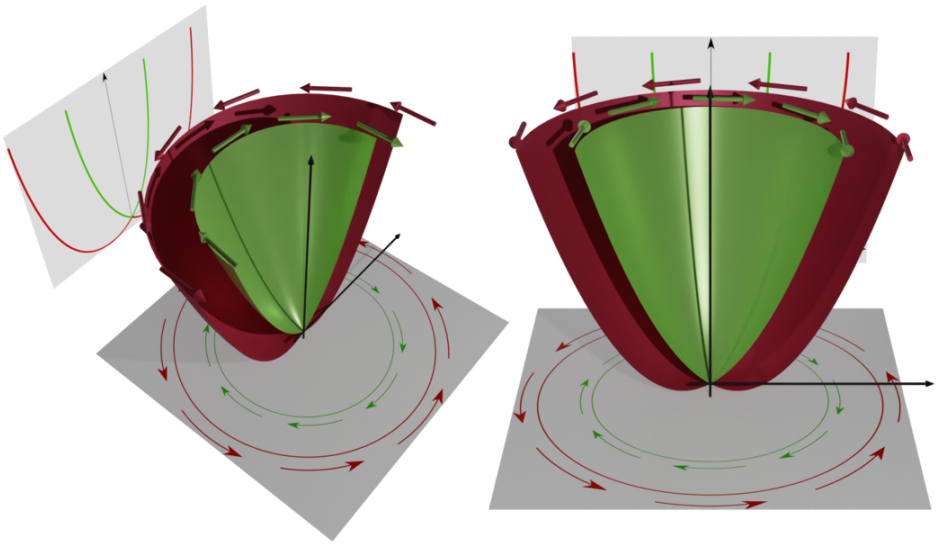

Figure 1.3.: Dispersion curves for a system with Rashba spin-orbit coupling. **Left:** Seen from above. **Right:** Seen from the front. The projection into the xy-plane is shown, as well as a cross section in a plane perpendicular to the xy-plane. The spin of the two states are shown as arrow above the dispersion curves, which defines the chirality of each state. Notice, as is most easily seen in the projection, that the two solutions together form a pair of parabolas separated in momentum.

1.6. Weyl and Dirac cones in condensed matter physics

Dirac and Weyl cones are the emergence of non-gapped linear energy bands in condensed matter physics, in effect exhibiting relativistic behavior at non-relativistic speeds. We here give a brief introduction to these materials. The system and its relation to high energy physics is discussed first. Then, several perturbations of the system are introduced. The topological nature of the system is considered in the context of Chern numbers and Berry curvature. Lastly, we go into tilted Dirac cones in some more depth. The reader is also advised to consult the many recent reviews on the topic, notably Armitage, Mele, and Vishwanath [AMV18] for a general introduction and overview of the field, Jia, Xu, and Hasan [JXH16] with a focus on material realizations, and Chernodub et al. [Che+21] which is the most directly relevant for our work, discussing in particular thermal transport and the analogy to high energy physics. For an intuitive and non-formal introduction to the latter, the lecture by Vozmediano [Voz21] given at the theoretical physics colloquium at Arizona State University is also recommended.

The standard model for metals in condensed matter physics is the Landau Fermi liquid [Che+21; Lan56], where electrons are described by the Hamiltonian $p^2/2m^*$, with m^* some effective mass. The model works remarkably well for many systems, but fails for the vanishing density of Dirac materials [Che+21; Voz21], where the electrons behave as "Dirac fermions". The notion of a "Dirac fermion" is almost comical from a high energy point of view [Che+21; Voz21] – what else can they be? A fermion is by its very definition a Dirac spinor. In condensed matter language, however, we mean by fermion that it obeys the Pauli exclusion principle and follows the Fermi-Dirac distribution. By Dirac fermion in condensed matter we mean fermions whose effective low-energy Hamiltonian is linear in momenta, they obey an effective Dirac equation.

This field unifies concepts from high and low energy physics; a "new era of grand unification of low and high energy physics" as Chernodub et al. [Che+21] puts it. The emergent Dirac and Weyl cones in condensed matter physics follow in beautiful analogy their high energy counterparts. Thus, the theory and results from high energy physics may be applied in these emergent Dirac systems. Likewise, these materials offer the opportunity to probe the fundamental theories of our universe, and beyond, at much lower energy and cost scales. Unfortunately, the language of QFT and high energy physics is somewhat inaccessible for condensed matter physicists. At the same time, the condensed matter descriptions have been difficult to relate back to the QFT formalism. So while the intersection of the two fields offers the possibility

of great new insight, it also comes with some misunderstandings. Some phenomena are known under different names, while different phenomena may be mistaken for the same. The recent and excellent review paper by Chernodub et al. [Che+21] attempts to make the topics approachable for researchers from both fields, with its "main purpose ... to present the basic notions underlying new developments in condensed matter in a language equally accessible to both high energy and condensed matter communities".

We wish here to briefly illuminate the connection between the high energy Dirac theory and the Dirac and Weyl semimetals of condensed matter physics, assuming the reader to be an expert in neither. The (massive) Dirac equation reads

$$(i\not{\partial} - m)\psi = 0, \tag{1.43}$$

where $\not{\partial} = \gamma^\mu \partial_\mu$, γ^μ are the so-called *gamma matrices*,[3] m is some mass parameter, and ψ the Dirac spinor. Note also that natural units $c = \hbar = 1$, as usual, is used and that the systems is 4×4. It may of course be written as a Schrödinger equation [Che+21] $i\partial_t \psi = H\psi$, with $H = \gamma^0 m + \gamma^0 \gamma^i p_i$. The great insight of Dirac was that due to the requirement of Lorentz invariance, the momentum and time operators had to appear at the same order, as opposed to the standard free particle $H = p^2/2m$. Shortly after Dirac published his theory, Weyl commented that for a massless particle, the equation could be decomposed into two 2×2 equations – a Weyl decomposition. This yields two independent subsystems, themselves also linear in momentum,

$$H_\pm = \pm \boldsymbol{\sigma} \cdot \boldsymbol{p}, \tag{1.44}$$

with the $\pm$ defining the *chirality*[4] of the Weyl component.

Interestingly, massless Dirac fermions may appear in condensed matter as low energy effective descriptions of electronic systems near a two-band crossing. Instead of obeying the Landau Fermi liquid theory, they obey a Dirac equation, with the speed of light being replaced by the Fermi velocity v_F. As in the high energy case, the Dirac equation may be decomposed into chiral Weyl equations

$$H_D = s v_F \boldsymbol{\sigma} \boldsymbol{p}, \tag{1.45}$$

where $\boldsymbol{\sigma}$ are the Pauli matrices, v_F the Fermi velocity, $\boldsymbol{p}$ the momentum, and $s = \pm 1$ denotes the chirality. It is here important to note that the Pauli matrices represent either real spin degree of freedom or some pseudo spin

[3] Also known as the Dirac matrices. They are any irreducible matrix representation of the Clifford algebra.

[4] For massless particles equivalent to the helicity.

degree of freedom. Examples of pseudo spin are that of bipartite lattices, such as graphene, in which case one must be careful when for example applying time-reversal, as only real spin is odd under this operation, and not pseudo spin.

These linear low energy emergent systems may appear in both 2D and 3D. There are, however, important differences depending on the dimensionality. When we here refer to Dirac and Weyl materials, we always mean 3D systems.

The dispersion of the Hamiltonian (1.45) has a band crossing at $\boldsymbol{p} = 0$. For the two-dimensional case, a perturbation on the form $m\sigma_z$, with m some parameter, opens a gap in the dispersion. This is easily verified by writing out the Hamiltonian and solving the eigenproblem

$$H_D^{(2D)} = sv_F(p_x\sigma_x + p_y\sigma_y) + m\sigma_z, \tag{1.46}$$

$$\left|H_D^{(2D)} - E\right| = 0. \tag{1.47}$$

As the Hamiltonian commutes with the momentum operator, we replace the momentum operator with its eigenvalues

$$E_\pm = \pm v_F\hbar\sqrt{k_x^2 + k_y^2 + \frac{m^2}{\hbar^2 v_F^2}}. \tag{1.48}$$

For a non-zero m, there are no solutions k_x, k_y making the energy levels degenerate (i.e. $E_\pm = 0$). The crossing is thus only protected by symmetry considerations, and is not *topologically protected*.

In three dimensions the situation is somewhat different, with the Hamiltonian

$$H_D^{(3D)} = sv_F(p_x\sigma_x + p_y\sigma_y + p_z\sigma_z). \tag{1.49}$$

In this case, no perturbing term may open a gap at the crossing. There is no 2×2 matrix σ_4 that anticommutes with the Pauli matrices and while also being linearly independent, i.e. there is no "fourth" Pauli matrix; therefore no perturbative term will open the gap. Say for example we add a term like $m\sigma_z$, where the z-direction was chosen arbitrarily. The only effect this will have on the crossing is to translate it in k_z. Tying this back to the accidental degeneracy of Section 1.4, we see that no matter the perturbation, the three-dimensional momentum space will always have a point of degeneracy, i.e., a crossing. The crossing is *topologically protected*. A more formal approach to topological materials is that of topological invariants – numbers related to the topology of the material. Having a non-trivial topological invariant number is the very definition of topological materials, and we will in Section 1.6.1 show that Dirac cones make the Chern number of these materials non-trivial.

Lorentz breaking perturbations

As opposed to high energy physics, the emergent Dirac equation in condensed matter physics need of course not be Lorentz invariant. We may therefore introduce terms that break Lorentz invariance. Introduce to the system a pseudospin degree of freedom, thus extending the system to 4×4-matricies; in effect re-constructing the full Dirac equation from the Weyl equations, and then introduce perturbations. The Hamiltonian of the system

$$H = v_F \tau_x \otimes \boldsymbol{\sigma} \boldsymbol{p} + m \tau_z \otimes I_2 + b I_2 \otimes \sigma_z + b' \tau_z \otimes \sigma_x, \tag{1.50}$$

with $\boldsymbol{\tau}$ the Pauli matrices related to the pseudospin, and I_2 the identity matrix of dimension 2. The perturbing parameters m, b, b' are a mass parameter, and Zeeman fields in the z and x direction, respectively [AMV18]. Ignore for now b', i.e. $b' = 0$, which is related to a state known as the line node semimetal. Notice that the b term breaks time-reversal symmetry in the system, as the real spin σ is odd under time-reversal. The eigenvalues of this system [AMV18]

$$E_{s\mu}(\boldsymbol{k}) = s \left[m^2 + b^2 + v_F^2 k^2 + 2\mu b \sqrt{v_F^2 k_z^2 + m^2} \right]^{\frac{1}{2}}, \tag{1.51}$$

with $s = \pm 1, \mu = \pm 1$ encoding the degeneracies related to the spin and pseudospin degrees of freedom, respectively. There are still linear dispersions for $b > m$. For $b < m$, a gap opens, and the dispersion is non-linear. In fact, for $b > m$, the perturbation is simply a shift in k_z of the Dirac cone, similar to what was discussed in the 2×2 case, as is seen by rewriting

$$E_{s\mu}(\boldsymbol{k}) = s v_F \left[k_x^2 + k_y^2 + \left(\sqrt{k_z^2 + \frac{m^2}{v_F^2}} + \mu \frac{b}{v_F} \right)^2 \right]^{\frac{1}{2}}. \tag{1.52}$$

This still has Weyl node solutions at $k_z^2 = (b^2 - m^2)/v_F^2$, where the dispersion is linear in the vicinity of the nodal solutions. The effect is thus to separate the two Dirac nodes in momentum space, giving a *Weyl* semimetal. This also illustrates that the decomposition in Eq. (1.45) is valid around either of the shifted nodes. Expanding around one of the Dirac points of the Weyl semimetal, the Hamiltonian is exactly Eq. (1.45), after decomposing the 4×4 Hamiltonian into its two chiral 2×2 Weyl constituents. If one instead perturbs the system with a Zeeman field in the x-direction, $b' \neq 0$, the separation is instead in energy, giving a nodal loop where the two cones intersect. We will not go into any depth on these types of materials.

The three cases described here: unperturbed, where the two cones are superimposed; perturbed by b, where the cones are separated in momentum; and perturbed by b', where the cones are separated in energy, are shown in Fig. 1.4. Notice that in the two latter cases, the Dirac points, i.e. crossings, are not superimposed. As will be substantiated more in Section 1.6.1, this makes the crossings very robust, as the two nodes must merge before a gap may be opened.

The Hamiltonian in Eq. (1.45) is not the most general 2×2 Weyl system if we allow for anisotropy in the system. In three dimensions we have more generally the *tilted* Weyl Hamiltonian

$$H_s = (\boldsymbol{t}^s + s\boldsymbol{\sigma})(\boldsymbol{v} \odot \boldsymbol{p}), \tag{1.53}$$

where $\boldsymbol{t}^s$ is the *tilt vector*, $\boldsymbol{v}$ is some anisotropic velocity, $(\boldsymbol{v} \odot \boldsymbol{p})_i = v_i p_i$ is the Hadamard product of the anisotropic velocity and the momentum, and $\boldsymbol{\sigma}$ are the Pauli matrices corresponding to spin degree of freedom. By a simple rescaling of the momenta, we may in general consider a system with isotropic Fermi velocity v_F, giving

$$H_s = sv_F\boldsymbol{\sigma}\boldsymbol{p} + v_F\boldsymbol{t}^s\boldsymbol{p}. \tag{1.54}$$

The energy bands are

$$E_s(\boldsymbol{k}) = \pm v_F|k| + v_F\boldsymbol{t}^s\boldsymbol{k}, \tag{1.55}$$

as shown in Fig. 1.5. These types of systems, which are the systems of interest for this thesis, are considered in detail in Section 1.6.2.

1.6.1. Chern number of the Weyl point

In order to more explicitly demonstrate the topological nature of the tilted Weyl cone in Eq. (1.45), we will find a non-zero topological invariant associated with that state. Thereby showing that the material is topological. The topological number we will calculate is the Chern number, related to the Berry curvature of the bands in some enclosed surface. In order to calculate the Chern number, we must first find an expression for the Berry curvature of our system. This derivation will follow closely Berry's original derivation [Ber84] of the Berry phase of a two-level system with the Hamiltonian

$$H(\boldsymbol{R}) = \frac{1}{2}\boldsymbol{\sigma}\boldsymbol{R}. \tag{1.56}$$

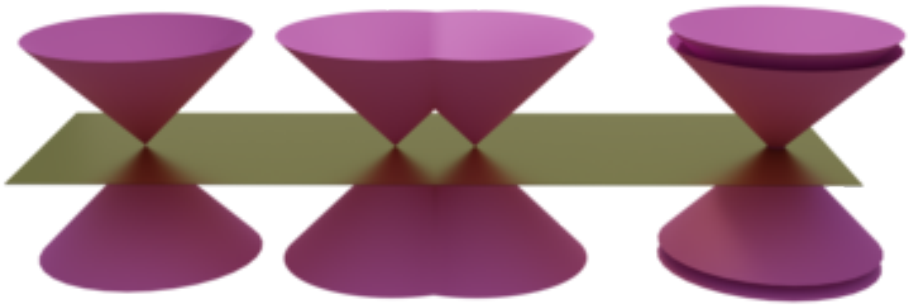

Figure 1.4.: Dirac cones in the plane, with the perpendicular momentum set to zero. **(Left)** Dirac material with superimposed cones. **(Center)** Time-reversal symmetry broken, giving a Weyl material with the cones separated in momentum space. **(Right)** The cones shifted in energy, giving a nodal loop.

Figure 1.5.: Tilted Dirac cones in the plane, with the perpendicular momentum set to zero. From left to right the tilt increases, from no tilt in the first cone to overtilt in the last. The three first are Type-I Weyl semimetals, the last is a Type-II semimetal. The Fermi surface is marked in red. See main text for details.

Some notation has been modernized with inspiration from the treatment of the Berry phase of the spin-1/2 particle in an external magnetic field in Holstein [Hol89].

Suppose we have a Hamiltonian $H(t)$, and that its t-dependence can be parameterized by $\boldsymbol{R} = \boldsymbol{R}(t)$, as in $H(t) = H(\boldsymbol{R}(t))$. Any evolution of the Hamiltonian through time, may then be described as a geometric path through the $\boldsymbol{R}$-space. As the reader might be aware, Berry's most famous discovery was that a closed path through $\boldsymbol{R}$-space gives an observable phase to the system, unlike the non-physical dynamical phase, which may be removed by a suitable choice of gauge. Here we will however focus on the so-called Berry curvature, $\boldsymbol{B}$, a vector field that will be shown to be useful in the categorization of topological materials. Note that there is some variation in the literature on the naming of the various quantities, and the sign convention used. In particular, the term *Berry curvature* will in some literature refer to a rank two tensor; what we call Berry curvature is referred to as the *Berry field strength*. In particular, if we let the rank two tensor be denoted F_{ij}, the Berry curvature is given by

$$B_i = \epsilon_{ijk} F_{jk}. \tag{1.57}$$

The Berry curvature for the state n is explicitly defined as [Ber84]

$$\boldsymbol{B_n}(\boldsymbol{R}) = -Im \sum_{m \neq n} \frac{\langle n(\boldsymbol{R}) | \boldsymbol{\nabla}_{\boldsymbol{R}} H | m(\boldsymbol{R}) \rangle \times \langle m(\boldsymbol{R}) | \boldsymbol{\nabla}_{\boldsymbol{R}} H | n(\boldsymbol{R}) \rangle}{(E_m(\boldsymbol{R}) - E_n(\boldsymbol{R}))^2}, \tag{1.58}$$

where $\times$ denotes the cross product. Notice that for a degenerate point where $E_n = E_m$ there will be a pole in $\boldsymbol{B_n}$. Considering the Berry curvature as a field in $\boldsymbol{R}$-space, this resembles a source, as will become relevant later. This may now be applied to for example the Weyl semimetal, both in the interest of solidifying the above theory, and as it will be useful in future consideration.

The Hamiltonian around the (untilted) Weyl point is

$$H = v_F \boldsymbol{\sigma} \cdot \boldsymbol{p}, \tag{1.59}$$

with v_F the Fermi velocity, $\boldsymbol{\sigma}$ the Pauli matrices, and $\boldsymbol{p}$ the momentum operator. By letting $\boldsymbol{R} = v_F \boldsymbol{p}$, the Berry curvature of the Hamiltonian can be found. The eigenvalues of this system are[5]

$$E_+ = -E_- = |R|. \tag{1.60}$$

[5] Technically, this is sloppy notation, as the eigenvalues are of course $E_+ = -E_- = v_F|k|$. We chose to use the above notation for clarity and to be more true to Berry's original derivation, even though that included implicit interchanging of $\boldsymbol{k} \leftrightarrow \boldsymbol{p}$.

The aforementioned degeneracy is here of course the Weyl point, where $E_+ = E_- = 0$. Noting that

$$\nabla_{\boldsymbol{R}} H = \boldsymbol{\sigma}, \tag{1.61}$$

we can calculate the Berry curvature easily. Denote by $|+\rangle$ the state with the eigenvalue E_+ and $|-\rangle$ the state with the eigenvalue E_-. Take also, without loss of generality, $\boldsymbol{R}$ to be in the z-direction. This gives

$$\boldsymbol{B}_+ = -Im\frac{\langle +|\boldsymbol{\sigma}|-\rangle \times \langle -|\boldsymbol{\sigma}|+\rangle}{4R^2}. \tag{1.62}$$

As $|+\rangle$ and $|-\rangle$ are eigenstates of σ_z and orthogonal to each other, only the z-component of the cross product may contain non-zero contributions.

$$\begin{aligned} \boldsymbol{B}_+ &= -\frac{\hat{z}}{4R^2} Im\left(\langle +|\sigma_x|-\rangle \langle -|\sigma_y|+\rangle - \langle +|\sigma_y|-\rangle \langle -|\sigma_x|+\rangle\right) \\ &= -\frac{\hat{z}}{2\boldsymbol{R}^2}. \end{aligned} \tag{1.63}$$

Here, the effect of the Pauli matrices on the eigenvectors was used, according to

$$\sigma_x |\pm\rangle = |\mp\rangle \tag{1.64}$$

$$\sigma_y |\pm\rangle = \pm i |\mp\rangle \tag{1.65}$$

Returning to general axis orientations, one has

$$B_+ = -\hat{R}/2\boldsymbol{R}^2 = -\boldsymbol{R}/2\boldsymbol{R}^3. \tag{1.66}$$

For the $|+\rangle$-band, the Weyl point thus takes the form of a negative monopole in R-space; this motivates the requirement that Weyl points must always appear in pairs of opposite chirality, as the divergence of the Berry curvature must always be zero over the entire sample.

Extending the calculation to a tilted Weyl cone

$$H = v_F \boldsymbol{\sigma} \cdot \boldsymbol{p} + v_F \boldsymbol{t} \cdot \boldsymbol{p}, \tag{1.67}$$

is trivial. The energies gain a factor $v_F \boldsymbol{t} \cdot \boldsymbol{p} = \boldsymbol{t} \cdot \boldsymbol{R}$, however, this does not change the difference between the energies of the states. Furthermore, the gradient of the Hamiltonian, Eq. (1.61), gains a factor

$$\nabla_{\boldsymbol{R}} H = \boldsymbol{\sigma} + \boldsymbol{t}, \tag{1.68}$$

which does not affect the result, as $\langle \pm|\boldsymbol{t}|\mp\rangle = 0$. Consequently, tilting does not affect the Berry curvature.

As mentioned, the Chern number is one of several numbers that is used to classify topological materials. The Chern number is defined as

$$C = \frac{1}{2\pi} \oint_{\partial C} \boldsymbol{B}_+ \cdot \mathrm{d}\boldsymbol{S}, \tag{1.69}$$

where the integral is taken over the closed surface ∂C, enclosing the volume C. Noting that the Berry curvature has the shape of a monopole source at $\boldsymbol{p} = 0$, we immediately know the value of this quantity from electromagnetism. We will, however, carry out the computation explicitly here. With the divergence theorem in mind, it behooves us to find the divergence of the Berry curvature. This divergence is zero everywhere except in the monopole source, giving

$$\nabla \cdot \boldsymbol{B}_+ = -\frac{1}{2} \nabla \cdot \hat{R}/R^2 = -2\pi\delta(\boldsymbol{p}), \tag{1.70}$$

where δ is the Dirac delta distribution. By virtue of the divergence theorem, the Chern number is then found to be

$$C = \frac{1}{2\pi} \int_C \nabla \cdot \boldsymbol{B}_+ \mathrm{d}C = -1, \tag{1.71}$$

where the property of integrals over Dirac delta distributions was used.

Note that some literature will have a Chern number differing from Eq. (1.71) by the sign of the Fermi velocity,

$$C = -\operatorname{sign}(v_F). \tag{1.72}$$

This simply comes from the definition of the eigenstates. We have put the sign dependence in the state, making the E_+ state always have positive eigenenergy. In the literature that instead defines $E_+ = v_F|R|$ the state's energy will depend on the sign of the Fermi velocity, and as a consequence, the sign dependence will end up in the Chern number instead.

The overall divergence of Berry curvature must be zero, or equivalently, the sum of the Chern numbers must be zero. The Hamiltonian Eq. (1.56) chosen with the opposite chirality,

$$H(\boldsymbol{R}) = -\frac{1}{2} \boldsymbol{\sigma} \boldsymbol{R}, \tag{1.73}$$

has the opposite Berry curvature, and also the opposite Chern number. Thus, Dirac cones must appear in pairs of opposite chirality, either superimposed as the Dirac semimetal case or separated in momentum space, as the Weyl semimetal.

In light of the interpretation of the Dirac point as a monopole of Berry curvature, the discussion in Section 1.6, on page 17, on the stability of the band crossing in two and three dimensions gets an intuitive and geometric interpretation. In Fig. 1.6 the Berry curvature pole is shown in p-space, together with a plane parallel to the xy-plane, which we will denote the *state plane*. In the two-dimensional case, the state is confined to the state plane, with the z-position of the plane given by any mass terms $m\sigma_z$. In the three-dimensional case, the state is not confined to this plane, as the parameter k_z is a free variable, or alternatively, it may be considered as the freedom to move the state plane freely, with its initial position simply shifted by any mass terms. It is thus obvious that one may never reach the monopole in the two-dimensional case, and thus for no $\boldsymbol{k}$ is there a band crossing. Importantly, the Berry curvature is indeed non-zero, however any closed curve of integration will give a Chern number of zero; the monopole has been moved outside the dimensionality of freedom.

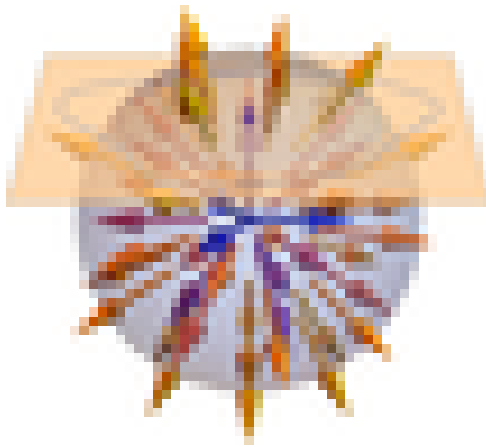

Figure 1.6.: The state plane, transparent yellow, parallel to the xy-plane and a Berry curvature monopole at the origin. An integration contour is shown in blue dashed. See main text for details.

1.6.2. Tilted Dirac semimetals

The conic section problem with the intersecting plane restricted to pass through the node of the cone is trivially seen to have two solutions: a point and two intersecting lines, shown schematically in Fig. 1.7. Despite this, the possibility of a Weyl cone tilted beyond the Fermi level was never considered before Soluyanov et al. [Sol+15] described this new class of Weyl semimetals in 2015. This now seemingly obvious possibility made an already rich field even more exciting, opening up for a wider range of novel and interesting effects [FZB17; SGT17; Sol+15; TCG16; YYY16].

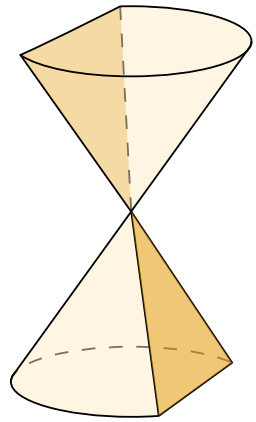

Figure 1.7.: The conic section.

In this section, we investigate in more detail the tilted Weyl cone, the star of this thesis. The tilted Hamiltonian was introduced in Eq. (1.54)

$$H_s = sv_F\boldsymbol{\sigma p} + v_F\boldsymbol{t}^s\boldsymbol{p},$$

where we chose isotropic Fermi velocity. As discussed earlier, the proper Dirac equation of particle physics cannot include such a tilting term, as it obviously breaks Lorentz invariance. The emergent Dirac equation of condensed matter physics, however, need not respect the Lorentz invariance and such a tilting term is no problem.

As was alluded to in the introduction to the section, the Weyl cone has two distinct phases: Type-I and Type-II. Tilting the Weyl cone, the upper and lower bands will at some tilt angle touch the Fermi level, a *critical* tilt. Going beyond this, the upper (lower) band dips below (above) the Fermi level, and we have what is known as a Type-II Weyl semimetal. Although the two states are similar in many ways, they also have hugely important differences separating them from one another. In the Type-I regime, the density of states goes to zero at the Fermi level. In the Type-II regime, however, particle and hole pockets appear – the intersection of the cone and the Fermi level goes from a singular point to two infinite lines (shown in Fig. 1.5 on page 20), making the density of states non-zero. This abrupt change of the topology of the Fermi surface, from closed to open, is known as a topological Lifshitz transition [Vol17]. This gives Type-II Weyl semimetals manifestly different properties from Type-I, useful both in practical applications and as an interesting phenomenon seen from a purely scientific perspective.

Linear Dirac equation from tight binding model

We will firstly consider a slightly more realistic tight binding toy model for a Weyl semimetal, with a parameter taking the system from a Type-I to a Type-II. This is instructive both in order to more intuitively see the origin of the terms causing the tilting of the Dirac cone, and also to discuss the validity of the linear model in different contexts. We will linearize the model around the Weyl points, regaining the familiar form of a Dirac cone, with an additional anisotropy term causing the tilt.

We will use the general time-reversal breaking model described by McCormick, Kimchi, and Trivedi [MKT17][6]

$$\begin{aligned} H(\boldsymbol{k}) = &[(\cos k_y + \cos k_z - 2)m - 2\gamma_0(\cos k_x - \cos k_0)]\,\sigma_1 \\ &- 2\gamma_0 \sin k_y \sigma_2 - 2\gamma_0 \sin k_z \sigma_3 + t_0(\cos k_x - \cos k_0). \end{aligned} \tag{1.74}$$

There are Weyl nodes at $\boldsymbol{K}' = (\pm k_0, 0, 0)$, and the parameter t_0 controls the tilting of the emerging cones. For $k_0 = \pi/2$, the cones are isotropic in low-energy expansion. As k_0 is reduced, the cones are brought closer together and made anisotropic, as the effective Fermi velocity is not the same in all directions, as shown in Fig. 1.8a, where two cones are moved until they meet at the origin. Fig. 1.8b shows the eigenvalues of the system, as t_0 is increased from 0 to $3\gamma_0$. A value of $t_0 = 0$ gives no tilt, while for $t > |2\gamma_0|$ the Type-II system emerges. The t_0-term "warps" the bands, and in the limit of Type-II the hole band crosses the Fermi level into positive energy, while the particle band crosses the Fermi level into negative energies. We call these electron and hole pockets, respectively. Note that in this model, the pockets are shared between the two nodes. One may also construct tight binding models with isolated pockets [MKT17].

Linearizing around the Weyl nodes the Hamiltonian reduces to the familiar expression of a Dirac cone

$$H(\boldsymbol{K}'^{\pm} + \boldsymbol{k}) \approx \mp 2\gamma_0 k_x \sin k_0 \sigma_1 - 2\gamma_0(k_y\sigma_2 + k_z\sigma_3) \mp t_0 k_x \sin k_0 \sigma_0, k_x, k_y, k_z \ll 1. \tag{1.75}$$

When the separation between the two nodes is π, i.e. $k_0 = \pi/2$, the linearized Hamiltonian around the cone is

$$H'(\boldsymbol{k}) = \mp 2\gamma_0 k_x \sigma_x - 2\gamma_0 k_y \sigma_y - 2\gamma_0 k_z \sigma_z \mp t_0 k_x, \tag{1.76}$$

with $\mp$ corresponding to the node at $\boldsymbol{K}'^{\pm}$. For a system

$$H = t_i k_i + k_i A_{ij} \sigma_j, \tag{1.77}$$

[6] Where we adapted the notation to match that used in the rest of the thesis.

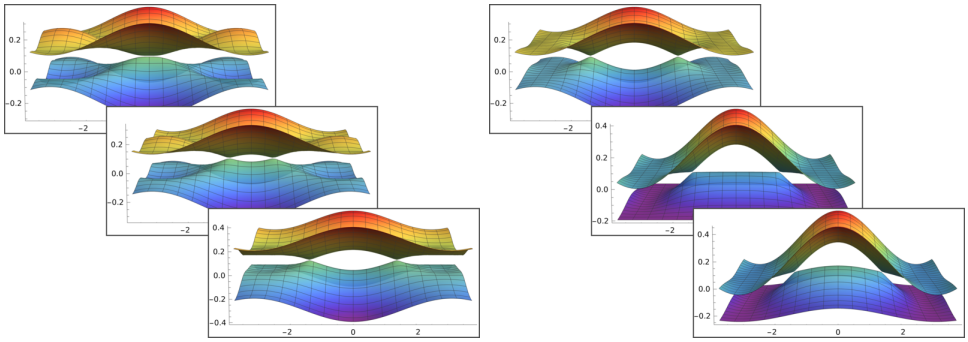

(a) A Type-I Weyl semimetal with separation between the nodes $2k_0 = 0, \pi/2, \pi$.

(b) The "warping" parameter t_0 increased from left to right, $t_0 = 0, 2\gamma_0, 3\gamma_0$, transitioning the system from Type-I to Type-II.

Figure 1.8.: Two-band tight binding model for a tilted Dirac semimetal. Shown are the two energy bands plotted in the xz-plane in momentum space; the separation of the nodes is in the x-direction. In (a) the separation between the two nods is adjusted. In (b) the bands are "warped" to induce tilt. See main text for details of the model.

the chirality of the node $s = \det(A_{ij})$ [MKT17], and we see this gives a negative cone at $k_x = \pi/2$ and positive at $k_x = -\pi/2$. We could arrive at a more familiar form of the expression by letting $2\gamma_0 \to v_F, t_0 \to v_F t$, explicitly introduce s for the chirality, and do a π rotation around x at the positive cone, giving

$$H'^{s}(\boldsymbol{k}) = s v_F \boldsymbol{k} \cdot \boldsymbol{\sigma} + s v_F t k_x. \tag{1.78}$$

The model thus gives rise to a pair of Weyl cones, with an inversion symmetric tilt, i.e. they tilt with equal magnitude in the opposite direction. Moving the two nodes closer together, the effective Fermi velocity in the x-direction is rescaled, and the system is anisotropic even for no tilt ($\gamma = 0$). As discussed earlier, this may be mitigated by a rescaling of k_x.

The linearized model is accurate in describing low-energy interactions around the Dirac point. For higher energies, its validity falls apart, and more complex models are warranted. For our calculations, we will take the linear model to be sufficient. It is much easier to work with and sufficient in most cases.

One of the most obvious differences between the tight-binding model and the continuous linear model is the finiteness of the former. This is particularly

important with regard to two aspects: the Dirac sea and the topology of the Fermi surface. In high energy physics, the Dirac sea is infinitely deep [Bur16; Voz21], whereas, in condensed matter physics, it is not. As is seen from the tight-binding model, the Dirac sea of the two cones is really connected; this has consequences for, among others, the interpretation of the chiral anomaly. In our context, also the topology of the Fermi surface is of importance. As mentioned, in the topological Lifshitz transition from Type-I to Type-II, the Fermi surface goes from being closed to open in the linear model. This is not the case in the tight-binding model, whose Fermi surface is shown in Fig. 1.9. According to Ferreiros, Zyuzin, and Bardarson [FZB17] the linear model will be able to give qualitatively correct results for Type-II in the deep tilt limit. We propose yet another argument for this claim here. Consider again the Fermi surface in Fig. 1.9; as the (Type-II) tilt is increased the Fermi surface resembles more and more that of the linear model. At small (but still Type-II) tilt, the Fermi surface is highly non-linear. For larger tilt, the Fermi surface of the tight-binding model becomes more linear. Although this is in no way rigorous, it gives hope that the linear model may give qualitatively valid results for Type-II materials in the deep tilt limit.

A priori, it is not obvious when and how the linear model falls short, and a critical interpretation and evaluation of results derived from it is always warranted. It is, however, a very useful and interesting model. One of the more obvious and common remedies is a momentum cutoff, restricting the model to the region where it is the most correct [FZB17; SGT17].

The tilt term – symmetries and Type-I vs. Type-II

Recall the tilted Weyl Hamiltonian

$$H^s = sv_F\boldsymbol{\sigma}\boldsymbol{p} + v_F\boldsymbol{t}^s\boldsymbol{p},$$

with $s \pm 1$ the chirality of the cone. The tilt vector will in general depend on the chirality of the cone. As the cones always appear in pairs, $\boldsymbol{t}^s = s\boldsymbol{t}$ will give a system with inversion symmetry, as was the result from the tight binding model in the previous subsection. In the case of broken inversion symmetry, we will consider the case of a tilt equal in direction and magnitude between the two cones, $\boldsymbol{t}^s = \boldsymbol{t}$. In short, we define

$$\boldsymbol{t}^s = \begin{cases} \boldsymbol{t} & \text{broken inversion symmetry,} \\ s\boldsymbol{t} & \text{inversion symmetry.} \end{cases} \tag{1.79}$$

This convention is used in most literature [FZB17; vdWS19].

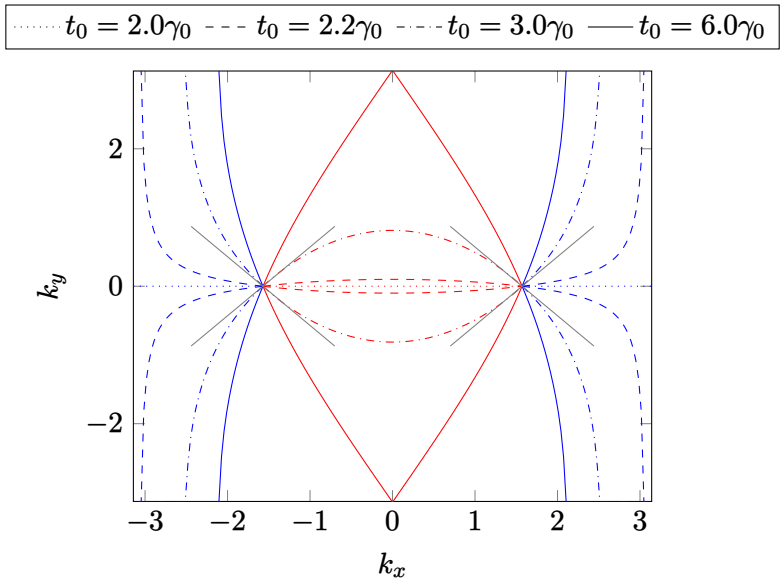

Figure 1.9.: The Fermi surface of the tight binding model in the Type-II phase, with the Fermi surface of the linear model for $t_0 = 3\gamma_0$ superimposed (gray, truncated). The Figure shows the k_x, k_y plane, with $k_z = 0$. Electron pockets are shown in red, hole pockets shown in blue. As the tilt is increased, the Fermi surface becomes more linear.

With no magnetic field, the eigenvalues of the system are

$$E_s(\boldsymbol{k}) = \pm v_F|k| + v_F \boldsymbol{t}^s \boldsymbol{k}, \tag{1.80}$$

where in the literature the first term is sometimes referred to as the *potential* term while the latter is the *kinetic* term. The definition for the system to be Type-II is that there exists a direction in momentum space for which the kinetic term dominates over the potential term [Sol+15]. The $\boldsymbol{t}$-vector is thus a convenient tool for categorization – if $t > 1$ we have a Type-II, else we have a Type-I.

Proof: We may always rotate our coordinate system such that, without loss of generality, $\boldsymbol{t} = t\hat{x}$. In that case, the first term dominates in the x-direction, when $t > 1$. □

The definition is equivalent to defining Type-I as tilted cones with a point like Fermi surface and Type-II as cones with a finite Fermi surface. In other words, Type-II occurs when the bands cross the Fermi surface.

When considering the symmetry properties of the system, we must consider the full 4×4 Dirac equation. The 2×2 Weyl equation describing one cone does not capture the symmetries of the full system, which involve both Weyl cones. Let

$$H = v_F \tau_z \otimes \boldsymbol{\sigma} \boldsymbol{p},$$

where τ is some pseudo spin degree of freedom, transforming like $\boldsymbol{r}$. This system describes two superimposed cones at the origin, with opposite chirality. The effect of parity $\mathcal{P}$ and time-reversal $\mathcal{T}$ is

$$\begin{aligned} \mathcal{P}\tau\mathcal{P}^\dagger &= -\tau, \quad \mathcal{T}\tau\mathcal{T}^\dagger = +\tau, \\ \mathcal{P}\sigma\mathcal{P}^\dagger &= +\sigma, \quad \mathcal{T}\sigma\mathcal{T}^\dagger = -\sigma, \\ \mathcal{P}\boldsymbol{k}\mathcal{P}^\dagger &= -\boldsymbol{k}, \quad \mathcal{T}\boldsymbol{k}\mathcal{T}^\dagger = -\boldsymbol{k}, \end{aligned} \tag{1.81}$$

compactly summarized in Table 1.1. Obviously then, the Hamiltonian is

Table 1.1.: The transformation rules for τ, σ, p under parity $\mathcal{P}$ and time-reversal $\mathcal{T}$.

	$\mathcal{P}$	$\mathcal{T}$
τ	-	+
σ	+	-
p	-	-

both time-reversal and parity invariant, as $\mathcal{P}\mathcal{P}^\dagger = \mathcal{T}\mathcal{T}^\dagger = 1$. Notice that as $\mathcal{P}\tau\mathcal{P}^\dagger = -\tau$, the chiralities of the cones are interchanged under a parity transformation.

The tilt term takes the form $v_F \tau_z^i \otimes \mathcal{I}_2 \, \boldsymbol{t} \cdot \boldsymbol{p}$, where $i = 1$ for inversion symmetric systems ($\boldsymbol{t}^s = s\boldsymbol{t}$) and $i = 2$ for broken inversion symmetry ($\boldsymbol{t}^s = \boldsymbol{t}$). We thus see explicitly, by applying the parity and time-reversal operators, that the term breaks time-reversal symmetry, and that we get self-consistency for the parity transformation. This is also shown pictorally in Fig. 1.10.

The unperturbed Dirac Hamiltonian is Lorentz invariant, given that we consider an "effective speed of light", namely the Fermi velocity, instead of the actual speed of light c. Specifically, Lorentz invariance means invariance under the *Lorentz group*. The Lorentz group is the $O(1,3)$ Lie group that conserves

$$x_\mu x^\mu = t^2 - x^2 - y^2 - z^2,$$

i.e. all isometries of Minkowski space. More specifically, the group consists of all 3D rotations, $O(3)$, and all *boosts*. A boost is a hyperbolic rotation from a

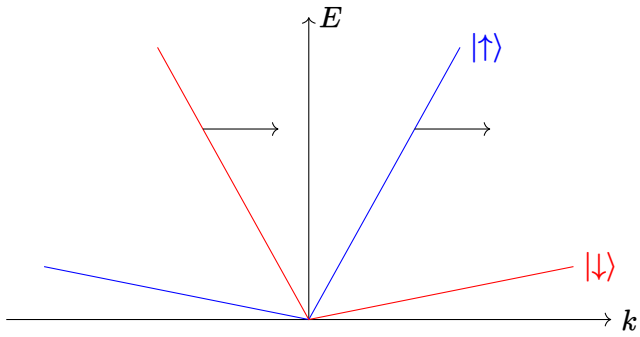

Figure 1.10.: One dimension of a tilted Dirac cone, with the two other momenta set to zero, pictorally showing the time-reversal symmetry breaking of the tilt. The two Weyl constituents are marked in red and blue, respectively. Black arrows indicate spin direction, which for $|\uparrow\rangle$ is parallel to $\boldsymbol{k}$ while for $|\downarrow\rangle$ is parallel to $-\boldsymbol{k}$.

spacial dimension to the temporal dimension. If we now direct our focus at the Hamiltonian of the Dirac cone

$$H = \pm v_F \boldsymbol{\sigma} \boldsymbol{p},$$

we may easily show the Lorentz invariance of the system. The time independent Schrödinger equation is

$$H|\psi\rangle = E|\psi\rangle \implies (H^2 - E^2) = 0. \tag{1.82}$$

As

$$p^\mu = \left(\frac{E}{c}, \boldsymbol{p}\right),$$

the operator in Eq. (1.82) is nothing more than

$$H^2 - E^2 = v_F^2 \boldsymbol{p}^2 - c^2 \left(p^0\right)^2, \tag{1.83}$$

where we used the anticommutation relation

$$\{\sigma_i, \sigma_j\} = 2\delta_{ij}$$

of the Pauli matrices. Using now the effective speed of light $c = v_F$, Eq. (1.82) is

$$-v_F^2 p_\mu p^\mu = 0. \tag{1.84}$$

The invariance of $x^\mu x_\mu$ is the very definition of the Lorentz group, and so is obviously Lorentz invariant.

Consider now a *tilted* Dirac cone

$$H = \pm v_F \boldsymbol{\sigma} \boldsymbol{p} + v_F t_x p_x, \tag{1.85}$$

where we, without loss of generality, chose the tilt to be in the x-direction. By the same argumentation as above, the eigen-equation

$$H|\psi\rangle = E|\psi\rangle \implies (H^2 - E^2) = 0$$

leads to the equation

$$-v_F^2 p^\mu p_\mu + v_F t_x p_x (2E - v_F t_x p_x) = 0. \tag{1.86}$$

This is *not* invariant under a Lorentz transformation, as can be seen by, for example, a rotation around the z-axis.

2 Linear Response Theory

We will now introduce the Kubo formalism of linear response theory. Later, the theory will be specialized to thermoelectric response. The material of this section is mostly inspired by the explanations given in Giuliani and Vignale [GV05]. The specialization to the electric response and Luttinger's method is also inspired by Mahan [Mah00].

We are interested in expressing the response of the observable A to some field F coupling to another observable B. Let the uncoupled system be described by the Hamiltonian H_0 and the coupling term be $H_F(t) = F(t)B$. Assume also that the coupling field F is turned on at $t = t_0$, such that $H_F(t) = 0$ for $t < t_0$. Let the unperturbed Hamiltonian be H_0, which will be assumed time independent. The total Hamiltonian describing the coupled system is

$$H(t) = H_0 + H_F(t) = H_0 + F(t)B. \tag{2.1}$$

Linear response theory tells us then that the response δA is given by [GV05]

$$\delta A = -\frac{i}{\hbar}\int_{t_0}^{t} \langle [A(t), B(t')] \rangle_0 \, F(t')\mathrm{d}t', \tag{2.2}$$

where $[A, B]$ is the operator commutator and $\langle \ldots \rangle_0$ denotes the average in the thermal equilibrium ensemble. A non-rigorous motivation for this form of the response is the fact that

$$\dot{A} = -\frac{i}{\hbar}[A, H] + \frac{\partial A_S}{\partial t}, \tag{2.3}$$

with A_S the Schrödinger picture operator, whose derivative is from here on assumed zero. Taking $H = H_F$, the part of the Hamiltonian whose dynamics we are interested in, and integrating over the interaction time, the result is reminiscent of Eq. (2.2). For a proper derivation see for example Giuliani and Vignale [GV05, Chapter 3.3].

We will now try to make this expression slightly more manageable, and in the process, we will highlight some important physical properties of the expression. Firstly, by taking advantage of the time translation invariance of the uncoupled Hamiltonian H_0, we may realize that the average taken in the

unperturbed basis may be taken at a more convenient time, preserving the time separation of the operators

$$\langle [A(t), B(t')] \rangle_0 = \langle [A(t-t'), B(0)] \rangle_0 . \tag{2.4}$$

Inserting this back to Eq. (2.2), and performing a change of variable $\tau = t - t'$ we have

$$\delta A = -\frac{i}{\hbar} \int_0^{t-t_0} \langle [A(\tau), B(0)] \rangle_0 F(t-\tau) \mathrm{d}\tau. \tag{2.5}$$

In this form the retardedness of the coupling is apparent – no observable can be affected by a future perturbation, shown schematically in Fig. 2.1.

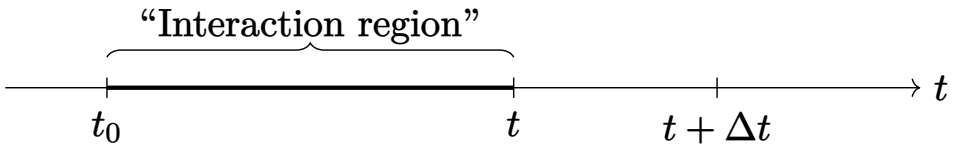

Figure 2.1.: Interacting region of a perturbation turned on at t_0. Note that the perturbation in the future, $t + \Delta t$, does not interact, as this is the retarded interaction.

For future convenience, and convention, we will in this last step introduce the *response function*

$$\chi_{AB}(\tau) = -\frac{i}{\hbar} \Theta(\tau) \langle [A(\tau), B(0)] \rangle_0 , \tag{2.6}$$

where the step-function Θ was introduced to make the response function explicitly *retarded*. Then our final expression for the response of A is

$$\delta A = \int_0^{t-t_0} \chi_{AB}(\tau) F(t-\tau) \mathrm{d}\tau. \tag{2.7}$$

Note of course that the limits could be altered to $\int_{-\infty}^{\infty}$ given that the coupling field is zero for times earlier than t_0 and we have chosen the retarded response function.

2.1. Charge current from electromagnetic coupling

We will now discuss the electric *conductivity* in light of the Kubo formalism, as an example to better understand and demonstrate the preceding discussion.

Firstly the concept of conductivity will be presented, then it will be derived using the machinery of the Kubo formula. As mentioned above, this part follow the derivation of Mahan [Mah00].

The charge current $\boldsymbol{J}$ that is induced from an electric field $\boldsymbol{E}$ in the linear scheme is expressed by Ohm's law

$$\boldsymbol{J}_i(\boldsymbol{r},t) = \int_V \mathrm{d}\boldsymbol{x} \int_{-\infty}^{t} \mathrm{dt}\ \sigma_{ij}(\boldsymbol{r},t,\boldsymbol{x},s)\boldsymbol{E}_j(\boldsymbol{x},s). \tag{2.8}$$

Above the Einstein summation convention is used, and σ_{ij} is the *conductivity tensor*. We see of course that this has the familiar form of a response relation. In the case of a simple and isotropic material, meaning symmetric under SO(n) and with no transverse response, the tensor is diagonal with $\boldsymbol{\sigma} = \sigma I$ and one gets the more well-known version of Ohm's law $\boldsymbol{J} = \sigma \boldsymbol{E}$.

Again, by the principle of causality, the response of $\boldsymbol{J}$ can only depend on $\boldsymbol{E}$ in the *past*; thus $\sigma_{ij}(\boldsymbol{r},t,\boldsymbol{x},s)$ can be finite only where the time separation $t-s$ is less than the time light takes to cover the spatial separation $\boldsymbol{r}-\boldsymbol{x}$. Moreover, if we assume spatial and temporal invariance, i.e. that the response only depends on the separation $t-s$ and $\boldsymbol{r}-\boldsymbol{x}$, the expression is simplified somewhat more by transforming it to the Fourier domain. Note that this assumption is *not* valid on an atomic scale; it is here used under the assumption that currents are averaged over multiple unit cells, a common practice in electromagnetism of solids. Let $\sigma_{ij}(\boldsymbol{r}-\boldsymbol{x},t-s) \equiv \sigma_{ij}(\boldsymbol{r},t,\boldsymbol{x},s)$ and introduce the Fourier transform

$$A(\boldsymbol{q},\omega) = \iint \mathrm{dtd}\boldsymbol{r} e^{i(\omega t - \boldsymbol{q}\boldsymbol{r})} A(\boldsymbol{r},t), \quad A(\boldsymbol{r},t) = \iint \frac{\mathrm{d}\omega \mathrm{d}\boldsymbol{q}}{(2\pi)^4} e^{-i(\omega t - \boldsymbol{q}\boldsymbol{r})} A(\boldsymbol{q},\omega). \tag{2.9}$$

Recognizing the right-hand side of Eq. (2.8)

$$\int \mathrm{d}\boldsymbol{x} \int \mathrm{dt} \sigma_{ij}(\boldsymbol{r}-\boldsymbol{x},t-s)\boldsymbol{E}_j(\boldsymbol{x},s) \tag{2.10}$$

as a convolution, we can write Eq. (2.8) as

$$\boldsymbol{J}_i(\boldsymbol{q},\omega) = \sigma_{ij}(\boldsymbol{q},\omega)\boldsymbol{E}_j(\boldsymbol{q},\omega), \tag{2.11}$$

by using the well known result that the Fourier transform of a convolution is the product of the transformed functions of the convolution [Rot95]. Alternatively, the same result is found by simply inserting the definition Eq. (2.9) for both $\boldsymbol{E}$ and σ in Eq. (2.8), and use

$$\int \mathrm{d}x e^{-ixa} = 2\pi\delta(a).$$

We now attempt to conclude at the result (2.11) using the Kubo formalism. The current couple to the electromagnetic potential $\boldsymbol{A}$ by a Hamiltonian term

$$H_{\boldsymbol{A}} = -\int \mathrm{d}\boldsymbol{r}\boldsymbol{A}(\boldsymbol{r},t)\cdot\boldsymbol{J}(\boldsymbol{r}). \tag{2.12}$$

Comparing with the notation introduced earlier for general linear response, where the perturbing Hamiltonian in Eq. (2.1) was

$$F(t)B,$$

we identify the perturbing field F as $\boldsymbol{A}$ and the observable B as the current density. We thus identify the *response function*

$$\chi_{ij}(\boldsymbol{r},t,\boldsymbol{x},s) = -\frac{i}{\hbar}\Theta(t-s)\left\langle[\boldsymbol{J}_i(\boldsymbol{r},t),\boldsymbol{J}_j(\boldsymbol{x},s)]\right\rangle_0. \tag{2.13}$$

This gives the response

$$\delta\boldsymbol{J}_i(\boldsymbol{r},t) = \int_{t_0}^{t}\mathrm{d}s\int \mathrm{d}\boldsymbol{x}\chi_{ij}(\boldsymbol{r},t,\boldsymbol{x},s)\boldsymbol{A}_j(\boldsymbol{x},s). \tag{2.14}$$

Assuming spatial and temporal translational invariance,

$$\chi_{ij}(\boldsymbol{r}-\boldsymbol{x},t-s) \equiv \chi_{ij}(\boldsymbol{r},t,\boldsymbol{x},s), \tag{2.15}$$

the expression can be simplified quite a bit. Firstly, we will make a change of variables, and then Fourier transform both the spatial and temporal argument. With $\tau = t-s$ and $\boldsymbol{x}' = \boldsymbol{r}-\boldsymbol{x}$,

$$\delta\boldsymbol{J}_i(\boldsymbol{r},t) = \int_0^{t-t_0}\mathrm{d}\tau\int \mathrm{d}\boldsymbol{x}'\chi_{ij}(\boldsymbol{x}',\tau)\boldsymbol{A}_j(\boldsymbol{r}-\boldsymbol{x}',t-\tau). \tag{2.16}$$

By the Fourier transformation introduced in Eq. (2.9)

$$\boldsymbol{A}(\boldsymbol{q},\omega) = \iint \mathrm{d}t\mathrm{d}\boldsymbol{r}e^{i(\omega t-\boldsymbol{q}\boldsymbol{r})}\boldsymbol{A}(\boldsymbol{r},t),$$

the time transformed version of Eq. (2.16) is

$$\delta\boldsymbol{J}_i(\boldsymbol{r},\omega) = \int_0^{t-t_0}\mathrm{d}\tau\int \mathrm{d}\boldsymbol{x}'\chi_{ij}(\boldsymbol{x}',\tau)\underbrace{\int_{-\infty}^{\infty}\mathrm{d}t e^{i\omega t}\boldsymbol{A}_j(\boldsymbol{r}-\boldsymbol{x}',t-\tau)}_{\equiv e^{i\omega\tau}\boldsymbol{A}_j(\boldsymbol{r}-\boldsymbol{x}',\omega)}. \tag{2.17}$$

Similarly, Fourier transforming the spatial component yields

$$\delta \boldsymbol{J}_i(\boldsymbol{q},\omega) = \int_0^{t-t_0} \mathrm{d}\tau \int \mathrm{d}\boldsymbol{x}' \chi_{ij}(\boldsymbol{x}',\tau) e^{i\omega\tau} \underbrace{\int \mathrm{d}\boldsymbol{r}\; e^{-i\boldsymbol{q}\boldsymbol{r}} \boldsymbol{A}_j(\boldsymbol{r}-\boldsymbol{x}',\omega)}_{\equiv e^{-i\boldsymbol{q}\boldsymbol{x}'}\boldsymbol{A}_j(\boldsymbol{q},\omega)} . \tag{2.18}$$

Identifying the remaining part as the Fourier transform of the response function, we finally end up with,

$$\delta \boldsymbol{J}_i(\boldsymbol{q},\omega) = \chi_{ij}(\boldsymbol{q},\omega)\boldsymbol{A}_j(\boldsymbol{q},\omega). \tag{2.19}$$

One could of course also have used the observation that the original expression is a convolution or the direct insertion of the Fourier transform for χ and $\boldsymbol{A}$, as shown earlier.

In the current derivation, the scalar field potential ϕ is taken to be zero, as transverse electric field is assumed, so the electric field is related to the vector potential as

$$\boldsymbol{E}(\boldsymbol{r},t) = -\partial_t \boldsymbol{A}(\boldsymbol{r},t) \implies \boldsymbol{E}(\boldsymbol{r},\omega) = -i\omega \boldsymbol{A}(\boldsymbol{r},\omega). \tag{2.20}$$

Thus, the response can be written as

$$\delta \boldsymbol{J}_i(\boldsymbol{q},\omega) = \frac{i}{\omega}\chi_{ij}(\boldsymbol{q},\omega)\boldsymbol{E}_j(\boldsymbol{q},\omega). \tag{2.21}$$

The expression (2.21) found using the Kubo formalism may now be compared to Ohm's equation (2.11), where we see that, re-inserting the component indices explicitly,

$$\sigma_{ij}(\boldsymbol{q},\omega) = \frac{i}{\omega}\chi_{ij}(\boldsymbol{q},\omega), \tag{2.22}$$

$$\begin{aligned}\chi_{ij}(\boldsymbol{q},\omega) &= \int \mathrm{d}\boldsymbol{x} \int \mathrm{d}t\; e^{i\omega t - i\boldsymbol{q}\boldsymbol{x}} \chi_{ij}(\boldsymbol{x},t) \\ &= -\frac{i}{\hbar}\int \mathrm{d}\boldsymbol{r} \int \mathrm{d}t\; e^{i\omega t - i\boldsymbol{q}\boldsymbol{x}} \Theta(t) \left\langle [\boldsymbol{J}_i(\boldsymbol{r},t), \boldsymbol{J}_j(0,0)] \right\rangle_0 .\end{aligned} \tag{2.23}$$

It is here important to remember that it was here assumed only transverse current. If that was not the case, there would be an additional contribution to the σ_{ii} components.

2.2. The Luttinger approach to thermal transport

Thermal transport, i.e. response to thermal gradients, is more convoluted than the response to an electromagnetic field, as there is no well-defined Hamiltonian describing the temperature gradient, which of course is a statistical

property of the system. In his now illustrious paper [Lut64] Luttinger seeks to make the theory of transport due to temperature gradients more formal and "mechanical", as he puts it. Inspired by the mechanical derivation of Kubo for the electric transport, he introduces a method where the transport may be derived mechanically from a phenomenological term in the Hamiltonian – the *Luttinger term*. Earlier calculations of the transport properties of temperature gradients were conducted from local variable theories; Luttinger [Lut64] mentions the derivations of Green and Mori, where they respectively had assumed a Markoff process and "local equilibrium distribution". Luttinger's method attempts to put the results of those calculations on a "more solid basis".

We will here simply outline the basic idea of Luttinger, without a rigorous derivation. Introduce to the Hamiltonian a *gravitational* scalar potential field ψ coupling to the energy density, here denoted by the T^{00} component of the energy-momentum tensor,[1] of the (flat) system [Lut64]

$$H_L = \int \mathrm{d}\boldsymbol{r}\psi T^{00}. \tag{2.24}$$

Note that the T^{00} component of the energy-momentum tensor must not be confused with the temperature T. Luttinger showed that the system is in equilibrium, i.e. the thermal and gravitational driving forces balance out, given that the gravitational field is related to the temperature by

$$\nabla\psi + \frac{\nabla T}{T} = 0. \tag{2.25}$$

Borrowing the language of Tatara [Tat15], this is essentially a trick to be able to calculate transport coefficients without introducing temperature gradients in the Hamiltonian. Instead, one introduces the fictitious field ψ, for which the origin is not addressed, and finds the transport coefficients for this system. The situation is depicted in Fig. 2.2, where the temperature field is shown, together with an accompanying gravitational field.

A temperature gradient, together with external electric field $\boldsymbol{E}$ and chemical potential μ, gives a response in the electrical current $\boldsymbol{J}$ and energy current $\boldsymbol{J}_E$ [Mah00]. One commonly defines the transport coefficient tensors L^{ab}, $a, b = 1, 2$ containing the response functions such that

$$J_i = -eL_{ij}^{11}\left[E_j - T\nabla_j\frac{\mu}{T}\right] - eL_{ij}^{12}T\nabla_j\frac{1}{T}, \tag{2.26}$$

$$J_{E,i} = L_{ij}^{21}\left[E_j - T\nabla_j\frac{\mu}{T}\right] + L_{ij}^{22}T\nabla_j\frac{1}{T}, \tag{2.27}$$

[1] Also known as the *stress-energy tensor* and *stress-energy-momentum tensor*.

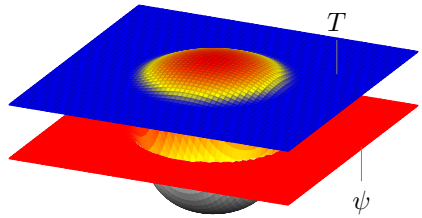

Figure 2.2.: Illustration of Luttinger's solution to heat transport. To include a temperature fluctuation T, couple the system to some (possibly fictious) gravitational potential ψ giving the same current response as the temperature fluctuation.

with the electric charge $e = |e|$. Or, more compactly,

$$\begin{pmatrix} -J_i/e \\ J_{E,i} \end{pmatrix} = \boldsymbol{L}_{ij} \begin{pmatrix} E_j - T\nabla_j \frac{\mu}{T} \\ T\nabla_j \frac{1}{T} \end{pmatrix}. \tag{2.28}$$

Importantly, note that these relations are valid when $\boldsymbol{J}, \boldsymbol{J}_E$ are understood as the *transport* currents, as opposed to the total currents containing also local non-transporting currents. This is discussed more with regard to the results of this thesis in Section 4.1.1. The coefficients of transportation, $\boldsymbol{L}_{ij}$ is a widely used convention, however, several slight variations are used, which at times may cause confusion. In particular, these differences are on which factors of T and μ are included explicitly; the reason for choosing other definitions might be to have more convenient expressions for the Onsager relation, Seebeck coefficient, thermal conductivity tensor, etc. [Che+21; LLF14; Mah00]. The success of Luttinger's method was that the transport coefficients could now be calculated directly, and yielded the same results as had previously been found by less formal approaches.

By the introduction of the Hamiltonian perturbation H_L, the response may now be investigated in the Kubo formalism. By the response in Eq. (2.2) the electric current generated from the gravitational perturbation is

$$\langle \boldsymbol{J}^i \rangle (t, \boldsymbol{r}) = \int \mathrm{d}t' \mathrm{d}\boldsymbol{r}' \left\{ \frac{-i}{\hbar} \Theta(t - t') \left\langle \left[\boldsymbol{J}^i(t, \boldsymbol{r}), T^{00}(t', \boldsymbol{r}') \right] \right\rangle \right\} \psi(t', \boldsymbol{r}'), \tag{2.29}$$

where the integration is taken over the entire spacetime. In order to express this as a response to the thermal gradient, we wish to get the gradient of the gravitational potential. To do this, firstly the 00-element of the energy-momentum tensor will be expressed in terms of derivatives of T^{j0}, and then a partial integration will swap the derivative between the energy-momentum

tensor and gravitational potential. Note first that in the flat system the conservation law of the energy and momentum is simply[2]

$$\partial_t T^{00}(t,\boldsymbol{r}) + v_F \partial_i T^{i0}(t,\boldsymbol{r}) = 0, \tag{2.30}$$

where v_F is the Fermi velocity. By the fundamental theorem of calculus this obviously gives for the zero-zero component of the energy-momentum tensor

$$T^{00}(t,\boldsymbol{r}) = -\int_{-\infty}^{t} \mathrm{d}t' v_F \partial_i T^{i0}(t',\boldsymbol{r}). \tag{2.31}$$

Introduce Eq. (2.31) in the response relation Eq. (2.29), and use integration by parts

$$\int uv' = uv - \int u'v, \tag{2.32}$$

giving

$$\langle \boldsymbol{J}^i \rangle (t,\boldsymbol{r}) = \int_{-\infty}^{t} \mathrm{d}t' \int \mathrm{d}\boldsymbol{r}' \int_{-\infty}^{t'} \mathrm{d}t'' \left\{ \frac{-iv_F}{\hbar} \left\langle \left[\boldsymbol{J}^i(t,\boldsymbol{r}), T^{j0}(t'',\boldsymbol{r}') \right] \right\rangle \right\} \partial'_j \psi(t',\boldsymbol{r}'), \tag{2.33}$$

where we have defined $\partial'_i = \partial/\partial r'_i$. By Luttinger's relation

$$\langle \boldsymbol{J}^i \rangle (t,\boldsymbol{r}) = \int_{-\infty}^{t} \mathrm{d}t' \int \mathrm{d}\boldsymbol{r}' \int_{-\infty}^{t'} \mathrm{d}t'' \left\{ \frac{iv_F}{\hbar} \left\langle \left[\boldsymbol{J}^i(t,\boldsymbol{r}), T^{j0}(t'',\boldsymbol{r}') \right] \right\rangle \right\} \frac{\partial'_j T(t',\boldsymbol{r}')}{T(t',\boldsymbol{r}')}, \tag{2.34}$$

where care must be taken to distinguish the energy-momentum tensor T^{j0} and the temperature T, differentiated by the indices, or lack thereof.

[2] We used the conservation law of the energy-momentum tensor $\partial_\mu T^{\mu\nu} = 0$, and $\partial_0 = \partial_t / v_F$.

3 Anomalies in Quantum Field Theory

"I have an equation; do you have one too?"

(Paul Dirac[1])

From Noether's theorem, described in the following section, we know that any continuous symmetry of the Lagrangian $\mathcal{L}$ in a classical consideration will lead to a conserved current. However, we know from the path integral formulation of QFT that for a system with fields ϕ and an external source J, it is the generating functional

$$Z[J] \equiv \int \mathcal{D}\phi \exp\left[i\left(S[\phi] + \int \mathrm{d}^4x J(x)\phi(x)\right)\right] \tag{3.1}$$

that must be invariant for a transformation to be a symmetry operation of the system. Quantum corrections from the second quantization can lead to the symmetry group of the generating functional to be smaller than the symmetry group of the classical action, in which case we say there is an *anomaly*. In that case, the conserved current predicted by Noether's theorem is no longer protected by symmetry, as the operation is indeed not a symmetry of the system. The terms breaking the classical conservation are called *anomalies*.

It should also be noted that the terminology *anomaly* and *breaks the classical symmetry* are somewhat misleading; there is no actual symmetry breaking – in the quantum theory there is no symmetry to begin with, and a more fitting language to describe the situation is that there is an anomalous symmetry in the classical Lagrangian, which is not there in the "real" theory. Thus, the situation must not be confused with spontaneous symmetry breaking, and there is no Goldstone boson present.

3.1. Noether's theorem

The following section is inspired by the derivation of Kachelriess [Kac18].

Noether's theorem is one of the most central results in theoretical quantum physics. It relates continuous symmetries with conserved quantities, which for example explain fundamental principles such as conservation of momentum and conservation of energy. Given a Lagrangian $\mathcal{L}(\phi_a, \partial_\mu \phi_a)$ dependent on the

[1] As quoted in [Zee10].

fields ϕ_a, we will consider the variations $\delta\phi_a$ that leave the action, and thus equations of motion, invariant. That is, the variations that are generators for some continuous symmetry of the system. Firstly, we will restrict our consideration to the case where the Lagrangian itself is invariant

$$0 = \delta\mathcal{L} = \frac{\delta\mathcal{L}}{\delta\phi_a}\delta\phi_a + \frac{\delta\mathcal{L}}{\delta\partial_\mu\phi_a}\delta\partial_\mu\phi_a. \tag{3.2}$$

In the last term use that the variation and derivation may be exchanged, $[\delta\partial_\mu, \partial_\delta\delta] = 0$, and in the first term use the Lagrange equations

$$\frac{\delta\mathcal{L}}{\delta\phi_a} = \delta_\mu\left(\frac{\delta\mathcal{L}}{\delta\partial_\mu\phi_a}\right). \tag{3.3}$$

By the product rule it follows that

$$0 = \delta\mathcal{L} = \partial_\mu\left(\frac{\delta\mathcal{L}}{\delta\partial_\mu\phi_a}\right)\delta\phi_a + \frac{\delta\mathcal{L}}{\delta\partial_\mu\phi_a}\partial_\mu\delta\phi_a = \partial_\mu\left(\frac{\delta\mathcal{L}}{\delta\partial_\mu\phi_a}\delta\phi_a\right). \tag{3.4}$$

Thus, we see that the quantity in the parenthesis after the last equality must be conserved. We denote this quantity j^μ and call it a *current*.

So far, we have the result that for any variation $\delta\phi_a$ that leave the Lagrangian invariant, there is a conserved current

$$j^\mu = \frac{\delta\mathcal{L}}{\delta\partial_\mu\phi_a}\delta\phi_a, \quad \partial_\mu j^\mu = 0. \tag{3.5}$$

There is, however, an even stronger formulation of Noether's theorem. As the equations of motion are only dependent on the transformation being a symmetry transformation of the action, we realize that even a change in the Lagrangian of the form $\delta\mathcal{L} = \partial_\mu K^\mu$ will not change the equations of motion, as long as boundary terms of the integral over the Lagrangian may be dropped ($K \to 0, r \to \infty$). Thus, altering the starting point in Eq. (3.4) to $0 = \delta\mathcal{L} - \partial_\mu K^\mu$ we get Noether's theorem, theorem 1.

Theorem 1 (Noether's theorem)**.** *For any continuous transformation that leave the Lagrangian $\mathcal{L}$ invariant up to a total derivative $\partial_\mu K^\mu$, there must be an associated conserved current*

$$j^\mu = \frac{\delta\mathcal{L}}{\delta\partial_\mu\phi_a}\delta\phi_a - K^\mu, \quad \partial_\mu j^\mu = 0. \tag{3.6}$$

3.2. The axial/chiral anomaly

We will first give a quick and somewhat superficial introduction to the axial anomaly,[2] and why it matters in condensed matter physics. That discussion will be based on the discussion given in Wehling, Black-Schaffer, and Balatsky [WBB14] and Tong [Ton, Ch. 3]. Then we will present a more thorough derivation of the anomaly, based on the derivation of Zee [Zee10] and Kachelriess [Kac18].

In the massless case, the Dirac equation reduces to two Weyl equations, whose solutions are right- and left-moving fermions. In 1+1 dimensions they have the energy dispersion

$$\epsilon_{\pm} = \pm|p|,$$

where the $\pm$ indicates positive and negative energy solutions. Consider the case now in the Dirac sea picture. The negative energy solutions, antiparticles in high energy physics and holes in condensed matter physics, are all filled, with the energy band going to $\pm\infty$ momentum. The particles with energy $\epsilon = +p$ are right-moving solutions, while $\epsilon = -p$ represent left-moving solutions. Note that in this language, an antiparticle with negative momentum, is right moving, and of course, a particle with positive momentum is right moving. The situation is shown in the left pane of Fig. 3.1. Introduce now an electric field E. This will cause the states to shift, according to $\dot{p} = eE$, with e being the electric coupling, which is here taken to be the fundamental charge; note that this shift does not discriminate against left- and right-movers, they are both shifted the same. For a field $E > 0$ the right-movers are shifted towards higher energies and the left-movers are shifted towards lower energies, shown in the right pane of Fig. 3.1. This also shifts the densities of left- and right-movers! Denote by n_+ the right-movers and n_- the left-movers. The total density $n = n_+ + n_-$ is constant, however, the difference $n_+ - n_-$ is not conserved. Identifying $J = n_+ + n_-$ as the vector current and $J_A = n_+ - n_-$ as the axial current, we see that the vector current is conserved, but the *axial* current is not! Notice how the origin of the anomaly in this context, is the infinite depth of the Dirac sea.

The above argumentation gives an intuitive explanation and interpretation of the anomaly, but it is obviously not rigorous. We here give a purely field theoretical derivation of the axial anomaly. Consider a massless QFT $\mathcal{L} = \bar{\psi} i\gamma^\mu \partial_\mu \psi$, which under the gauge transformation

$$\psi \to e^{i\theta + i\theta\gamma^5}\psi \tag{3.7}$$

[2] Also known as the chiral anomaly.

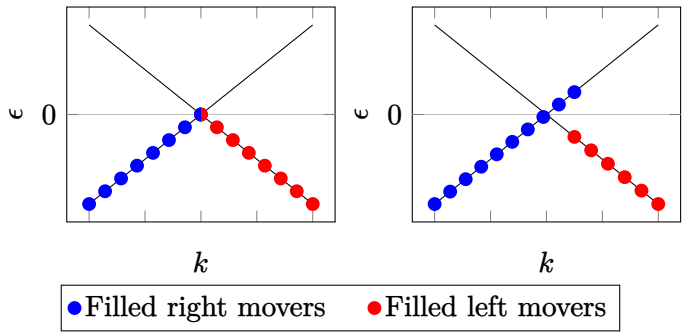

Figure 3.1.: Dispersion of Weyl fermions, black showing unfilled states, blue filled right-movers, and red filled left-movers. **(Left)** No electric field applied, Fermi level at the crossing. **(Right)** Electric field in the positive direction applied, shifting the filled states. See main text for details.

is invariant. It can be shown that the associated conserved Noether currents are the vector current $J^\mu = \bar{\psi}\gamma^\mu\psi$ and the axial current $J_5^\mu = \bar{\psi}\gamma^\mu\gamma^5\psi$ [Zee10]. In the following, we will show that the two currents *cannot* be simultaneously conserved – that is the chiral anomaly. As is often the case, there are many ways to do this. For example, one could show directly that the measure of the path integral is not invariant under a transformation. We will, however, show it in a somewhat crude way, but where there are no complicated formal considerations, only brute force calculation which is hopefully more readily appreciated by those not familiar with the concept. The calculation also has some historical importance, as the problem we will solve is exactly the same as the problem that led to the discovery of anomalies [Adl69; BJ69]![3]

We will calculate the triangle diagram

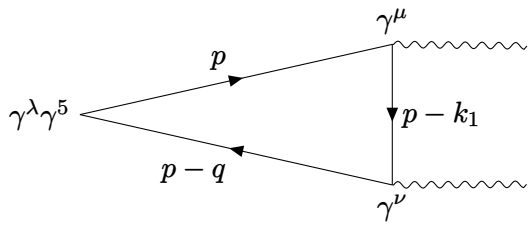

and show that this leads to the conclusion that either the vector current or

[3]The anomaly was discovered independently by Adler [Adl69] and Bell and Jackiw [BJ69] in 1969. See Tong [Ton] for a more in-depth historic commentary.

the axial current is non-conserved. The amplitude of the diagram is

$$\left\langle 0 \left| T J_5^\lambda J^\mu J^\nu \right| 0 \right\rangle, \tag{3.8}$$

with the vector current $J^\mu = \bar{\psi}\gamma^\mu\psi$ and the axial current $J_5^\mu = \bar{\psi}\gamma^\mu\gamma^5\psi$. Written out explicitly in momentum space

$$\begin{aligned}\mathcal{A}^{\lambda\mu\nu}(k_1,k_2) &= (-1)i^3\int\frac{\mathrm{d}^4p}{(2\pi)^4}\\ &\times \mathrm{Tr}\left(\gamma^\lambda\gamma^5\frac{1}{\not{p}-\not{q}}\gamma^\nu\frac{1}{\not{p}-\not{k}_1}\gamma^\mu\frac{1}{\not{p}}+\gamma^\lambda\gamma^5\frac{1}{\not{p}-\not{q}}\gamma^\mu\frac{1}{\not{p}-\not{k}_2}\gamma^\nu\frac{1}{\not{p}}\right),\end{aligned} \tag{3.9}$$

where $q = k_1 + k_2$. For the vector current to be conserved the requirement $k_{1\mu}\mathcal{A}^{\lambda\mu\nu} = k_{2\nu}\Delta^{\lambda\mu\nu} = 0$ must hold. For the axial current to be conserved, the requirement is $q_\lambda\mathcal{A}^{\lambda\mu\nu} = 0$ [Zee10].

One must be careful when carrying out this calculation, as is also stressed in many textbooks dealing with this issue, for example [Kac18] and [Zee10]. Consider the criterion for the vector current to be conserved

$$k_{1\mu}\mathcal{A}^{\lambda\mu\nu}(k_1,k_2) = i\int\frac{\mathrm{d}^4p}{(2\pi)^4}\,\mathrm{Tr}\left(\gamma^\lambda\gamma^5\frac{1}{\not{p}-\not{q}}\gamma^\nu\frac{1}{\not{p}-\not{k}_1}-\gamma^\lambda\gamma^5\frac{1}{\not{p}-\not{k}_2}\gamma^\nu\frac{1}{\not{p}}\right)=0. \tag{3.10}$$

When calculating the integral it might be tempting to simply perform a change of variables, rendering the two terms equal and thus concluding that the criterion is met. However, we must notice that the integrand goes like $1/p^2$ while the boundary surface of a 3-sphere is proportional to p^3. The boundary terms do therefore not vanish, and there is an extra term associated with performing such a change of variables.

Consider that we want to integrate over the function f

$$\int \mathrm{d}^d p f(p). \tag{3.11}$$

If we perform the change of variables $p \to p + a$, one could in theory get an extra contribution from boundary terms, which we will now find. We will calculate

$$\int \mathrm{d}^d p\,[f(p+a) - f(p)], \tag{3.12}$$

where we in the first term has "naively" performed a change of variables, without considering the boundary terms. Thus, the result of this integral is

indeed the boundary terms. Firstly, we will perform a Wick rotation into Euclidean space

$$\int \mathrm{d}_E^d p\,[f(p+a)-f(p)] = \int \mathrm{d}_E^d p\,[a^\mu \partial_\mu f(p) + \dots]\,. \tag{3.13}$$

Ignoring the higher order terms, the RHS may be rewritten as a surface integral by Gauss's theorem. Taking the average over the surface integral, and denoting by $S_d(r)$ the surface of a d-sphere with radius r, we write the integral as

$$\lim_{P\to\infty} a^\mu \left(\frac{P_\mu}{P}\right) f(P) S_{d-1}(P). \tag{3.14}$$

Rotating back to Minkowski space we gain an additional i, with

$$\int \mathrm{d}^d p\,[f(p+a)-f(p)] = \lim_{P\to\infty} i a^\mu \left(\frac{P_\mu}{P}\right) f(P) S_{d-1}(P). \tag{3.15}$$

We will now perform such a shift of variables in the second term of the trace in Eq. (3.10), as we notice that shifting $p \to p - k_1$ makes the two terms cancel, leaving only the boundary term. Let

$$f(p) = \mathrm{Tr}\left(\gamma^\lambda \gamma^5 \frac{1}{\not{p}-\not{k}_2}\gamma^\nu \frac{1}{\not{p}}\right) = \frac{\mathrm{Tr}\left(\gamma^5(\not{p}-\not{k}_2)\gamma^\nu \not{p}\gamma^\lambda\right)}{(p-k_2)^2 p^2} = \frac{4i\epsilon^{\tau\nu\sigma\lambda}k_{2\tau}P_\sigma}{(p-k_2)p^2}. \tag{3.16}$$

Here we used in the first equality the property $1/\not{a} = \not{a}/a^2$ twice, and the cyclic permutation invariance of the trace, $\mathrm{Tr}(ABC) = \mathrm{Tr}(BCA)$. In the second equality, we first wrote the Feynman slash operator by its definition $\not{a} = \gamma^\mu a_\mu$, and then used the property

$$\mathrm{Tr}(\gamma^5\gamma^\tau\gamma^\nu\gamma^\sigma g^\lambda) = -4i\epsilon^{\tau\nu\sigma\lambda}, \tag{3.17}$$

where ϵ is the totally antisymmetric tensor. The trace can be split into two terms, where the first vanishes as it is proportional to $\epsilon^{\tau\nu\sigma\lambda}p_\tau p_\sigma$, and one is left with the expression in Eq. (3.16). Thus, Eq. (3.10) becomes

$$k_{1\mu}\mathcal{A}^{\lambda\mu\nu} = \frac{i}{(2\pi)^4}\lim_{P\to\infty} i(-k_1)^\mu \frac{P_\mu}{P}\frac{4i\epsilon^{\tau\nu\sigma\lambda}k_{2\tau}P_\sigma}{P^4}2\pi^2 P^3 = \frac{i}{8\pi^2}\epsilon^{\lambda\nu\tau\sigma}k_{1\tau}k_{2\sigma}. \tag{3.18}$$

Consider now, however, what happens if we shift $p \to p + k_2$ in the first term of Eq. (3.10) instead. Surely, if our answer above is correct, any arbitrary

shift must yield the same answer. Similarly to before, let

$$\begin{aligned} f(p) &= \operatorname{Tr}\left(\gamma^\lambda\gamma^5\frac{1}{\not{p}-\not{q}}\gamma^\nu\frac{1}{\not{p}-\not{k}_1}\right) = \frac{\operatorname{Tr}\left(\gamma^5(\not{p}-\not{q})\gamma^\nu(\not{p}-\not{k}_1)\gamma^\lambda\right)}{(p-q)^2(p-k_1)^2} \\ &= \frac{-4i\epsilon^{\tau\nu\sigma\lambda}k_{2\tau}(k_{1\sigma}-p_\sigma)}{(p-q)^2(p-k_1)^2}, \end{aligned} \tag{3.19}$$

where we as above removed all terms symmetric under $\sigma \leftrightarrow \tau$. Now, Eq. (3.10) becomes

$$k_{1\mu}\mathcal{A}^{\lambda\mu\nu} = \frac{i}{(2\pi)^4}\lim_{P\to\infty} ik_2^\mu\frac{P_\mu}{P}\frac{-4i\epsilon^{\tau\nu\sigma\lambda}k_{2\tau}(k_{1\sigma}-p_\sigma)}{P^4}2\pi^2P^3 = \frac{i\epsilon^{\lambda\nu\tau\sigma}}{8\pi^2}k_{2\tau}k_{2\sigma}. \tag{3.20}$$

Where we used that the only term contributing is the p_σ, as the term with $k_{1\sigma}$ goes like P^{-1}. Our results differ depending on the non-physical shift of variables! As is shown by several textbooks, see [Kac18; Zee10], this comes from the fact that the integral we started with is in fact linearly divergent – its value is not well-defined. What we will have to do, is consider an arbitrary shift a in the integration variable of the amplitude Eq. (3.9), which we will show changes the amplitude by a quantity dependent on a. To cancel this, a counter term must be inserted; however, as we will see, this counter term can only make either the axial current or the vector current conserved! Consider now a shift in the integration variable $p \to p - a$ in the amplitude Eq. (3.9), where we denote the amplitude with shifted integration variable

$$\begin{aligned} &\mathcal{A}^{\lambda\mu\nu}(a,k_1,k_2) \\ &\quad= (-1)i^3\int\frac{\mathrm{d}^4p}{(2\pi)^4}\operatorname{Tr}\left(\gamma^\lambda\gamma^5\frac{1}{\not{p}-\not{a}-\not{q}}\gamma^\nu\frac{1}{\not{p}-\not{a}-\not{k}_1}\gamma^\mu\frac{1}{\not{p}-\not{a}}\right. \\ &\qquad\qquad\left. + \gamma^\lambda\gamma^5\frac{1}{\not{p}-\not{a}-\not{q}}\gamma^\mu\frac{1}{\not{p}-\not{a}-\not{k}_2}\gamma^\nu\frac{1}{\not{p}-\not{a}}\right). \end{aligned} \tag{3.21}$$

From Eq. (3.15) we already have a formula for the difference

$$\mathcal{A}^{\lambda\mu\nu}(a,k_1,k_2) - \mathcal{A}^{\lambda\mu\nu}(k_1,k_2), \tag{3.22}$$

by choosing

$$f(p) = \frac{i}{(2\pi)^4}\operatorname{Tr}\left(\gamma^\lambda\gamma^5\frac{1}{\not{p}-\not{q}}\gamma^\nu\frac{1}{\not{p}-\not{k}_1}\gamma^\mu\frac{1}{\not{p}}\right).$$

Ignore for now the prefactor, and note that in the limit

$$\begin{aligned}\lim_{p\to\infty} f(p) &= \frac{\mathrm{Tr}(\gamma^\lambda\gamma^5 \not{p}\gamma^\nu \not{p}\gamma^\mu \not{p})}{p^6} \\ &= \frac{2\,\mathrm{Tr}(\gamma^\lambda\gamma^5 \not{p}\gamma^\nu \not{p}) - p^2\,\mathrm{Tr}(\gamma^\lambda\gamma^5 \not{p}\gamma^\nu\gamma^\mu)}{p^6} \\ &= \frac{4ip_\sigma\epsilon^{\sigma\nu\mu\lambda}}{p^4}.\end{aligned} \tag{3.23}$$

In the second equality we used the anti-commutation relation of gamma matrices in $\not{p}\gamma^\mu = 2p^\mu - \gamma^\mu\not{p}$ and $\not{a}^2 = a^2$. In the last equality, we used again Eq. (3.17), and the vanishing of all terms symmetric under interchanging indices when contracted with the fully antisymmetric tensor. We now find the amplitude difference (3.22). Firstly, we simplify the expression slightly as

$$\Delta\mathcal{A}^{\lambda\mu\nu}(a,k_1,k_2) \equiv \int \mathrm{d}^4p f(p-a) - f(p) + \{(k_1,\mu)\leftrightarrow(k_2,\nu)\}, \tag{3.24}$$

where the last term indicates to repeat the preceding expression with interchange of $k_1 \leftrightarrow k_2$ and $\mu\leftrightarrow\nu$. Thus, by Eq. (3.15),

$$\begin{aligned}\Delta\mathcal{A}^{\lambda\mu\nu}(a,k_1,k_2) &= \lim_{p\to\infty} ia^\mu\left(\frac{p_\mu}{p}\right)\frac{i}{(2\pi)^4}\frac{4ip_\sigma\epsilon^{\sigma\nu\mu\lambda}}{p^4}2\pi^2p^3 \\ &\quad + \{(k_1,\mu)\leftrightarrow(k_2,\nu)\} \\ &= \lim_{p\to\infty}\frac{-ia^\mu}{2\pi^2}\frac{p_\mu p_\sigma}{p^2}\epsilon^{\sigma\nu\mu\lambda} + \{(k_1,\mu)\leftrightarrow(k_2,\nu)\} \\ &= -\frac{ia_\sigma}{8\pi^2}\epsilon^{\sigma\nu\mu\lambda} + \{(k_1,\mu)\leftrightarrow(k_2,\nu)\}.\end{aligned} \tag{3.25}$$

Now is the time to take a break from the calculations and consider in some detail what this result means, before we will finally carry out the derivation to its end and show the anomaly. A priori $\mathcal{A}^{\lambda\mu\nu}(a,k_1,k_2)$ should be just as valid as $\mathcal{A}^{\lambda\mu\nu}(k_1,k_2)$, i.e. setting $a=0$. In fact, that formulation is quite the misnomer, as $a=0$ is no less arbitrary than any $a\neq 0$ in this setting; p is simply a name by which we denote the moment transfer in our diagram. *However*, using Eq. (3.25), leading to

$$\begin{aligned}&k_{1\mu}\mathcal{A}^{\lambda\mu\nu}(a,k_1,k_2) - k_{1\mu}\mathcal{A}^{\lambda\mu\nu}(a=0,k_1,k_2) \\ &\quad = -\frac{i}{8\pi^2}\left[\epsilon^{\sigma\nu\mu\lambda}a_\sigma + \{(k_1,\mu)\leftrightarrow(k_2,\nu)\}\right]k_{1\mu},\end{aligned} \tag{3.26}$$

we see that the criterion for vector current conservation, Eq. (3.10), may or may not be met depending on our choice of a! Owning to a trick from Zee

[Zee10], we will show that the resolve of this is to chose one particular a, and the choice will be that a which preserves the consistency of our theory. Now, this may indeed seem both strange and ad-hoc, how can we justify *choosing* some parameter to get the result we want? This is, in fact, common in QFT. Recall that both the UV-cutoff and dimensional regularization schemes introduce a parameter, which must be determined "outside" of our theory.

Let $a = \alpha(k_1 + k_2) + \beta(k_1 - k_2)$. This is allowed as k_1, k_2 are independent, and the only parameters of our equations. The α term is obviously symmetric under interchange of k_1, k_2, while the β term is antisymmetric. Thus, we see that in Eq. (3.26) only the β part survives when adding the pair with interchanged indices and momenta. Thus,

$$\begin{aligned} k_{1\mu}\mathcal{A}^{\lambda\mu\nu}(a, k_1, k_2) &= -\frac{i}{4\pi^2}\epsilon^{\sigma\nu\mu\lambda}\beta(k_{1\sigma} - k_{2\sigma})k_{1\mu} + k_{1\mu}\mathcal{A}^{\lambda\mu\nu}(k_1, k_2) \\ &= \frac{i}{8\pi^2}\left(\epsilon^{\lambda\nu\tau\sigma}k_{1\tau}k_{2\sigma} - 2\epsilon^{\sigma\nu\mu\lambda}\beta(k_{1\sigma} - k_{2\sigma})k_{1\mu}\right) \\ &= \frac{i}{8\pi^2}\epsilon^{\lambda\nu\tau\sigma}k_{1\tau}k_{2\sigma}(1 + 2\beta). \end{aligned} \tag{3.27}$$

Here we inserted our previous result for $k_{1\mu}\mathcal{A}^{\lambda\mu\nu}$ given in Eq. (3.18). In the last equality, we used that $k_{1\sigma}k_{1\mu}$ vanishes when contracted with the Levi Cevita symbol, and relabeled the dummy indices. It is now apparent that choosing $\beta = -1/2$ makes the criterion for conservation of vector current hold!

By choosing the shift appropriately, the vector current is preserved. However, it does come at a price. The requirement for the axial current to be conserved, as mentioned earlier, is

$$q_\lambda \mathcal{A}^{\lambda\mu\nu} = 0.$$

This amplitude is in fact also set by the parameter β, as also here α drops out; we have no free parameter to tune after fixing β. With the choice $\beta = -1/2$, required to conserve the vector current, the axial current will not be conserved! This is the chiral anomaly.

We could have, of course, instead chosen β such that the axial current is conserved, at the expense of the conservation of the vector current. However, as Zee [Zee10] describes, this would have catastrophic consequences, rendering the entire theory useless. A non-conserved vector current would make the fermion number not conserved, clearly non-acceptable. We therefore chose to sacrifice the axial current instead of the vector current.

3.3. The conformal/scale anomaly

Consider massless QED (quantum electrodynamics)

$$\mathcal{L} = -\frac{1}{4}F^{\mu\nu}F_{\mu\nu} + i\bar{\psi}\not{D}\psi, \tag{3.28}$$

with ψ the Dirac field, $\bar{\psi} = \psi^\dagger\gamma^0$, $\not{D} = \gamma^\mu D_\mu$, D the covariant derivative $D_\mu = \partial_\mu - ieA_\mu$, γ^μ the Dirac matrices. A_μ is the electromagnetic potential, $F_{\mu\nu} = \partial_\mu A_\nu - \partial_\nu A_\mu$ the electromagnetic field, and e is the coupling, here the fundamental charge. The theory is classically scale-invariant. That is, under the transformation

$$x \to \lambda^{-1}x, \quad A_\mu \to \lambda A_\mu, \quad \psi \to \lambda^{\frac{3}{2}}\psi, \tag{3.29}$$

the Lagrangian transforms as

$$\mathcal{L} \to \lambda^4\mathcal{L}, \tag{3.30}$$

which is canceled by the transformation of measure $\mathrm{d}^4x \to \mathrm{d}^4x\lambda^{-4}$ in the action. As the action is invariant, thus so are the equations of motion.

By Noether's theorem, there must be some conserved current corresponding to this symmetry transformation, which we will now show is the dilation current $j^\mu_D = T^{\mu\nu}x_\nu$, where $T^{\mu\nu}$ is the energy-momentum tensor. Consider a conformal transformation of the type $g_{\mu\nu} = e^{2\tau}\eta_{\mu\nu}$, also known as a Weyl transformation of the metric. The variation of the metric is obviously $\delta g_{\mu\nu} = 2\tau\eta_{\mu\nu}$. Recall also that the energy-momentum tensor is defined as the response of the action to a variation of the metric[4]

$$T_{\mu\nu} = \frac{2}{\sqrt{|g|}}\frac{\delta S}{\delta g^{\mu\nu}}, \tag{3.31}$$

where g is the determinant of the metric. Now, using this we see that

$$\begin{aligned}
\delta S &= \int \mathrm{d}^4x \frac{\delta S}{\delta g^{\mu\nu}}\delta g^{\mu\nu} \\
&= \int \mathrm{d}^4x \frac{\sqrt{|g|}}{2}T_{\mu\nu}\delta g^{\mu\nu} \\
&= \int \mathrm{d}^4x T_{\mu\nu}\sqrt{|g|}\tau(x)\eta^{\mu\nu}(x) \\
&= \int \mathrm{d}^4x \sqrt{|g|}\tau(x)T^\mu_\mu.
\end{aligned} \tag{3.32}$$

[4]This defines the *dynamical* energy-momentum tensor. See Section 4.1.2 for more details.

As the scaling is a symmetry operation, Eq. (3.32) must be zero. As the scaling factor τ is an arbitrary function, we conclude that the trace T^{μ}_{μ} must vanish. The vanishing trace ensures the conservation of the dilation current as

$$\begin{aligned} \partial_\mu J^\mu_D &= T^{\mu\nu}\partial_\mu x_\nu + (\overbrace{\partial_\mu T^{\mu\nu}}^{0})x_\nu \\ &= T^{\mu\nu}\delta_{\mu\nu} = T^\mu_\mu, \end{aligned} \tag{3.33}$$

where we used the property of the energy-momentum tensor that $\partial_\mu T^{\mu\nu} = 0$. As the trace is zero, the dilation current is conserved in the classical picture.

However, this symmetry does not hold when quantum corrections are taken into account. Loop effects give non-vanishing contributions to the trace, and by Eq. (3.33) this makes the dilation current non-conserved. Due to this, the conformal anomaly is also often referred to as the trace anomaly. Recall that when calculating the propagators of the QED theory, we end up with infinities. These, we regularize and renormalize, for example with dimensional regularization or UV-cutoff. In any case, this introduces some dimensionful scale, μ, the renormalization scale and the cutoff energy respectively for the regulators mentioned. This scale dependence is encoded in the beta function of the theory, encoding the dependence of the coupling e on the scale,

$$\beta(e) = \frac{\partial e}{\partial \log \mu}; \tag{3.34}$$

if the beta function does not vanish, our theory now has a scale dependence, rendering our theory no longer scale-invariant!

When taking into account the loop effects, the trace of the energy-momentum tensor is [Kac18]

$$T^\mu_\mu = \frac{\beta(e)}{2e} F_{\mu\nu}F^{\mu\nu}, \tag{3.35}$$

where $\beta(e)$ is the beta function of the theory. This beta function makes the anomaly not exact in one loop, as opposed to the axial anomaly. In one loop, the massless fermion beta function is [Che16]

$$\beta^{(1)} = \frac{e^3}{12\pi^2}. \tag{3.36}$$

Thermoelectric Effect from the Conformal Anomaly

4

In 2016 Chernodub [Che16] showed that the conformal anomaly of QED leads to electrical currents in an inhomogeneous gravitational background. This effect was further explored by Chernodub, Cortijo, and Vozmediano [CCV18], showing through Luttinger's method that such an anomalous transport could be generated from a temperature gradient, giving additional contributions to the Nernst current. The same effect was shortly after derived more formally through the Kubo formalism, by Arjona, Chernodub, and Vozmediano [ACV19].

In this chapter, we extend the Kubo calculation to tilted Weyl cones. Firstly, the result for the untilted system is rederived, where we also show several simplifications compared to previous computations. The results for the untilted cone are then generalized to tilted cones. The computation is quite lengthy, and the thesis is explicit in each step, with the goal being that a graduate-level student should be able to comfortably follow the calculations.

The chapter is divided into sections, each representing a somewhat contained part of the calculation. The text is not, however, written such that a reader should expect to understand a section without reading the preceding one. Due to the nature of the work, certain sections are rather technical. For the benefit of the reader, we have included summaries of intermediate results, enabling the reader to skip the more technical parts. In particular, the latter part of Section 4.2.2 and Section 4.5.1 may be skipped without much loss.

We will find the current response of a single Weyl cone, with a temperature gradient $\nabla_y T$ and a magnetic field B_z. The current response of interest in the given geometry is thus in the x-direction,

$$J^x = \chi^{xy}\left(\frac{-\nabla_y T}{T}\right), \tag{4.1}$$

with χ^{xy} being the response function.[1] This geometry is shown in Fig. 4.1. For the untilted case, the first calculation by Chernodub, Cortijo, and Vozmediano [CCV18] used direct application of the scale magnetic effect [Che16] to thermally perturbed condensed matter systems using the Luttinger formalism,

[1] The sign in Eq. (4.1) may differ in the literature due to different sign conventions, as noted in [ACV19]. We follow that of [ACV19], differing from [CCV18].

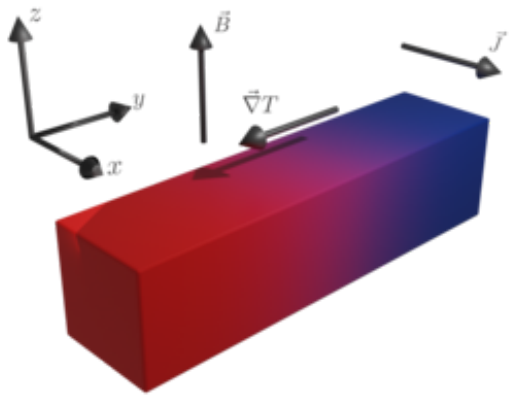

Figure 4.1.: Sketch of the geometry used in the derivation. Note that we consider only bulk response, and the finite sample is only for illustration purposes.

where the response function

$$\chi^{xy} = \frac{e^2 v_F B}{18\pi^2 \hbar} \tag{4.2}$$

was found. Later, Arjona, Chernodub, and Vozmediano [ACV19] found

$$\chi^{xy} = \frac{e^2 v_F B}{4\pi^2 \hbar}. \tag{4.3}$$

The results differ only by numerical prefactors, with the dependence on parameters of the system otherwise equal. As we will show, the response function for the tilted system differs from the untilted case only by a numerical prefactor as well, dependent on the tilt.

The tilt $\boldsymbol{t}$ may in general take any direction. We separate between tilt perpendicular to and parallel to the magnetic field, as the two cases give qualitatively different behavior of the Landau levels. The perpendicular component is, in the given geometry, thus in the xy-plane. In this work, we have restricted the perpendicular component to be parallel[2] to the charge current. The first part of the calculation, however, is general for any tilt, and the specialization to $\boldsymbol{t}_\perp = t_\perp \hat{x}$ is first made in Section 4.5.

[2]Parallel is here taken to mean "proportional to", i.e. either parallel or antiparallel.

Recall the linear response from the Kubo formalism in Eq. (2.34), found through Luttinger's approach.

$$\langle J^i \rangle (t, \boldsymbol{r}) = \underbrace{\int_{-\infty}^{t} \mathrm{d}t' \int \mathrm{d}\boldsymbol{r}' \int_{-\infty}^{t'} \mathrm{d}t'' \left\{ \frac{-iv_F}{\hbar} \left\langle [J^i(t, \boldsymbol{r}), T^{j0}(t'', \boldsymbol{r}')] \right\rangle \right\}}_{\chi^{ij}} \left(\frac{-\partial'_j T(t', \boldsymbol{r}')}{T} \right), \tag{4.4}$$

where, as before, $\partial'_j = \partial / \partial r'_j$. Fourier transforming to the frequency and momentum domain will be beneficial in our calculations. The non-perturbed system will be taken to be time and position invariant, such that the correlator in Eq. (4.4) can be taken to depend only on the differences $t - t''$ and $\boldsymbol{r} - \boldsymbol{r}'$. Starting with Fourier transforming the position part, notice that the structure of Eq. (4.4) is

$$\langle J^i \rangle (\boldsymbol{r}) = \int \mathrm{d}\boldsymbol{r}' \chi(\boldsymbol{r} - \boldsymbol{r}') \left(-\frac{\partial'_j T(\boldsymbol{r}')}{T} \right),$$

where the temporal parts were dropped for clarity. This is a convolution, and the Fourier transform is thus simply given by the product of the two factors [Rot95].

$$\langle J^i \rangle (\boldsymbol{q}) = -\chi(\boldsymbol{q})(iq_j) T(\boldsymbol{q}) / T, \tag{4.5}$$

where it was also used that the Fourier transform of a derivative gives the component of the variable. Showing explicitly how to find the form of the response χ in momentum space is often overlooked in much literature, and as it does involve some finesse, we want to show it here. This trick is courtesy of Chang [Cha18]. By definition, the Fourier transform of the response is, where the variable of integration has been chosen to be $\boldsymbol{r} - \boldsymbol{r}'$ for later convenience,

$$\chi(\boldsymbol{q}) = \int \mathrm{d}(\boldsymbol{r} - \boldsymbol{r}') e^{-i\boldsymbol{q}(\boldsymbol{r} - \boldsymbol{r}')} \chi(\boldsymbol{r} - \boldsymbol{r}') \tag{4.6}$$

$$= \int \mathrm{d}(\boldsymbol{r} - \boldsymbol{r}') e^{-i\boldsymbol{q}(\boldsymbol{r} - \boldsymbol{r}')} C \left\langle \left[J^i(\boldsymbol{r}), T^{j0}(\boldsymbol{r}') \right] \right\rangle, \tag{4.7}$$

$$\tag{4.8}$$

where C denotes t-dependent prefactors and integrals over time are omitted, again for clarity of notation. Note that

$$\int \mathrm{d}(\boldsymbol{r} - \boldsymbol{r}') = \frac{1}{\mathcal{V}} \int \mathrm{d}\boldsymbol{r} \mathrm{d}\boldsymbol{r}', \tag{4.9}$$

where $\mathcal{V}$ is the volume of the system. Thus,

$$\begin{aligned}\chi(\boldsymbol{q}) &= \frac{1}{\mathcal{V}}\int \mathrm{d}\boldsymbol{r}\mathrm{d}\boldsymbol{r}' e^{-i\boldsymbol{q}(\boldsymbol{r}-\boldsymbol{r}')} C\left\langle\left[J^i(\boldsymbol{r}), T^{j0}(\boldsymbol{r}')\right]\right\rangle \\ &= \frac{C}{\mathcal{V}}\left\langle\left[J^i(\boldsymbol{q}), T^{j0}(-\boldsymbol{q})\right]\right\rangle.\end{aligned} \tag{4.10}$$

Considering now the temporal part, the procedure is simpler. The linear response still has the form of a convolution, as the response function is only dependent on the difference $t-t'$ by

$$\chi(t-t') = \int_{-\infty}^{0} \mathrm{d}t''\Theta(t-t')\left\langle\left[J^i(t-t'), T^{j0}(t'')\right]\right\rangle, \tag{4.11}$$

where t'' was shifted by t', and then the translational invariance of the correlator was used. In frequency space

$$\chi(\omega) = \int \mathrm{d}t e^{i\omega t}\chi(t) \tag{4.12}$$

$$= \int \mathrm{d}t e^{i\omega t}\int_{-\infty}^{0} \mathrm{d}t''\Theta(t)\left\langle\left[J^i(t), T^{j0}(t'')\right]\right\rangle. \tag{4.13}$$

In frequency and momentum space the response function is thus

$$\chi^{ij}(w,\boldsymbol{q}) = \frac{-iv_F}{\mathcal{V}\hbar}\int \mathrm{d}t e^{i\omega t}\int_{-\infty}^{0} \mathrm{d}t'\Theta(t)\left\langle\left[J^i(t,\boldsymbol{q}), T^{j0}(t',-\boldsymbol{q})\right]\right\rangle. \tag{4.14}$$

4.1. General remarks

Before beginning the computation, we here briefly mention some complications and considerations important to our result. Firstly we discuss how the charge current from a Kubo calculation relates to experimentally measurable currents. Secondly, we discuss the ambiguity related to the energy-momentum tensor.

4.1.1. Transport and magnetization

Recall from Eq. (2.26) that we generally define the transport coefficients

$$J^i = -eL_{ij}^{11}\left[E_j - T\nabla_j\frac{\mu}{T}\right] - eL_{ij}^{12}T\nabla_j\frac{1}{T},$$

where J^i is the electrical current. In our work, we focus on the L^{12} coefficient, however, the following discussion is valid also more generally. The definition of transport currents becomes more subtle in systems with broken time-reversal symmetry [Che+21; vdWS19]. In such systems, unobservable, circulating *magnetization* currents arise. These currents do not contribute to transport, but the Kubo treatment derives the local current, which in general also includes non-transporting currents. Let

$$\boldsymbol{J} = \boldsymbol{J}_{\mathrm{tr}} + \boldsymbol{J}_M, \tag{4.15}$$

where $\boldsymbol{J}$ is the total local current, $\boldsymbol{J}_{\mathrm{tr}}$ is the transport current, and $\boldsymbol{J}_M$ is the circulating magnetization current. The Kubo formalism generally gives the response to the total local current, χ; we are more interested in the experimentally measurable transport response L_{ij}^{12}, related to our Kubo result as [Che+21]

$$L_{ij}^{12} = -\chi_{ij}/e + \epsilon^{ijl} M_l, \tag{4.16}$$

with M_l the magnetization. For zero chemical potential, however, these magnetization currents have been shown to go to zero as $T \to 0$ [vdWS19]. The result from the Kubo calculation is therefore the actual transport current.

4.1.2. Comment on the energy-momentum tensor

There is some ambiguity regarding the definition of the energy-momentum tensor [Che+21; FR04; Kac18; vdWS19]. The *canonical* energy-momentum tensor, derived from the Lagrangian formalism, is defined as

$$T^{\mu\nu} = \frac{\partial \mathcal{L}}{\partial \partial_\mu \psi_i} \partial^\nu \psi_i - \eta^{\mu\nu} \mathcal{L}. \tag{4.17}$$

On the other hand, from general relativity, the *dynamical* energy-momentum tensor is defined by the variation of the (matter) action with respect to the metric [Kac18]

$$T^{\mu\nu}_{\mathrm{dyn}} = \frac{2}{\sqrt{g}} \frac{\delta S}{\delta g_{\mu\nu}}. \tag{4.18}$$

Immediately, we see that the first definition is in general not symmetric, while the latter is, as the metric is always symmetric.[3] As the energy-momentum tensor is an observable, this presents a problem: how should the tensor be defined? This issue is not trivial and has puzzled physicists for decades [FR04].

[3] In a torsionless manifold. For manifolds with torsion, the definitions are still generally different.

Superficially, we make the following observations. The *defining* property of the energy-momentum tensor is its conservation law

$$\partial_\mu T^{\mu\nu} = 0, \tag{4.19}$$

on a flat manifold. This, of course, only defines the tensor up to a total divergence. Denote by $T^{\mu\nu}$ the *canonical* energy-momentum tensor. We can then define another tensor

$$\hat{T}^{\mu\nu} = T^{\mu\nu} + \partial_\alpha S^{\alpha\mu\nu}. \tag{4.20}$$

By letting $S^{\alpha\mu\nu}$ be antisymmetric in α and μ, the last term of Eq. (4.20) is divergence free. This is easily shown as

$$\begin{aligned} \partial_\mu\partial_\alpha S^{\alpha\mu\nu} &= -\partial_\mu\partial_\alpha S^{\mu\alpha\nu} \\ &= -\partial_\alpha\partial_\mu S^{\mu\alpha\nu} \\ &= -\partial_\mu\partial_\alpha S^{\alpha\mu\nu}, \end{aligned} \tag{4.21}$$

where we used the commutation of partial derivatives and relabelling of the dummy indices μ, α. By an appropriate choice of $S^{\alpha\mu\nu}$ the canonical energy-momentum tensor may be symmetrized, importantly while still abiding by the conservation law. The correction that symmetrizes the energy-momentum tensor is known as the "Belinfante tensor", which for the Dirac Lagrangian is [Che+21]

$$S^{\alpha\mu\nu} = \frac{1}{8}\bar{\Psi}\left[\gamma^\alpha, \sigma^{\mu\nu}\right]\Psi, \tag{4.22}$$

which gives

$$\hat{T}^{\mu\nu} = T^{\mu\nu}_{\text{dyn}} = \frac{1}{4}\bar{\Psi}(\gamma^\mu D^\nu + \gamma^\nu D^\mu)\Psi. \tag{4.23}$$

Which, in the case of the Dirac Lagrangian, so happens to correspond to the naive symmetrization

$$T^{\mu\nu}_s = \frac{T^{\mu\nu} + T^{\nu\mu}}{2}. \tag{4.24}$$

It is also instructive for our work to consider a more naive line of reasoning. The energy-momentum tensor is used in this work through its conservation law Eq. (4.19), whose first component gives the conservation of energy. Writing it out explicitly

$$\partial_0 T^{00} + \partial_i T^{i0} = \partial_0 \epsilon + \partial_i j^i_\epsilon = 0, \tag{4.25}$$

with ϵ the energy density and j_ϵ the energy density current, the question is really seen to be finding the energy density current, ignoring all formal

arguments about the energy-momentum tensor in a general context. Using such a line of reasoning van der Wurff and Stoof [vdWS19] argued that the appropriate form of the energy-momentum tensor that should be used in linear response calculations of Dirac material systems is the unsymmetrized canonical tensor. In this work, we will therefore use the canonical energy-momentum tensor, as opposed to the symmetric form used in the linear response calculation of an untilted cone done by Arjona, Chernodub, and Vozmediano [ACV19]. In the untilted case, even though the two definitions are generally different, they give the same contribution, while for a tilted cone, the response from the two definitions differs.

We here show explicitly how the response differs for the two choices of the energy-momentum tensor. The discussion relies on results found later in the text, however, we find it instructive to include the discussion already here. For an untilted system, the components of interest of the canonical energy-momentum tensor reads

$$T^{y0} = \frac{si}{4}\left[\phi^\dagger \sigma_y \partial_0 \phi - \partial_0 \phi^\dagger \sigma_y \phi\right], \tag{4.26a}$$

$$T^{0y} = \frac{v_F}{4}\left[\phi^\dagger p_y \phi - p_y \phi^\dagger \phi\right], \tag{4.26b}$$

where $\phi, \phi^\dagger$ are the fields. The symmetrized energy-momentum tensor used by Arjona, Chernodub, and Vozmediano [ACV19]

$$T_s^{y0} = \frac{T^{y0} + T^{0y}}{2}. \tag{4.27}$$

Using this, the response was found to be

$$\chi = [\dots] \sum_{\substack{m,n \\ N=M-1}} \int \mathrm{d}\kappa_z (F^{(1)} + F^{(2)}) \alpha^2_{\kappa_z m s}, \tag{4.28}$$

with $[\dots]$ prefactors not relevant here, and $F^{(i)}$, $i = 1, 2$ the contribution from T^{y0} and T^{y0}, respectively. They are

$$F^{(1)} = \epsilon_{\kappa_z m s} + \epsilon_{\kappa_z n s}, \tag{4.29}$$

$$F^{(2)} = s\alpha_{\kappa_z n s}\sqrt{M-1} + \frac{s\sqrt{M}}{\alpha_{\kappa_z m s}}, \tag{4.30}$$

where $\epsilon_{\kappa_z m s}$ and κ_z are dimensionless energy and momentum, and

$$\alpha_{k_z m s} = -\frac{s\sqrt{M}}{\epsilon_m - s\kappa_z}$$

is a normalization factor of the eigenstate. Using the explicit form of the energy

$$\epsilon_m = \text{sign}(m)\sqrt{M + \kappa_z^2},$$

it is not difficult to show that

$$F^{(2)} = \epsilon_{\kappa_z ms} + \epsilon_{\kappa_z ns} = F^{(1)}. \tag{4.31}$$

A tilt vector parallel to the magnetic field $\boldsymbol{t} \parallel \boldsymbol{B}$ does not alter the eigenstates, it only changes the eigenvalues by a factor $tv_F k_z$ [TCG16; YYY16], as we will show later. The results from the untilted case may thus be applied directly, with rescaled energies. As the normalization factor $\alpha_{\kappa_z ms}$ is invariant under the tilt, $F^{(2)}$ does not change. However, $F^{(1)}$ changes to

$$F^{(1)} = \epsilon_{\kappa_z ms} + \epsilon_{\kappa_z ns} = \epsilon^0_{\kappa_z ms} + \epsilon^0_{\kappa_z ns} + 2\kappa_z t, \tag{4.32}$$

where $\epsilon^0_{\kappa_z ms}$ are the energy levels of the untilted system. The last term in Eq. (4.32) gives a non-zero contribution to the total response, and so the results for a tilted cone is generally dependent on the choice of the energy-momentum tensor.

As mentioned, we have used the non-symmetric canonical energy-momentum tensor. The calculation presented in the thesis has for completeness been carried out for the symmetric energy-momentum tensor as well. The result is presented in Appendix B.

4.2. Eigenvalue problem of the Landau levels of a Weyl Hamiltonian

To evaluate the correlator of the response function, the matrix elements of the current and energy-momentum tensor must be found. In order to do this, we find eigenstates in the Landau basis of the system. We will first consider the untilted Hamiltonian, which we will then use to find the Landau levels of the tilted Hamiltonian.

4.2.1. The untilted Hamiltonian

Couple the Weyl Hamiltonian to the magnetic field through minimal coupling

$$H_s = sv_F\sigma^i \left(p_i + eA_i\right), \tag{4.33}$$

with s being the chirality, p_i the momentum operator, and $e = |e|$ the coupling constant to the electromagnetic field $\boldsymbol{A}$. Choose coordinates such that

$\boldsymbol{B} = B_z\hat{\boldsymbol{z}}$, which in the Landau gauge gives $\boldsymbol{A} = -B_z y\,\hat{\boldsymbol{x}}$. As the Hamiltonian is invariant in x and z, take the plane wave ansatz $\phi(\boldsymbol{r}) = e^{ik_x x + ik_z z}\phi(y)$. It then follows

$$H_s\phi(\boldsymbol{r}) = E\phi(\boldsymbol{r}) \implies \tilde{H}_s\phi(y) = E\phi(y), \tag{4.34}$$

where $\tilde{H}$ is the result of replacing $p_z \to k_z, p_x \to k_x$ in H_s, as the plane wave part of ϕ have these eigenvalues. Absorb the chirality s as a sign in the velocity v_F, for more concise notation. Thus, writing everything explicitly, the spectrum is given by

$$-v_F\begin{pmatrix} -k_z & \partial_y + eyB_z/ - k_x \\ -\partial_y + eyB_z/ - k_x & k_z \end{pmatrix}\phi(y) = E\phi(y). \tag{4.35}$$

We will now find the spectrum E of the Hamiltonian.

Inspired by the derivation for the spectrum of the 2D Dirac Hamiltonian in [WBB14], we introduce the length scale $l_B = 1/\sqrt{eB}$, and the dimensionless quantity $\chi = y/l_B - k_x l_B$. In dimensionless quantities Eq. (4.35) is

$$-\frac{v_F}{l_B}\begin{pmatrix} -k_z l_B & \partial_\chi + \chi \\ -\partial_\chi + \chi & k_z l_B \end{pmatrix}\phi(y) = E\phi(y). \tag{4.36}$$

Let the operators $a = (\chi + \partial_\chi)/\sqrt{2}$, $a^\dagger = (\chi - \partial_\chi)/\sqrt{2}$. One may easily verify the commutation relation $[a, a^\dagger] = 1$; they are ladder operators of the harmonic oscillators, whose eigenstates are $|n\rangle$, with $a|n\rangle = \sqrt{n}\,|n-1\rangle$, $a^\dagger|n\rangle = \sqrt{n+1}\,|n+1\rangle$. In terms of these operators, the system is

$$-\frac{\sqrt{2}v_F}{l_B}\begin{pmatrix} -\frac{k_z l_B}{\sqrt{2}} & a \\ a^\dagger & \frac{k_z l_B}{\sqrt{2}} \end{pmatrix}|\phi\rangle = E\,|\phi\rangle\,. \tag{4.37}$$

Take the ansatz

$$|\phi\rangle = \begin{pmatrix} \beta\,|n-1\rangle \\ \alpha\,|n\rangle \end{pmatrix}, \tag{4.38}$$

which is the most general form of $|\phi\rangle$ with any hope of being an eigenstate. This leads to

$$-\frac{\sqrt{2}v_F}{l_B}\begin{pmatrix} (-\gamma\beta + \alpha\sqrt{n})\,|n-1\rangle \\ (\beta\sqrt{n} + \gamma\alpha)\,|n\rangle \end{pmatrix} = E\,|\phi\rangle\,, \tag{4.39}$$

with $\gamma = k_z l_B/\sqrt{2}$. For $n > 0$ this leads to the equation for ϕ to be an eigenfunction

$$-\gamma + \frac{\alpha}{\beta}\sqrt{n} = \frac{\beta}{\alpha}\sqrt{n} + \gamma. \tag{4.40}$$

Solving for α/β this gives

$$\frac{\alpha}{\beta} = \frac{\gamma}{\sqrt{n}} \pm \sqrt{1 + \frac{\gamma^2}{n}}, \tag{4.41}$$

and thus

$$E = \pm v_F \sqrt{\frac{2n}{l_B^2} + k_z^2} = \pm s v_F \sqrt{2neB + k_z^2}, \tag{4.42}$$

where we reintroduced the explicit s. For $n = 0$ the annihilation operator a destroys the vacuum state $|0\rangle$, and the energy is instead $E_0 = -sk_z v_F$. The excited energy states are doubly degenerate; we choose to denote the energy levels by $m \in \mathbb{Z}$, where the sign from $\pm s$ is taken care of by the sign of this quantum number, and the harmonic oscillator levels n are given by its absolute value $|m|$. The energy levels are

$$E_{k_z m s} = \operatorname{sign}(m) v_F \sqrt{2|m|eB + k_z^2} \qquad \text{for } m \neq 0, \tag{4.43a}$$

$$E_{k_z 0 s} = -sk_z v_F \qquad \text{for } m = 0. \tag{4.43b}$$

We now find the corresponding eigenvectors of the system. The solution to the one dimensional harmonic oscillator in position space is, in dimensionless coordinates ξ, [Olv+, Eq. 18.39.5]

$$\langle \xi | n \rangle = \phi_n(\xi) = \frac{1}{\sqrt{2^n n!}} \pi^{-\frac{1}{4}} e^{-\frac{\xi^2}{2}} H_n(\xi), \tag{4.44}$$

where H_n are the Hermite polynomials. Thus,

$$\langle \chi | \phi \rangle = \begin{pmatrix} \beta \langle \chi | n-1 \rangle \\ \alpha \langle \chi | n \rangle \end{pmatrix} = e^{-\frac{\chi^2}{2}} \begin{pmatrix} \frac{\beta}{\sqrt{2^{n-1}(n-1)!\sqrt{\pi}}} H_{n-1}(\chi) \\ \frac{\alpha}{\sqrt{2^n n!\sqrt{\pi}}} H_n(\chi) \end{pmatrix}, \tag{4.45}$$

where we defined $H_{-1} = 0$ in order to get a more general expression. Choosing

$$\alpha = \sqrt{\frac{\gamma^2}{n}} \implies \beta = \frac{1}{1 \pm \sqrt{1 + \frac{n}{\gamma^2}}} = \pm \frac{\gamma^2}{n} \left(\sqrt{1 + \frac{n}{\gamma^2}} - 1 \right), \tag{4.46}$$

gives

$$\phi(\chi) = e^{-\frac{\chi^2}{2}} \sqrt{\frac{\gamma^2}{n}} \begin{pmatrix} \frac{\pm\sqrt{\frac{\gamma^2}{n}} \left(\sqrt{1+\frac{n}{\gamma^2}} - 1 \right)}{\sqrt{2^{n-1}(n-1)!\sqrt{\pi}}} H_{n-1}(\chi) \\ \frac{1}{\sqrt{2^n n!\sqrt{\pi}}} H_n(\chi) \end{pmatrix}. \tag{4.47}$$

There are thus four quantum numbers related to the eigenvectors, k_x, k_z, m, s. Reintroducing $\chi = (y - k_x l_B^2)/l_B$ and normalizing we get:

Summary 1

The Landau levels of a Weyl cone coupled to a magnetic field B_z has the eigenvalues

$$E_{k_z ms} = \operatorname{sign}(m) v_F \sqrt{2eBM + k_z^2} \qquad \text{for } m \neq 0, \tag{4.48a}$$

$$E_{k_z 0s} = -s k_z v_F \qquad \text{for } m = 0. \tag{4.48b}$$

The eigenstates are

$$\phi_{kms}(\boldsymbol{r}) = \frac{e^{ik_x x} e^{ik_z z}}{\sqrt{L_x L_z}} \frac{e^{-\frac{\left(y - k_x l_B^2\right)^2}{2 l_B^2}}}{\sqrt{\alpha_{k_z ms}^2 + 1}} \begin{pmatrix} \frac{\alpha_{k_z ms}}{\sqrt{2^{M-1}(M-1)!\sqrt{\pi} l_B}} H_{M-1}\left(\frac{y - k_x l_B^2}{l_B}\right) \\ \frac{1}{\sqrt{2^M M!\sqrt{\pi} l_B}} H_M\left(\frac{y - k_x l_B^2}{l_B}\right) \end{pmatrix}, \tag{4.49}$$

where $\boldsymbol{k} = (k_x, k_z)$, and with the normalization factor

$$\alpha_{k_z ms} = \frac{-s\sqrt{2eBM}}{\frac{E_{k_z ms}}{v_F} - s k_z}. \tag{4.50}$$

Here, capital letters indicate absolute value of corresponding quantity, $M = |m|$, a convention we will use throughout the chapter.

4.2.2. The tilted Hamiltonian

As we have seen, the eigenvalues of a Type-II Weyl semimetal are simple to find, and are not qualitatively different from those of Type-I, other than the appearance of particle and hole pockets at the Fermi level. We will also consider the Landau levels of these materials, which importantly are very different from Type-I. In fact, erroneous treatment of the Landau spectrum of Type-II semimetals caused the original paper describing Type-II materials to mistakenly assert that the chiral anomaly would not be present for certain directions of a background magnetic field [SGT17; Sol+15].

The issue with the Landau level description is that for certain directions of the B-field, the Landau levels break down. For Type-I materials, the description is valid for all directions of the B-field, but as the cone tilts into a Type-II material, the description breaks down when the B-field and tilt direction are perpendicular [SGT17], and as the magnitude of the tilt increases, the Landau levels are only valid up to a certain angle between the tilt direction and magnetic field. We will in this section derive and elucidate

the Landau levels and their regions of validity.

Consider again the Hamiltonian

$$H = v_F \boldsymbol{t}^s \boldsymbol{p} + s v_F \boldsymbol{p}\boldsymbol{\sigma}, \tag{4.51}$$

with the *tilt vector* as defined in Eq. (1.79)

$$\boldsymbol{t}^s = \begin{cases} \boldsymbol{t} & \text{broken inversion symmetry,} \\ s\boldsymbol{t} & \text{inversion symmetry.} \end{cases}$$

To find the Landau levels in a magnetic field $\boldsymbol{B} = B_z \hat{z}$, we will "Lorentz boost" the system to a frame where the cone is not tilted, where we may use the usual approach for finding the Landau levels.

Generally, consider $\boldsymbol{t}$ to consist of two components: $\boldsymbol{t}_\parallel$ which is parallel to the magnetic field, and $\boldsymbol{t}_\perp$ perpendicular to the magnetic field. Without loss of generality, we take the magnetic field to be in the z-direction, with the Landau gauge $\boldsymbol{A} = -B_z y \hat{x}$. By a rotation around z, we may also in general take $\boldsymbol{t}_\perp \parallel \hat{x}$.[4] Thus, let $\boldsymbol{t} = (t_\perp, 0, t_\parallel)$, and introduce the magnetic field through the minimal coupling $\boldsymbol{p} \to \boldsymbol{p}^B = \boldsymbol{p} + e\boldsymbol{A}$.

The Landau level equation is

$$(H_B - E)\,|\psi\rangle = 0, \tag{4.52}$$

with

$$H_B = v_F \left(t^s_\perp p^B_x + t^s_\parallel p^B_z \right) \mathcal{I}_2 + \sum_i s v_F p^B_i \sigma_i, \tag{4.53}$$

where $\mathcal{I}_2$ is the identity matrix of size 2. We may again make the plane wave ansatz $\phi(\boldsymbol{r}) = e^{ik_x x + ik_z z}\phi(y)$, similar to what was done for the untilted Hamiltonian in Section 4.2.1, to replace $p_{(x/z)} \to k_{(x/z)}$. In order to use the ladder operator method used for the untilted cone, we must get rid of the k^B_x on the diagonal of the Hamiltonian.[5] To achieve this, we will use a "Lorentz boost", which as we will show only leaves k_z and E in the diagonal. Act with the hyperbolic rotation operator $R = \exp[\Theta/2\sigma_x]$ on Eq. (4.52) from the left, and insert identity on the form RR^{-1} before the state vector. By introducing the state in the rotated frame $|\tilde{\psi}\rangle = R^{-1}\mathcal{N}\,|\psi\rangle$, with $\mathcal{N}$ a normalization

[4] The setup considered in the response calculation does not have $U(1)$ symmetry around the $\boldsymbol{B}$-field, due to the temperature gradient ∇T. However, the Landau levels are here computed generally, and when later introducing the symmetry-breaking components like the temperature gradient, we simply rotate to an appropriate frame.

[5] One could, in principle, have solved the system directly without such a transformation, however, it would be very tedious. [TCG16]

factor compensating for the non-unitarity of the transformation, we get the eigenvalue equation

$$(RH_BR - ER^2)\,|\tilde{\psi}\rangle = 0. \tag{4.54}$$

We now make the fortunate observation that the diagonal elements of

$$R\sigma_i R$$

are zero for $i = y$ and non-zero for $i = x, z$. The x- and z-components may thus be rotated in and out of the diagonal, without accidentally rotating the y-components into the diagonal.

We will now find the boost parameter that eliminates k_x from the diagonal. Note that

$$R^2 = e^{\Theta\sigma_x} = \begin{pmatrix} \cosh\theta & \sinh\theta \\ \sinh\theta & \cosh\theta \end{pmatrix} \tag{4.55}$$

and as $[R, \sigma_x] = 0$,

$$R\sigma_x R = R^2\sigma_x = \begin{pmatrix} \sinh\theta & \cosh\theta \\ \cosh\theta & \sinh\theta \end{pmatrix}, \tag{4.56}$$

as the effect of σ_x is to transpose the rows. The problematic part of the Hamiltonian in regard to finding the Landau levels, are the terms containing k_x^B on the diagonal, i.e.

$$v_F t_\perp^s k_x^B \mathcal{I}_2 + s v_F k_x^B \sigma_x.$$

The requirement for k_x^B to be rotated out of the diagonal is thus

$$t_\perp^s \cosh\theta + s \sinh\theta = 0. \tag{4.57}$$

Solving for θ we get

$$\theta = \log(\pm\frac{\sqrt{s - t_\perp^s}}{\sqrt{s + t_\perp^s}}). \tag{4.58}$$

Alternatively, written in a slightly suggestive form,

$$\tanh\theta = -st_\perp^s, \tag{4.59}$$

which is of course on the form of the *rapidity* known from Lorentz transformations, with $-st_\perp^s$ taking the place of the $\beta = v/c$ factor. From this observation, we also find it instructive to introduce the Lorentz factor

$$\gamma = \frac{1}{\sqrt{1 - \beta^2}} = \frac{1}{\sqrt{1 - t_\perp^2}}. \tag{4.60}$$

The required hyperbolic tilt angle to eliminate the k_x^B in the diagonal elements of the Hamiltonian, originating from the tilt, is thus

$$\theta = -s \tanh^{-1} t_\perp^s. \tag{4.61}$$

The inverse of tan, of course, diverges as the argument approaches ± 1, as shown in Fig. 4.2. For $|t_\perp| < 1$ we can find an angle θ which transforms our Hamiltonian into a form that we may solve. For $|t_\perp| \geq 1$, however, no (real) solution of θ exits, and the Landau level description collapses. More concretely, as we will show later, the separation of the Landau levels is reduced as the perpendicular tilt increases, and as $|t_\perp| \to 1$, the level separation $\Delta E \to 0$.

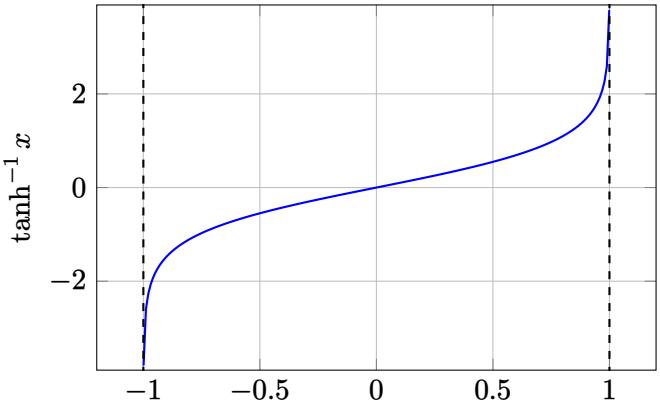

Figure 4.2.: Plot of $\tanh^{-1}$, which diverges as the argument goes to ± 1.

Interestingly, there are no restrictions on the parallel tilt, $t_\parallel$. The $\boldsymbol{t}$ parametrization of the tilt is conveniently visualized by plotting the $\boldsymbol{t}$-vector inside a unit sphere, shown in Fig. 4.3. If the vector is outside the unit sphere, it is a Type-II, if it is inside, it is a Type-I. Also, if the projection of the vector onto the x, y-plane is on the unit disk, the Landau level description is valid, if not, the Landau levels collapse. When the projection is on the unit disc, the system is in the *magnetic* regime, otherwise, we denote it by the *electric* regime. As the t-vector gets larger, the magnetic regime is restricted to smaller angles between $\boldsymbol{t}$ and $\boldsymbol{B}$. The magnetic regime is where the Landau levels are valid. All Type-I materials may thus be described by Landau levels, while for Type-II the Landau level description is only valid for certain directions of $\boldsymbol{t}$.

We now return to solving Eq. (4.54), using the solution angle we just found. By insertion, and after some clean up, we get

$$(RH_BR - ER^2)\,|\tilde{\psi}\rangle = v_F A\,|\tilde{\psi}\rangle = 0, \tag{4.62}$$

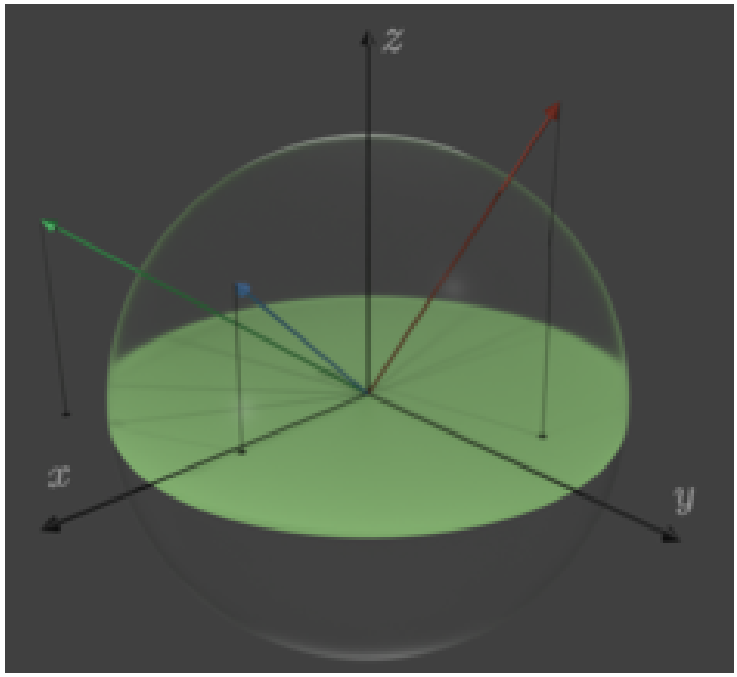

Figure 4.3.: Geometric visualization of the *tilt vector* $\boldsymbol{t}$. When the vector is inside the unit sphere ($t < 1$), the system is in the Type-I regime. When the vector is outside the unit sphere ($t > 1$), the system is in the Type-II regime. When the projection onto the xy-plane is on the unit disc, the system is in the *magnetic* regime, otherwise, it is in the *electric* regime. Shown are Type-I tilt (blue), Type-II magnetic (red), and Type-II electric (green). Figure inspired by Tchoumakov, Civelli, and Goerbig [TCG16].

with

$$\begin{aligned}
A_{11} &= k_z(s + t_\parallel^s \gamma) - E/v_F\gamma, \\
A_{12} &= -s(ik_y + k_z t_\perp t_\parallel \gamma - k_x/\gamma - E/v_F \gamma t_\perp^s), \\
A_{21} &= s(ik_y - k_z t_\perp t_\parallel \gamma + k_x/\gamma + E/v_F \gamma t_\perp^s), \\
A_{22} &= -k_z(s - t_\parallel^s \gamma) - E/v_F\gamma.
\end{aligned}$$

In order to simplify this further, absorb $\gamma t_\perp^s(k_z t_\parallel^s - E/v_F)$ into k_x. Thus, let

$$\begin{aligned}
\tilde{k}_x &= k_x/\gamma + \gamma t_\perp^s(E/v_F - k_z t_\parallel^s), \\
\tilde{k}_y &= k_y, \\
\tilde{k}_z &= k_z.
\end{aligned} \tag{4.63}$$

These expressions warrant some explanation, as the Lorentz boost is of course

$$\tilde{k}_x = \gamma(k_x - t_\perp \frac{E}{v_F}), \tag{4.64}$$

where E is the effective energy, and we used the four momentum $p^\mu = (\frac{E}{v_F}, \boldsymbol{p})$, and the effective speed of light v_F. It can thus look like our expression in Eq. (4.63) is wrong. The solution to this seeming inconsistency is that the proper effective energy is not $E - v_F k_z t_\parallel^s$, but rather $E - v_F k_z t_\parallel^s - v_F k_x t_\perp^s$ [YYY16].

The eigenvalue equation in the transformed momenta is simply

$$\left[\gamma\left(t_\parallel^s \tilde{k}_z - \frac{E}{v_F}\right)\mathcal{I}_2 + s\tilde{k}_i\sigma_i\right]|\tilde{\psi}\rangle = 0. \tag{4.65}$$

If we now again introduce the magnetic field using minimal coupling, $k_x \to k_x - eyB_z$, this corresponds to an effective field B_z/γ in the new quantities. This is because $\tilde{k}_x \to \tilde{k}_x - eyB_z/\gamma$. The Landau level equation thus reads

$$\left[\sum_i s v_F\left(\tilde{k}_i + e\tilde{A}_i\right)\sigma_i\right]|\tilde{\psi}\rangle = (E - t_\parallel^s v_F \tilde{k}_z)\gamma\,|\tilde{\psi}\rangle\,, \tag{4.66}$$

where $\tilde{\boldsymbol{A}} = -B_z/\gamma y\hat{x}$. We may thus use directly the result for the untilted cone, Eq. (4.43), giving

$$\left(E - t_\parallel^s v_F \tilde{k}_z\right)\gamma = \mathrm{sign}(m) v_F \sqrt{2|m|e\frac{B}{\gamma} + \tilde{k}_z^2}, \qquad m \neq 0, \tag{4.67a}$$

$$\left(E - t_\parallel^s v_F \tilde{k}_z\right)\gamma = -s\tilde{k}_z v_F, \qquad m = 0. \tag{4.67b}$$

Cleaning up and introducing explicitly the quantum numbers to the energy

$$E_{k_z m s} = t_\parallel^s v_F \tilde{k}_z + \mathrm{sign}(m)\frac{v_F}{\gamma}\sqrt{2|m|e\frac{B}{\gamma} + \tilde{k}_z^2}, \qquad m \neq 0, \tag{4.68a}$$

$$E_{k_z 0 s} = \tilde{k}_z v_F\left(t_\parallel^s - s/\gamma\right), \qquad m = 0. \tag{4.68b}$$

As the perpendicular tilt is increased, $\gamma = 1/\sqrt{1 - t_\perp^2}$ diverges to infinity. With the trivial substitution $\alpha = 1/\gamma$, which goes to zero, this gets an intuitive interpretation. As the perpendicular tilt increases, the Landau levels converge towards $t_\parallel v_F \tilde{k}_z$. In particular, the separation between Landau levels is reduced by a factor $\alpha^{3/2}$. The effect of the tilt on the Landau levels is to squeeze the

Landau levels together, and we will call the α the *squeezing factor*. We note that when approaching the degree of tilt where we are no longer able to find a boost that enables us to solve for the Landau levels, i.e. when $|t_\perp| \to 1$, the squeezing factor goes to zero. As the tilt exceeds this limit, the squeezing factor is imaginary.

The energy levels of the tilted cone expressed in terms of the energy levels of the untilted cone

$$E_{k_z ms} = t_\parallel^s v_F k_z + \alpha E^0_{m,\alpha B},$$

where $E^0_{m,\alpha B}$ is the energy in the untilted case, with magnetic field αB. We thus see that, in the Landau level picture, the energy levels are tilted by the $t_\parallel$-component, while the $t_\perp$-component squeezes the separation between the levels. The Landau levels cross the Fermi level at the transition from Type-I to Type-II, just like the energy bands do. The Landau levels are shown in Fig. 4.4 for different choices of $t_\perp$ and $t_\parallel$.

Recall the eigenstate of

$$H = v_F \sigma^i (p_i + eA_i),$$

with $A_i = -B_z y \delta_{ix}$, as given in summary 1 using the position basis,

$$\phi_{kms}(\boldsymbol{r}) = \frac{e^{ik_x x} e^{ik_z z}}{\sqrt{L_x L_z}} \frac{e^{-\frac{(y-k_x l^2)^2}{2l_B^2}}}{\sqrt{\alpha^2_{k_z ms}+1}} \begin{pmatrix} \frac{\alpha_{k_z ms}}{\sqrt{2^{M-1}(M-1)!\sqrt{\pi} l_B}} H_{M-1}\left(\frac{y-k_x l_B^2}{l_B}\right) \\ \frac{1}{\sqrt{2^M M!\sqrt{\pi} l_B}} H_M\left(\frac{y-k_x l_B^2}{l_B}\right) \end{pmatrix},$$

where capital letters indicate absolute value of corresponding quantity, $M = |m|, \boldsymbol{k} = (k_x, k_z)$, and with the normalization factor

$$\alpha_{k_z ms} = \frac{-\sqrt{2eBM}}{\frac{E_{k_z ms}}{s v_F} - k_z}. \tag{4.69}$$

Taking care to keep track of boosted and rescaled quantities, the eigenstate in the boosted frame is

$$\tilde{\phi}(\tilde{\boldsymbol{r}}) = \frac{e^{i\tilde{k}_x \tilde{x}} e^{ik_z z}}{\sqrt{L_x L_z}} \frac{e^{-\frac{\left(\tilde{y}-\tilde{k}_x l^2_{B'}\right)^2}{2l^2_{B'}}}}{\sqrt{\alpha^2_{\tilde{k}_z ms}+1}} \begin{pmatrix} \frac{\alpha_{\tilde{k}_z ms}}{\sqrt{2^{M-1}(M-1)!\sqrt{\pi} l_{B'}}} H_{M-1}\left(\frac{\tilde{y}-\tilde{k}_x l^2_{B'}}{l_{B'}}\right) \\ \frac{1}{\sqrt{2^M M!\sqrt{\pi} l_{B'}}} H_M\left(\frac{\tilde{y}-\tilde{k}_x l^2_{B'}}{l_{B'}}\right) \end{pmatrix}, \tag{4.70}$$

with

$$\alpha_{\tilde{k}_z ms} = \frac{-\sqrt{2eB'M}}{\gamma \frac{E_{\tilde{k}_z ms} - t_\parallel^s v_F \tilde{k}_z}{s v_F} - \tilde{k}_z}, \tag{4.71}$$

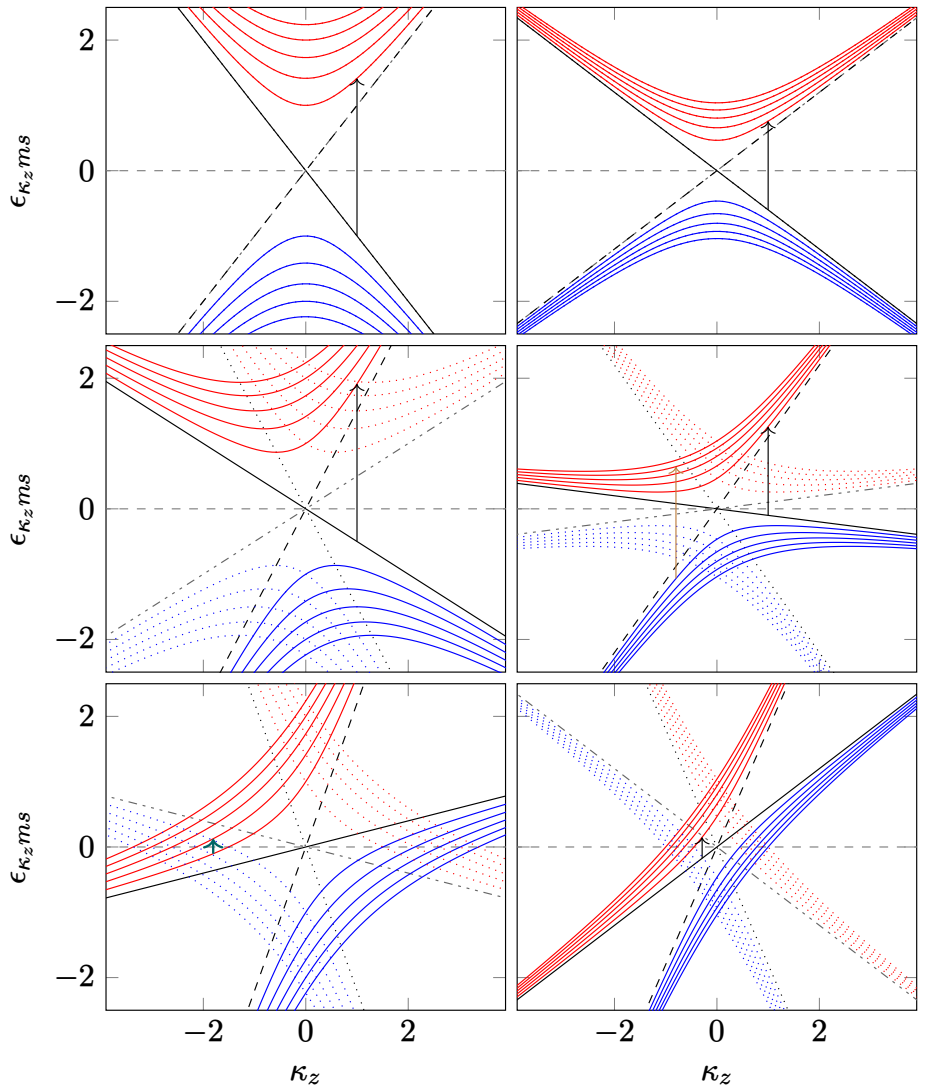

Figure 4.4.: Landau levels for different values of $t_\perp, t_\parallel$. The top two rows show Type-I, while the lowest row shows Type-II. Left column shows $t_\perp = 0$, right column $t_\perp = 0.64$ ($\alpha = 0.6$). The rows show $t_\parallel = 0, 0.5, 1.2$, from top to bottom. The dotted lines show the Landau levels with opposite sign of $t_\parallel$, and the dashed show the opposite chirality. The arrows indicate valid "transitions", namely the $0 \to 1$ interband in black, $-1 \to 4$ interband in brown, and $1 \to 2$ intraband in teal. See main text for details.

where

$$B' = B\alpha.$$

We note that $\alpha_{k_z 0s} = 0$, so using the explicit form of the energy we may simplify the expression some. For $m \neq 0$

$$\frac{E_{k_z ms} - t_\parallel^s v_F k_z}{s v_F} = \mathrm{sign}(m) s\alpha \sqrt{2MeB\alpha + k_z^2}$$

and thus

$$\alpha_{k_z ms} = \frac{-\sqrt{\alpha M}}{\mathrm{sign}(m) s \sqrt{\alpha M + \kappa^2} - \kappa} \tag{4.72}$$

where we defined the dimensionless $\kappa_z = \sqrt{2eB} k_z$.

The original eigenstate $|\psi\rangle = 1/\mathcal{N} e^{\theta/2\sigma_x} |\tilde{\psi}\rangle$ of the tilted system is easily found. Reinserting explicitly, in the boosted frame, that

$$\tilde{k}_x = \alpha k_x + \frac{t_\perp^s}{\alpha}(E_{k_z ms}/v_F - k_z t_\parallel^s) = \alpha k_x + t_\perp^s \frac{E^0_{m,\alpha B}}{v_F}$$

and $l_{B'} = \frac{l_B}{\sqrt{\alpha}}$ we define

$$\chi = \frac{y - \tilde{k}_x l_{B'}^2}{l_{B'}} = \sqrt{\alpha}(y - k_x l_B^2)/l_B + \frac{t_\perp^s l_B}{\sqrt{\alpha} v_F} E^0_{m,\alpha B}, \tag{4.73}$$

which is the argument of the Hermite polynomials. For later convenience, let us explicitly define

$$\tilde{\phi}_{kms}(\tilde{r}) = \frac{e^{i\tilde{k}_x \tilde{x} + i k_z z}}{\sqrt{L_x L_z}} \underbrace{\frac{e^{-\frac{1}{2}\chi^2} \sqrt[4]{\alpha}}{\sqrt{\alpha_{\tilde{k}_z ms}^2 + 1}} \begin{pmatrix} \frac{\alpha_{\tilde{k}_z ms}}{\sqrt{2^{M-1}(M-1)!\sqrt{\pi} l_B}} H_{M-1}(\chi) \\ \frac{1}{\sqrt{2^M M! \sqrt{\pi} l_B}} H_M(\chi) \end{pmatrix}}_{\tilde{\phi}_{kms}(y)}, \tag{4.74}$$

and thus

$$\tilde{\phi}_{kms}(y) = e^{-\frac{1}{2}\chi^2} \begin{pmatrix} a_{kms} H_{M-1}(\chi) \\ b_{kms} H_M(\chi) \end{pmatrix}, \tag{4.75}$$

with

$$a_{kms} = \frac{\alpha_{\tilde{k}_z ms} \sqrt[4]{\alpha}}{\sqrt{\alpha_{\tilde{k}_z ms}^2 + 1} \sqrt{2^{M-1}(M-1)! \sqrt{\pi} l_B}}, \tag{4.76}$$

$$b_{kms} = \frac{\sqrt[4]{\alpha}}{\sqrt{\alpha_{\tilde{k}_z ms}^2 + 1} \sqrt{2^M M! \sqrt{\pi} l_B}}. \tag{4.77}$$

We proceed now to find the normalization factor $\mathcal{N}$, as it will become necessary in later steps. Recall that

$$|\psi\rangle = \frac{1}{\mathcal{N}} e^{\theta/2\sigma_x} |\tilde{\psi}\rangle ,$$

and use that for $\theta = \tanh^{-1}(-st_\perp^s)$ the hyperbolic rotation

$$R^2 = e^{\theta\sigma_x} = \frac{1}{\alpha}\begin{pmatrix} 1 & -st_\perp^s \\ -st_\perp^s & 1 \end{pmatrix}.$$

The upper and lower part of the spinor are orthogonal, thus we have

$$\langle\psi|\psi\rangle = \frac{1}{\mathcal{N}^*\mathcal{N}}\frac{1}{\alpha}\langle\tilde{\psi}|\tilde{\psi}\rangle = 1 \implies \mathcal{N}^*\mathcal{N} = \frac{1}{\alpha}. \tag{4.78}$$

We choose $\mathcal{N} = \alpha^{-\frac{1}{2}}$.

Summary 2

The tilted Hamiltonian

$$H = v_F \boldsymbol{t}^s \boldsymbol{p} + s v_F \boldsymbol{p}\boldsymbol{\sigma}$$

in a magnetic field $\boldsymbol{B}$ has the Landau levels

$$E = \begin{cases} t_\parallel^s v_F k_z + \operatorname{sign}(m) v_F \alpha \sqrt{2eB\alpha M + k_z^2} & m \neq 0, \\ t_\parallel^s v_F k_z - s\alpha v_F k_z & m = 0, \end{cases}$$

with the squeezing factor $\alpha = \sqrt{1 - t_\perp^2}$. *The associated eigenstates in the position basis are*

$$\phi(\boldsymbol{r}) = \sqrt{\alpha} e^{\theta/2\sigma_x} \frac{e^{ik_x x + ik_z z}}{\sqrt{L_x L_z}} \tilde{\phi}(y),$$

where

$$\tilde{\phi}(y) = e^{-\frac{1}{2}\chi^2} \begin{pmatrix} a_{k_z m s} H_{M-1}(\chi) \\ b_{k_z m s} H_M(\chi) \end{pmatrix},$$

where we have defined $\chi = \sqrt{\alpha}\frac{y - k_x l_B^2}{l_B} + \frac{t_\perp^s l_B}{\sqrt{\alpha} v_F} E^0_{m,\alpha B}$ *and* $a_{k_z m s}, b_{k_z m s}$ *are given in Eqs.* (4.76) *and* (4.77).

4.3. Analytical expression for the response function

We will here find analytical expressions for the current operator $J^i(\omega, \boldsymbol{q})$ and energy-momentum tensor $T^{j0}(\omega, \boldsymbol{q})$, needed to calculate the correlation function. The fields are given, in the position basis, by

$$\psi = \sum_{kn} \langle \boldsymbol{r} | \boldsymbol{kns} \rangle \, a_{kns}(t) = \sum_{kn} \phi_{kns}(\boldsymbol{r}) a_{kns}(t), \tag{4.79}$$

$$\psi^\dagger = \sum_{kn} \langle \boldsymbol{kns} | \boldsymbol{r} \rangle \, a^\dagger_{kns}(t) = \sum_{kn} \phi^*_{kns}(\boldsymbol{r}) a^\dagger_{kns}(t). \tag{4.80}$$

Here $a^\dagger_\lambda(t) = \exp(iE_\lambda t/) a^\dagger_\lambda$ and $a^\dagger_\lambda, a_\lambda$ are the creation and annihilation operators of the state with quantum numbers λ.

4.3.1. Expressions for the operators

The current operator

The current operator $\hat{\boldsymbol{J}} = e\hat{\boldsymbol{v}}$, where $\hat{\boldsymbol{v}}$ is the velocity operator. Using the relation of Heisenberg operators $\dot{A} = -i[A, H]$ [SN17], for the operator A and Hamiltonian H, and with the minimal coupling $\boldsymbol{p}^B = \boldsymbol{p} + e\boldsymbol{A}$,

$$\begin{aligned} \boldsymbol{v} = \dot{\boldsymbol{r}} &= -i \left[\boldsymbol{r}, H \right] && (4.81) \\ &= -i v_F (s\boldsymbol{\sigma}_i + \boldsymbol{t}^s_i) \left[\boldsymbol{r}, p^B_i \right] && (4.82) \\ &= v_F (s\boldsymbol{\sigma} + \boldsymbol{t}^s), && (4.83) \end{aligned}$$

where we used the canonical commutation relation $[r_i, p_j] = i\delta_{ij}$ and that the position operator and magnetic potential $\boldsymbol{A}$ commute. We thus get

$$J^x = \psi^\dagger \hat{J}^x \psi = s v_F e \sum_{km,ln} \phi^*_{kms}(\boldsymbol{r}) \left(\sigma^x + s t^s_x \right) \phi_{lns}(\boldsymbol{r}) a^\dagger_{kms}(t) a_{lns}(t). \tag{4.84}$$

The energy-momentum tensor

The *canonical* energy-momentum tensor is generally defined by

$$T^{\mu\nu} = \frac{\delta \mathcal{L}}{\delta(\partial_\mu \phi_i)} \partial_\nu \phi_i - \eta^{\mu\nu} \mathcal{L}, \tag{4.85}$$

where the index i runs over the types of fields. This definition is correct for commuting fields, however, for non-commuting fields like ours, this formula is slightly wrong. This is often overlooked in many textbooks and papers, so we

will here elucidate the issue to some degree. While a proper derivation requires the use of Grassman variables and defining left and right derivation, which we will not do here, some simple considerations help in understanding the issue. In the standard textbook derivation of the canonical energy-momentum tensor, one expands the total derivative of the Lagrangian $\mathcal{L}(\psi_i, \partial\psi_i)$ in terms of the fields,

$$\frac{\mathrm{d}\mathcal{L}(\psi_i, \partial\psi_i)}{\mathrm{d}x_\nu} \equiv \mathrm{d}^\nu \mathcal{L} = \frac{\partial\mathcal{L}}{\partial(\partial_\mu\phi_i)}\frac{\partial(\partial_\mu\psi_i)}{\partial x_\nu} + \frac{\partial\mathcal{L}}{\partial\psi_i}\frac{\partial\psi_i}{\partial x_\nu}. \tag{4.86}$$

This expansion, however, ignores the non-commutative nature of the fields. For concreteness, consider $\psi_i = \bar{\psi}$. Heuristically, the correct expression would be obtained by reordering the factors in the two terms. By naively employing Eq. (4.85), the resulting canonical energy-momentum tensor of the Dirac theory would be

$$T^{\mu\nu} = \frac{\delta\mathcal{L}}{\delta(\partial_\mu\bar{\psi})}\partial^\nu\bar{\psi} + \frac{\delta\mathcal{L}}{\delta(\partial_\mu\psi)}\partial^\nu\psi - \eta^{\mu\nu}\mathcal{L}, \tag{4.87}$$

while the correct form is [IZ80, Eq. (3-153)]

$$T^{\mu\nu} = \partial^\nu\bar{\psi}\frac{\delta\mathcal{L}}{\delta(\partial_\mu\bar{\psi})} + \frac{\delta\mathcal{L}}{\delta(\partial_\mu\psi)}\partial^\nu\psi - \eta^{\mu\nu}\mathcal{L}. \tag{4.88}$$

The untilted Weyl Hamiltonian

$$H_s = s\sigma^i p_i, \tag{4.89}$$

where natural units ($c = v_F = 1$) are used, to have the expressions explicitly match those of QFT literature. The associated Lagrange density [Kac18]

$$\mathcal{L}_s = i\phi^\dagger\sigma_s^\mu\partial_\mu\phi, \tag{4.90}$$

with $\sigma_s^\mu = (I_2, s\boldsymbol{\sigma})$, i.e. $\sigma_{s=1}^\mu = \sigma^\mu, \sigma_{s=-1}^\mu = \bar{\sigma}^\mu$ known from the Dirac solutions. This is seen directly from the Dirac Lagrangian $i\bar{\psi}\partial\!\!\!/\psi$ by taking $\psi = (\phi_L, \phi_R)^T$ and setting, for example, $\phi_R = 0$. Symmetrize in daggered and undaggered fields[6]

$$\mathcal{L}_s = \frac{i}{2}(\phi^\dagger\sigma_s^\mu\partial_\mu\phi - \partial_\mu\phi^\dagger\sigma_s^\mu\phi), \tag{4.91}$$

[6]The Lagrangian itself is nonphysical, and we may transform it in any way that leaves the action $\int\mathcal{L}$ invariant.

which will prove more convenient to work with. From the definition of the canonical energy-momentum tensor for Dirac fields Eq. (4.88), one gets

$$T^{\mu\nu} = \frac{i}{2}(\phi^\dagger \sigma_s^\mu \partial_\nu \phi - \partial_\nu \phi^\dagger \sigma_s^\mu \phi - \eta^{\mu\nu}\mathcal{L}). \tag{4.92}$$

Consider now the tilted Weyl Hamiltonian

$$H_s = s\sigma^i k_i + (t^s)^i p_i. \tag{4.93}$$

Exactly analogous to the treatment of van der Wurff and Stoof [vdWS19] for the full 4×4 tilted Dirac Lagrangian, absorb the tilt term into the Pauli matrices, giving the Lagrangian density

$$\mathcal{L}_s = i\phi^\dagger \tilde{\sigma}_s^\mu \partial_\mu \phi, \tag{4.94}$$

where $\tilde{\sigma}_s^\mu = \sigma_s^\mu + (t^s)^\mu$, with $(t^s)^\mu = (0, t^s)$. The corresponding energy-momentum tensor, after again symmetrizing in the fields,

$$T^{\mu\nu} = \frac{i}{2}(\phi^\dagger \tilde{\sigma}_s^\mu \partial_\nu \phi - \partial_\nu \phi^\dagger \tilde{\sigma}_s^\mu \phi - \eta^{\mu\nu}\mathcal{L}). \tag{4.95}$$

Reintroducing the explicit effective speed of light v_F and recalling $\partial_0 = \partial_t / v_F$ this gives

$$\begin{aligned} T^{y_0}(t, \boldsymbol{r}) = \frac{1}{2} \sum_{km,ln} & \phi^*_{kms}(\boldsymbol{r})(s\sigma^y + t^s_y)\phi_{lns}(\boldsymbol{r}) \\ \times & \left[a^\dagger_{kms}(t) i\partial_t a_{lns}(t) - i\left(\partial_t a^\dagger_{kms}(t)\right) a_{lns}(t) - 2\mu a^\dagger_{kms}(t) a_{lns}(t) \right]. \end{aligned} \tag{4.96}$$

Here, also a non-zero potential μ is included by hand,[7] equal to what was done in Arjona, Chernodub, and Vozmediano [ACV19]. Our final result will be given at zero potential, however, it is included in the calculations as it for future work is interesting to consider small deviations from zero chemical potential. Recalling the time dependence of $a(t), a^\dagger(t)$ we have that

$$i\partial_t a_\lambda(t) = E_\lambda a_\lambda, \quad i\partial_t a^\dagger_\lambda(t) = -E_\lambda a^\dagger_\lambda,$$

which further simplifies the expression.

Summary 3

The current- and energy-momentum tensor operator are

[7] This is of course in no way a rigorous treatment of the chemical potential. Heuristically, one may argue that as the T^{y0} component is to be regarded as the energy flux, the contribution from chemical potential should be the chemical potential multiplied by the particle velocity operator.

$$J^x = sv_F e \sum_{km,ln} \phi^*_{kms}(r)\left(\sigma^x + st^s_x\right)\phi_{lns}(r) a^\dagger_{kms}(t) a_{lns}(t), \tag{4.97}$$

$$\begin{aligned} T^{y_0}(t,r) = \frac{1}{2}\sum_{km,ln} & \phi^*_{kms}(r)(s\sigma^y + t^s_y)\phi_{lns}(r) \\ & \times \left[E_{k_z ms} + E_{l_z ns} - 2\mu\right] a^\dagger_{kms}(t) a_{lns}(t). \end{aligned} \tag{4.98}$$

4.3.2. Response function in momentum space

Fourier transforming the position gives

$$J^x(t,\boldsymbol{q}) = \sum_{km,ln} J^x_{kms,lns}(\boldsymbol{q}) a^\dagger_{kms}(t) a_{lns}(t), \tag{4.99}$$

$$T^{y0}(t,-\boldsymbol{q}) = \sum_{km,ln} T^{y0}_{kms,lns}(\boldsymbol{q}) a^\dagger_{kms}(t) a_{lns}(t), \tag{4.100}$$

where the matrix elements in momentum space are given by

$$J^x_{kms,lns}(\boldsymbol{q}) = \int \mathrm{d}r e^{-iqr} sv_F e \phi^*_{kms}(r)(\sigma^x + st^s_x)\phi_{lns}(r), \tag{4.101}$$

$$T^{y0}_{kms,lns}(\boldsymbol{q}) = \frac{1}{2}\int \mathrm{d}r e^{iqr} \phi^*_{kms}(r)(s\sigma^y + t^s_y)(E_{k_z ms} + E_{l_z ns} - 2\mu)\phi_{lns}(r). \tag{4.102}$$

Note that as $T^{y0}(t,-\boldsymbol{q})$ will be used later, we here for convenience included the sign into the definition of the matrix element $T^{y0}_{kms,lns}$, as is reflected in the sign of the exponent of Eq. (4.102).

As was noted earlier, the eigenvectors are plane waves in the x- and z-directions, and the non-trivial part is the y-dependent $\phi(y)$. Thus, we want to express these matrix elements in terms of $\phi(y)$. The sum over $\boldsymbol{l}$ in Eq. (4.99) can be replaced by an integral, as it is a good quantum number. As usual, the measure in the integration is given by the density of states in momentum space, the well-known $L_i/2\pi$, with L_i being the length of the system in the i-direction.

$$\begin{aligned} J^x(t,\boldsymbol{q}) &= \sum_{km,n}\int \mathrm{d}l_x \mathrm{d}l_z \frac{L_x L_z}{4\pi^2} J^x_{kms,lns}(\boldsymbol{q}) a^\dagger_{kms}(t) a_{lns}(t) \\ &= \int \mathrm{d}l_x \mathrm{d}l_z \int \mathrm{d}y e^{-iq_y y}\delta(l_x - k_x - q_x)\delta(l_z - k_z - q_z) \\ &\quad \times sv_F e \phi^*_{kms}(y)(\sigma^x + st^s_x)\phi_{lns}(y). \end{aligned} \tag{4.103}$$

The Dirac delta functions appeared from taking the integrals from the matrix element over x and z, as the integrand in these variables was only plane waves. The exact same procedure may be done for the energy-momentum tensor in Eq. (4.100). Eliminating l by doing the integrals yields

$$J^x(t,\boldsymbol{q}) = \sum_{\boldsymbol{k},mn} J^x_{\boldsymbol{k}ms,\boldsymbol{k}+\mathrm{q}ns}(\boldsymbol{q}) a^\dagger_{\boldsymbol{k}ms}(t) a_{\boldsymbol{k}+\mathrm{q}ns}(t), \tag{4.104}$$

$$T^{y0}(t,-\boldsymbol{q}) = \sum_{\boldsymbol{\kappa},\mu\nu} T^{y0}_{\boldsymbol{\kappa}\mu s,\boldsymbol{\kappa}-\mathrm{q},\nu s}(\boldsymbol{q}) a^\dagger_{\boldsymbol{\kappa}\mu s}(t) a_{\boldsymbol{\kappa}-\mathrm{q}\nu s}(t), \tag{4.105}$$

where $\mathrm{q} = (q_x, q_z)$. Keeping in mind that $a^\dagger_\lambda(t) = e^{iE_\lambda t/}a^\dagger_\lambda$, and that

$$\left\langle \left[a^\dagger_{\boldsymbol{k}ms} a_{\boldsymbol{k}+\mathrm{q}ns}, a^\dagger_{\boldsymbol{\kappa}\mu s} a_{\boldsymbol{\kappa}-\mathrm{q}\nu s} \right] \right\rangle = \delta_{\boldsymbol{k},\boldsymbol{\kappa}-\mathrm{q}} \delta_{m,\nu} \delta_{\boldsymbol{k}+\mathrm{q},\boldsymbol{\kappa}} \delta_{n,\mu} \left[n_{\boldsymbol{k}ms} - n_{\boldsymbol{k}+\mathrm{q}ns} \right], \tag{4.106}$$

where $n_{\boldsymbol{k}ms}$ is the Fermi-Dirac distribution, the correlation function is given by

$$\begin{aligned} \left\langle \left[J^x(t,\boldsymbol{q}), T^{y0}(t',-\boldsymbol{q}) \right] \right\rangle = \sum_{\boldsymbol{k}mn} & e^{i(E_{k_z ms} - E_{k_z+\mathrm{q}_z ns})t} e^{i(E_{k_z+\mathrm{q}_z ns} - E_{k_z ms})t'} \\ & \times J^x_{\boldsymbol{k}ms,\boldsymbol{k}+\mathrm{q}ns}(\boldsymbol{q}) T^{y0}_{\boldsymbol{k}+\mathrm{q}ns,\boldsymbol{k}ms}(\boldsymbol{q}) \left[n_{\boldsymbol{k}ms} - n_{\boldsymbol{k}+\mathrm{q}ns} \right]. \end{aligned} \tag{4.107}$$

We are now ready to find the correlation function χ^{xy} given in Eq. (4.14)

$$\chi^{xy}(\omega,\boldsymbol{q}) = \frac{-iv_F}{\mathcal{V}} \int \mathrm{d}t e^{i\omega t} \int_{-\infty}^{0} \mathrm{d}t' \Theta(t) \left\langle \left[J^x(t,\boldsymbol{q}), T^{y0}(t',-\boldsymbol{q}) \right] \right\rangle. \tag{4.108}$$

Introduce as usual a decay factor $e^{-\eta(t-t')}$ to ensure convergence in the time integrals, and make a change of variables $t' \to -t'$. The integral part of Eq. (4.108), ignoring everything without time dependence for clarity, is then

$$\begin{aligned} & \lim_{\eta\to 0} \int_0^\infty \mathrm{d}t\mathrm{d}t' e^{\left[i\left(E_{k_z ms} - E_{k_z+\mathrm{q}_z ns} + \omega + i\eta\right)t\right]} e^{\left[i\left(E_{k_z ms} - E_{k_z+\mathrm{q}_z ns} + i\eta\right)t'\right]} \\ & = \lim_{\eta\to 0} i \left[E_{k_z ms} - E_{k_z+\mathrm{q}_z ns} + \omega + i\eta \right]^{-1} i \left[E_{k_z ms} - E_{k_z+\mathrm{q}_z ns} + i\eta \right]^{-1}. \end{aligned} \tag{4.109}$$

The response function then reads

$$\begin{aligned} \chi^{xy}(\omega,\boldsymbol{q}) = \frac{iv_F}{\mathcal{V}} \lim_{\eta\to 0} \sum_{\boldsymbol{k}mn} & J^x_{\boldsymbol{k}ms,\boldsymbol{k}+\mathrm{q}ns}(\boldsymbol{q}) T^{y0}_{\boldsymbol{k}+\mathrm{q}ns,\boldsymbol{k}ms}(\boldsymbol{q}) \left[n_{\boldsymbol{k}ms} - n_{\boldsymbol{k}+\mathrm{q}ns} \right] \\ & \times \left[E_{k_z ms} - E_{k_z+\mathrm{q}_z ns} + \omega + i\eta \right]^{-1} \left[E_{k_z ms} - E_{k_z+\mathrm{q}_z ns} + i\eta \right]^{-1}, \end{aligned} \tag{4.110}$$

where the matrix elements are

$$J^x_{kms,k+\mathtt{q}ns}(q) = \int \mathrm{d}y e^{-iq_y y} s v_F e \phi^*_{kms}(y)(\sigma^x + s t^s_x)\phi_{k+\mathtt{q}ns}(y), \tag{4.111}$$

$$\begin{aligned} T^{y0}_{k+\mathtt{q}ns,kms}(q) = \frac{1}{2}\int \mathrm{d}y e^{iq_y y}\phi^*_{k+\mathtt{q}ns}(y)(s\sigma^y + t^s_y)\phi_{kms}(y) \\ \times (E_{k_z ms} + E_{k_z+\mathtt{q}_z ns} - 2\mu)\,. \end{aligned} \tag{4.112}$$

We will for the rest of the calculation consider $\eta \to 0$. The calculation was also done with a finite impurity η, which gives no important contributions.

We will consider the response function in the static limit $\lim_{\omega\to 0}\lim_{\boldsymbol{q}\to 0}$. We may use the property of the limit of a product of functions $\lim A \cdot B = \lim A \cdot \lim B$ to write

$$\lim_{\omega\to 0}\lim_{\boldsymbol{q}\to 0}\chi^{xy}(\omega, \boldsymbol{q}) = \frac{iv_F}{\mathcal{V}}\sum_{kmn}\frac{J^x_{kms,kns}T^{y0}_{kns,kms}[n_{kms} - n_{kns}]}{(E_{k_z ms} - E_{k_z ns})^2}, \tag{4.113}$$

where the current and energy-momentum tensor matrix elements are the expression given in Eqs. (4.111) and (4.112) taken in the limit. Furthermore, we will take the zero temperature limit $T \to 0$, where $n_{kms} = \theta(\mu - E_{k_z ms})$.

4.4. Response of an untilted cone

We here evaluate Eq. (4.113) for the untilted cone.

4.4.1. Explicit form of the matrix elements

Compared to the procedure used by Arjona, Chernodub, and Vozmediano [ACV19], taking the limit of each matrix element by itself greatly simplifies the calculation.

Let

$$\phi_{kms}(y) = e^{-\frac{(y-k_x l_B^2)^2}{2l_B^2}}\begin{pmatrix} a_{k_z ms}H_{M-1}\left(\frac{y-k_x l_B^2}{l_B}\right) \\ b_{k_z ms}H_M\left(\frac{y-k_x l_B^2}{l_B}\right)\end{pmatrix}, \tag{4.114}$$

where $a_{k_z ms}, b_{k_z ms}$ are as defined in Eqs. (4.76) and (4.77), with $t = 0$.

The current operator

The matrix element

$$
\begin{aligned}
&J_{kms;k+\mathrm{q}ns}(\boldsymbol{q}) \\
&= \int \mathrm{d}y e^{-iq_y y} s v_F e \phi^*_{kms}(y) \sigma^x \phi_{k+\mathrm{q}ns}(y) && (4.115)\\
&= s v_F e \int \mathrm{d}y \exp\left\{-iq_y y - \frac{(y-k_x l_B^2)^2 + (y-(k_x+q_x)l_B^2)^2}{2l_B^2}\right\} && (4.116)\\
&\quad \times \left[a_{k_z ms} b_{k_z+\mathrm{q}_z ns} H_{M-1}\left(\frac{y-k_x l_B^2}{l_B}\right) H_N\left(\frac{y-(k_x+q_x)l_B^2}{l_B}\right)\right. \\
&\qquad \left. + b_{k_z ms} a_{k_z+\mathrm{q}_z ns} H_M\left(\frac{y-k_x l_B^2}{l_B}\right) H_{N-1}\left(\frac{y-(k_x+q_x)l_B^2}{l_B}\right)\right].
\end{aligned}
$$

We wish to write the exponent on the form $e^{-a(y+b)^2}$. Introduce $\mathrm{q}_y = (q_x, q_y)$, not to be confused with $\mathrm{q} = (q_x, q_z)$, and complete the square

$$
\begin{aligned}
J_{kms;k+\mathrm{q}ns}(\boldsymbol{q}) &= s v_F e \int \mathrm{d}y e^{-\left\{y + l_B^2(iq_y - 2k_x - q_x)/2\right\}^2 / l_B^2} e^{-\frac{1}{4} l_B^2 \left\{\mathrm{q}_y^2 + 2i(2k_x+q_x)q_y\right\}} \\
&\times \left[a_{k_z ms} b_{k_z+\mathrm{q}_z ns} H_{M-1}\left(\frac{y-k_x l_B^2}{l_B}\right) H_N\left(\frac{y-(k_x+q_x)l_B^2}{l_B}\right)\right. \\
&\qquad \left. + b_{k_z ms} a_{k_z+\mathrm{q}_z ns} H_M\left(\frac{y-k_x l_B^2}{l_B}\right) H_{N-1}\left(\frac{y-(k_x+q_x)l_B^2}{l_B}\right)\right].
\end{aligned} \tag{4.117}
$$

By introducing $\tilde{y} = \frac{y}{l_B} + l_B(iq_y - q_x - 2k_x)/2$ the matrix element may be rewritten

$$
\begin{aligned}
J_{kms;k+\mathrm{q}ns}(\boldsymbol{q}) &= s v_F e \int \mathrm{d}\tilde{y}\, l_B \exp\left[-\frac{1}{4} l_B^2 \left\{\mathrm{q}_y^2 + 2i(2k_x+q_x)q_y\right\}\right] e^{-\tilde{y}^2} \\
&\times \left[a_{k_z ms} b_{k_z+\mathrm{q}_z ns} H_{M-1}\left(\tilde{y} + \frac{l_B}{2}(q_x - iq_y)\right) H_N\left(\tilde{y} + \frac{l_B}{2}(-q_x - iq_y)\right)\right. \\
&\quad \left. + b_{k_z ms} a_{k_z+\mathrm{q}_z ns} H_M\left(\tilde{y} + \frac{l_B}{2}(q_x - iq_y)\right) H_{N-1}\left(\tilde{y} + \frac{l_B}{2}(-q_x - iq_y)\right)\right].
\end{aligned} \tag{4.118}
$$

Taking the limit we find the simple form

$$
J_{kms;kns} = J_{k_z mns} = s v_F e l_B \int \mathrm{d}\tilde{y} e^{-\tilde{y}} \left[a_{k_z ms} b_{k_z ns} H_{M-1}(\tilde{y}) H_N(\tilde{y}) + m \leftrightarrow n\right], \tag{4.119}
$$

where $m \leftrightarrow n$ are the repetition of the previous term under the interchange of m, n. We employ now the orthogonality relation of the Hermite polynomials [Olv+, Table 18.3.1]

$$\int_{-\infty}^{\infty} \mathrm{d}x e^{-x^2} H_n(x) H_m(x) = \sqrt{\pi} 2^n n! \delta_{n,m} \tag{4.120}$$

to write

$$J_{kms,kns} = J_{k_z mns} = s v_F e l_B \sqrt{\pi} (a_{k_z ms} b_{k_z ns} \delta_{M-1,N} 2^N N! + m \leftrightarrow n). \tag{4.121}$$

With

$$a_{kms} b_{kns} = \frac{\alpha_{k_z ms}}{\sqrt{\alpha_{k_z ms}^2 + 1}\sqrt{\alpha_{k_z ns}^2 + 1}} \left[2^{N+M-1}(M-1)!N!\pi l_B^2\right]^{-\frac{1}{2}}, \tag{4.122}$$

$$b_{kms} a_{kns} = \frac{\alpha_{k_z ns}}{\sqrt{\alpha_{k_z ms}^2 + 1}\sqrt{\alpha_{k_z ns}^2 + 1}} \left[2^{N+M-1}(N-1)!M!\pi l_B^2\right]^{-\frac{1}{2}}, \tag{4.123}$$

we find explicitly

$$J_{kms,kns} = J_{k_z mns} = s v_F e \frac{\alpha_{k_z ms}\delta_{M-1,N} + \alpha_{k_z ns}\delta_{M,N-1}}{\sqrt{\alpha_{k_z ms}^2 + 1}\sqrt{\alpha_{k_z ns}^2 + 1}}. \tag{4.124}$$

The energy-momentum tensor operator

Consider now the matrix element of the energy-momentum tensor

$$T^{y0}_{k+\mathfrak{q}ns,kms}(q) = \frac{1}{2}\int \mathrm{d}y e^{iq_y y} \phi^*_{k+\mathfrak{q}ns}(y) s\sigma^y (E_{k_z ms} + E_{k_z+\mathfrak{q}_z ns} - 2\mu)\phi_{kms}(y). \tag{4.125}$$

The form of the integrand is similar to the current matrix case, with the exchange of the Pauli matrix $\sigma^x \to \sigma^y$, thus giving an additional i and a negative sign to the first term.

$$T^{y0}_{k+\mathfrak{q}ns,kms}(q) = \frac{is}{2}(E_{k_z ms} + E_{k_z+\mathfrak{q}_z ns} - 2\mu)\int \mathrm{d}y e^{iq_y y} e^{-\frac{(y-k_x l_B^2)^2 + (y-(k_x+q_x)l_B^2)^2}{2l_B^2}}$$
$$\times \left[-a_{k_z+\mathfrak{q}_z ns} b_{k_z ms} H_{N-1}(\dots) H_M(\dots) + b_{k_z+\mathfrak{q}_z ns} a_{k_z ms} H_N(\dots) H_{M-1}(\dots)\right]. \tag{4.126}$$

Taking care to note that the factor from the Fourier transform, that was $e^{-iq_y y}$ in the current matrix element is here $e^{+iq_y y}$, a similar completion of the square is done

$$\begin{aligned} T^{y0}_{k+\mathrm{q}ns,kms}(\boldsymbol{q}) = \frac{is}{2}(E_{k_z ms} + E_{k_z+\mathrm{q}_z ns} - 2\mu) e^{-l_B^2\{\mathrm{q}_y^2 - 2iq_y(2k_x+q_x)\}/4} \\ \times \int \mathrm{d}y \exp\left[-\left\{ y + \frac{l_B^2}{2}(-iq_y - 2k_x - q_x) \right\}^2 / l_B^2 \right] \\ \times \Big[- a_{k_z+\mathrm{q}_z ns} b_{k_z ms} H_{N-1}(\dots) H_M(\dots) \\ + b_{k_z+\mathrm{q}_z ns} a_{k_z ms} H_N(\dots) H_{M-1}(\dots) \Big]. \end{aligned} \tag{4.127}$$

The arguments of the Hermite polynomials have been dropped for brevity of notation. As before make a change of variables to get the integral on the form of the orthogonality relation for the Hermite polynomials Eq. (4.120). Upon introducing $\tilde{y} = \frac{y}{l_B} + l_B(-iq_y - q_x - 2k_x)/2$ the orthogonality relation is used on the expression

$$\begin{aligned} T^{y0}_{k+\mathrm{q}ns,kms}(\boldsymbol{q}) = \frac{isl_B}{2}(E_{k\mu s} + E_{\lambda\nu s} - 2\mu) e^{-l_B^2\{\mathrm{q}_y^2 - 2iq_y(2k_x+q_x)\}/4} \int \mathrm{d}\tilde{y} e^{-\tilde{y}^2} \\ \times \left[-a_{k+\mathrm{q}ns} b_{kms} H_{N-1}\left(\tilde{y} + \frac{l_B}{2}(iq_y - q_x) \right) H_M\left(\tilde{y} + \frac{l_B}{2}(iq_y + q_x) \right) \right. \\ \left. + b_{k+\mathrm{q}ns} a_{kms} H_N\left(\tilde{y} + \frac{l_B}{2}(iq_y - q_x) \right) H_{M-1}\left(\tilde{y} + \frac{l_B}{2}(iq_y + q_x) \right) \right]. \end{aligned} \tag{4.128}$$

The terms in the integrand are exactly the same as in the current matrix element case, just in the reverse order and with $q_y \to -q_y$. In the limit $\boldsymbol{q} \to 0$

$$T^{y0}_{kns,kms}(\boldsymbol{q}) = \frac{is}{2} \frac{(E_{k_z ms} + E_{k_z ns} - 2\mu)}{\sqrt{\alpha^2_{k_z ms} + 1}\sqrt{\alpha^2_{k_z ns} + 1}} \left(\alpha_{k_z ms} \delta_{M-1,N} - \alpha_{k_z ns} \delta_{M,N-1} \right). \tag{4.129}$$

Summary 4

For an untilted Weyl cone, in the local limit $q \to 0$, we have the matrix

elements

$$J_{kms;kns} = \Gamma_{k_z mns} s v_F e \left(\alpha_{k_z ms}\delta_{M-1,N} + m \leftrightarrow n\right), \tag{4.130}$$

$$T^{y0}_{kns,kms} = \frac{is\Gamma_{k_z mns}}{2}\left(E_{k_z ms} + E_{k_z ns} - 2\mu\right)\left(\alpha_{k_z ms}\delta_{M-1,N} - m \leftrightarrow n\right), \tag{4.131}$$

where $m \leftrightarrow n$ represent the preceding term under the interchange of m, n and where we have defined $\Gamma_{k_z mns} = \left[(\alpha^2_{k_z ms}+1)(\alpha^2_{k_z ns}+1)\right]^{-\frac{1}{2}}$.

4.4.2. Computing the response function

It is now finally possible to write out the entire response function. We begin by replacing the sum over $\boldsymbol{k}$ with an integral. Firstly, we will show that the sum over k_x is restricted; recall that the eigenfunctions are exponentially centered around $y_0 = k_x l_B^2$, which for a finite sample we expect to be restricted to $0 \le y_0 \le L_y$. This restricts the k_x sum to $0 \le k_x \le L_y/l_B^2 = L_y eB$, resulting in the k_x summation giving a finite degeneracy contribution [Ton, Ch. 1.4.1; Lin17], as the integrand is independent of k_x.

$$\sum_{\boldsymbol{k}} = \sum_{k_x=0}^{L_y eB}\sum_{k_z} \to \frac{L_x L_z}{(2\pi)^2}\int_0^{L_y eB} \mathrm{d}k_x \int \mathrm{d}k_z \tag{4.132}$$

$$= \frac{\mathcal{V} eB}{(2\pi)^2}\int \mathrm{d}k_z. \tag{4.133}$$

Recall the response function (4.113)

$$\lim_{\omega\to 0}\lim_{q\to 0}\chi^{xy}(\omega, q) = \frac{iv_F}{\mathcal{V}}\sum_{kmn}\frac{J^x_{kms,kns}T^{y0}_{kns,kms}[n_{kms} - n_{kns}]}{(E_{k_z ms} - E_{k_z ns})^2}. \tag{4.134}$$

Firstly, introduce the dimensionless quantities $\kappa_z\sqrt{2eB} = k_z, \epsilon_{k_z ms}v_F\sqrt{2eB} = E_{k_z ms}$, in order to facilitate solving the integral over k_z. Collecting dimensionful quantities, the response function reads

$$\lim_{\omega\to 0}\lim_{q\to 0}\chi^{xy} = -\frac{e^2 v_F B}{2(2\pi)^2}\sum_{mn}\int \mathrm{d}\kappa_z [n_{\kappa_z ms} - n_{\kappa_z ns}][(\alpha^2_{\kappa_z ms}+1)(\alpha^2_{\kappa_z ns}+1)]^{-1}$$
$$\times \frac{(\epsilon_{\kappa_z ms} + \epsilon_{\kappa_z ns})(\alpha^2_{\kappa_z ms}\delta_{M-1,N} - \alpha^2_{\kappa_z ns}\delta_{N-1,M})}{(\epsilon_{\kappa_z ms} - \epsilon_{\kappa_z ns})^2}. \tag{4.135}$$

Let us now define

$$\xi(\kappa_z, m, n) = \lim_{\omega\to 0}\lim_{q\to 0} \frac{[n_{\kappa ms} - n_{\kappa+qns}]\left[(\alpha^2_{\kappa ms}+1)(\alpha^2_{\kappa+qns}+1)\right]^{-1}}{(\epsilon_{\kappa ms}-\epsilon_{\kappa+qns})(\epsilon_{\kappa ms}-\epsilon_{\kappa+qns}+\frac{\omega}{v_F\sqrt{2eB}})}. \quad (4.136)$$

As is shown in Table 4.1, in the limit, $\xi(\kappa_z, m, n)$ is odd under interchange of m, n. Using this, we may simplify our expressions. In the last term of Eq. (4.135), relabel the summation indices $m \leftrightarrow n$, and then use that ξ is odd under interchange of m, n. This renders the two terms equal, and we may consider

$$\alpha^2_{\kappa_z ms}\delta_{M-1,N} - \alpha^2_{\kappa_z ns}\delta_{N-1,M} \to 2\alpha^2_{\kappa_z ms}\delta_{M-1,N}.$$

The simplified expression is then

$$\lim_{\omega\to 0}\lim_{q\to 0}\chi^{xy} = -\frac{e^2 v_F B}{(2\pi)^2}\sum_{\substack{mn\\ N=M-1}}\int \mathrm{d}\kappa_z \xi(\kappa_z, m, n)(\epsilon_{\kappa_z ms}+\epsilon_{\kappa_z ns}-2\mu)\alpha^2_{\kappa_z ms}. \quad (4.137)$$

Table 4.1.: Sign change of factors under various transformations.

Transformation	$\xi(\kappa_z, m, n)$	$\epsilon_{\kappa_z ms}$	$\alpha_{\kappa_z ms}$
$(m, n, \kappa_z) \mapsto (-m, -n, -\kappa_z)$	-1	-1	-1
$(\kappa_z, s) \mapsto (-\kappa_z, -s)$	+1	+1	-1
$(m, n) \mapsto (n, m)$	-1		

Before solving the integral, we note that in addition to the $N = M - 1$ selection rule[8] of the sum, the distribution functions $n_{\kappa_z ms} - n_{\kappa_z ns}$ in $\xi(\kappa_z, m, n)$ impose further restrictions on which transitions are energetically allowed. We consider the limit $T \to 0$, where the distributions take the form of step functions, $n_{\kappa_z ms} \to \theta(-\epsilon_{\kappa_z ms})$. As the sign of energy level m, for $m \neq 0$, is given by the sign of m itself, this gives a rather simple restriction on the sum. For the zeroth energy level, the sign of the energy is given by $\mathrm{sign}(-s\kappa_z)$. The distribution factor is

$$n_{kms} - n_{kns} = \begin{cases} 0 & mn > 0 \text{ or } m, n = 0, \\ -\mathrm{sign}(m) & m, n \neq 0, \\ -\mathrm{sign}(m)\theta\left[\mathrm{sign}(m)s\kappa_z\right] & n = 0. \end{cases} \quad (4.138)$$

[8] Known as the *dipolar* selection rule [TCG16].

Combining this with the selection rule $N = M - 1$, we see that the only allowed transitions are

$$M \to -N = -(M-1),\ -M \to N = (M-1).$$

The sum may be further restricted by noting that as both $\xi(\kappa_z, m, n)$ and $\epsilon_{\kappa_z ms} + \epsilon_{\kappa_z ns}$ are odd under $(m, n, \kappa_z) \to (-m, -n, -\kappa_z)$, the two transitions above give the same contribution when $\mu = 0$. In the case of zero chemical potential, the expression may thus be simplified further, by considering only $-N \to M = N + 1$ transitions, adding a factor of 2.

Lastly, we now show that the contributions from cones of opposite chirality s are the same. Under the transformation $(\kappa_z, s) \mapsto (-\kappa_z, -s)$, the product $\kappa_z s$ is obviously invariant. Note that $\epsilon_{\kappa_z ms}$ only depends on s and κ_z through the product $\kappa_z s$. While it is not the case for $\alpha_{\kappa_z ms}$, it is the case for its square. Consequently, the integrand is invariant under $(\kappa_z, s) \mapsto (-\kappa_z, -s)$. Similar to the argumentation used above, as the integral goes over all κ_z, the integral is invariant under $s \mapsto -s$.

Summary 5

We have shown the following simplifications of Eq. (4.135):

- *The contributions from the terms $\alpha^2_{\kappa_z ms}\delta_{M-1,N}$ and $-\alpha^2_{\kappa_z ns}\delta_{N-1,M}$ are equal, and we consider therefore only one of them, adding a degeneracy factor 2.*
- *The difference of the step functions takes the form Eq. (4.138), which limits the transitions to states with energies of opposite signs. For each value of M, N, this means the only valid transitions are $m = M, n = -N$ and $m = -M, n = N$.*
- *As the integrand is invariant under $(m, n, \kappa_z) \mapsto (-m, -n, -\kappa_z)$, we may consider only one of the transitions mentioned in the previous point, adding once again a degeneracy factor of 2.*
- *We lastly showed that the contribution is independent of the chirality s.*

For zero chemical potential, the response function is

$$\lim_{\omega\to 0}\lim_{q\to 0}\chi^{xy} = -\frac{2e^2 v_F B}{(2\pi)^2}\sum_{i=0}\int \mathrm{d}\kappa_z \xi(\kappa_z, m, n)(\epsilon_{\kappa_z ms} + \epsilon_{\kappa_z ns})\alpha^2_{\kappa_z ms}\big|_{\substack{m=i+1\\ n=-i}}, \tag{4.139}$$

where the integration limits are $(-\infty, \infty)$ for $i \neq 0$, $(-\infty, 0)$ for $i = 0, s = -1$, and $(0, \infty)$ for $i = 0, s = 1$.

Including only the first term of the sum, we find

$$\lim_{\omega \to 0} \lim_{\boldsymbol{q} \to 0} \chi^{xy} = \frac{e^2 v_F B}{2(2\pi)^2 \hbar}, \tag{4.140}$$

where we have reinserted the explicit $\hbar$. Including contributions from the $\bar{N}$ lowest Landau levels, one acquire additional numerical prefactors,

$$\lim_{\omega \to 0} \lim_{\boldsymbol{q} \to 0} \chi^{xy} = \gamma_{\bar{N}} \frac{e^2 v_F B}{2(2\pi)^2 \hbar}. \tag{4.141}$$

Solving the integral analytically, we obtained the contribution from each term

$$\gamma_{\bar{N}} - \gamma_{\bar{N}-1} = 1 + 2\bar{N} \left\{ 1 - (1 + \bar{N}) \log(1 + \frac{1}{\bar{N}}) \right\}, \quad \bar{N} > 0. \tag{4.142}$$

The sum can be shown to equal the rather nasty expression

$$\begin{aligned} \gamma_{\bar{N}} = \gamma_0 + \frac{1}{3} \Big(& 6\zeta^{(1,0)}(-2, \bar{N} + 1) - 6\zeta^{(1,0)}(-2, \bar{N} + 2) + 6\zeta^{(1,0)}(-1, \bar{N} + 1) \\ & + 6\zeta^{(1,0)}(-1, \bar{N} + 2) + 12 \log(\xi) + 3\bar{N}^2 + 6\bar{N} - 1 \Big), \end{aligned} \tag{4.143}$$

where $\xi \approx 1.28243$ is Glaisher's constant. Specifically $\gamma_0 = 1, \gamma_{20} \approx 2$. Furthermore, $\gamma_{\bar{N}}$ goes like $\log \bar{N}$. The first 300 contributions are shown in Fig. 4.5.

4.5. The response of a tilted cone

The generalization to the tilted cone follows the same fundamental steps as that of the untilted cone. However, there are important technical and physical complications that must be handled with care. In this section, we compute the response of a tilted cone, following the same structure as was used in the untilted case. As mentioned in the introduction to the chapter, the tilt vector $\boldsymbol{t}$ may in general have any direction. However, we here specialize to having $\boldsymbol{t} = (t_\perp, 0, t_\parallel)$.

4.5.1. Explicit form of the matrix elements

We will here find an explicit form of the matrix elements, starting with the charge current

$$J_{kms;k+qns}(\boldsymbol{q}) = \int \mathrm{d}y e^{-iq_y y} s v_F e \phi^*_{kms}(y) (\sigma^x + s t_x^s) \phi_{k+qns}(y), \tag{4.144}$$

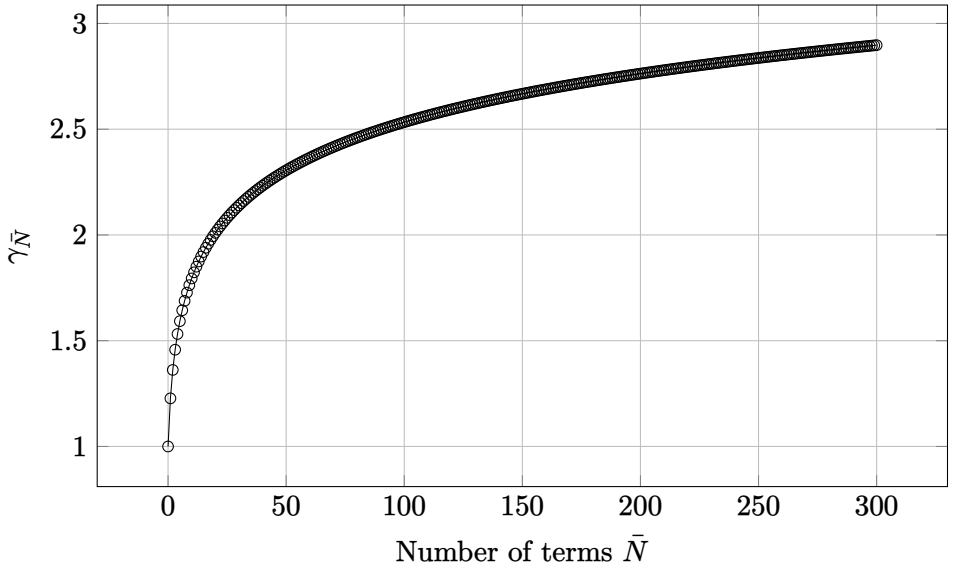

Figure 4.5.: Prefactor $\gamma_{\bar{N}}$ for a non-tilted system as a function of the number of included Landau levels $\bar{N}$.

which we will split into two parts, $J^{(1)}, J^{(2)}$, corresponding to the terms σ_x and st_x^s. For the first part, we must find the matrix product $\phi\sigma_x\phi$. Recall from summary 2 that $\phi = \sqrt{\alpha}e^{\theta/2\sigma_x}\tilde{\phi}$, and thus we must find

$$\phi^*\sigma_x\phi = \alpha\tilde{\phi}^* e^{\theta/2\sigma_x}\sigma_x e^{\theta/2\sigma_x}\tilde{\phi} = \alpha\tilde{\phi}^*\sigma_x e^{\theta\sigma_x}\tilde{\phi}.$$

As defined in summary 2

$$\tilde{\phi} = e^{-\frac{1}{2}\chi^2}\begin{pmatrix} a_{kms}H_{M-1}(\chi) \\ b_{kms}H_M(\chi)\end{pmatrix}, \quad \chi = \sqrt{\alpha}\frac{y - k_x l_B^2}{l_B} + \frac{t_\perp^s l_B}{\sqrt{\alpha}v_F}E^0_{m,\alpha B}.$$

With the previously found solution $\theta = -\tanh^{-1} t_x^s$, we get the rather simple form

$$e^{\theta\sigma_x} = \begin{pmatrix} 1 & -st_x^s \\ -st_x^s & 1\end{pmatrix}\frac{1}{\sqrt{1-t_x}}.$$

Where we in the untilted case only have off-diagonal contributions from σ_x, the hyperbolic rotation gives contributions on the diagonal as well.

First, let us consider the exponent of the product. We want to complete the square similarly to what was done for the untilted cone in Section 4.4.1. Due to the extra term in χ, this becomes more elaborate. The exponent in

the current matrix element Eq. (4.144) is of course

$$\exp\{-iq_y y - \frac{1}{2}\chi_k^2 - \frac{1}{2}\chi_{k+\mathrm{q}}^2\}. \tag{4.145}$$

A straightforward but tedious calculation shows that the argument of the exponent can be written as

$$-\frac{\alpha}{l_B^2}\left(y + \frac{l_B^2}{2\alpha}(iq_y - (q_x' + 2k_x'))\right)^2 - \frac{l_B^2}{4\alpha}(q_y^2 + 2i(q_x' + 2k_x')q_y + (q_x')^2), \tag{4.146}$$

where we have defined

$$q_x' = q_x\alpha - \frac{\beta}{v_F}(E^0_{n,\alpha B} - E^0_{m,\alpha B}), \tag{4.147}$$

$$k_x' = k_x\alpha - \frac{\beta}{v_F}E^0_{m,\alpha B}. \tag{4.148}$$

These must not be confused with the transformed momenta $\tilde{k}$, which are similar in form. Eq. (4.146) is on the same form as in the untilted cone case, and we may thus proceed with the same method. Make a change of variable

$$\tilde{y} = \frac{\sqrt{\alpha}}{l_B}\left(y + \frac{l_B^2}{2\alpha}(iq_y - 2k_x' - q_x')\right),$$

to get the exponent on the form $e^{-\tilde{y}^2}$. With this substitution,

$$\chi_k = \tilde{y} + \frac{l_B}{2\sqrt{\alpha}}\left(q_x' - iq_y\right), \tag{4.149}$$

$$\chi_{k+\mathrm{q}} = \tilde{y} + \frac{l_B}{2\sqrt{\alpha}}\left(-q_x' - iq_y\right). \tag{4.150}$$

The first part of the current matrix element, Eq. (4.144), is thus

$$\begin{aligned} J^{(1)}_{kms;k+\mathrm{q}ns}(\boldsymbol{q}) = \frac{sv_F e}{\sqrt{\alpha}}\int \mathrm{d}\tilde{y}\, l_B \exp\left[-\frac{l_B^2}{4\alpha}\left(q_y^2 + 2i(2k_x' + q_x')q_y + (q_x')^2\right)\right] \\ \times e^{-\tilde{y}^2}\left[a_{kms}b_{k+\mathrm{q}ns}H_{M-1}\left(\chi_k\right)H_N\left(\chi_{k+\mathrm{q}}\right)\right. \\ - st_x a_{kms}a_{k+\mathrm{q}ns}H_{M-1}\left(\chi_k\right)H_{N-1}\left(\chi_{k+\mathrm{q}}\right) \\ + b_{kms}a_{k+\mathrm{q}ns}H_M\left(\chi_k\right)H_{N-1}\left(\chi_{k+\mathrm{q}}\right) \\ \left. - st_x b_{kms}b_{k+\mathrm{q}ns}H_M\left(\chi_k\right)H_N\left(\chi_{k+\mathrm{q}}\right)\right]. \end{aligned} \tag{4.151}$$

Next consider the second term of the current operator,

$$J^{(2)}_{kms;k+\mathrm{q}ns}(\boldsymbol{q}) = ev_F t_x^s \int \mathrm{d}y e^{-iq_y y} \phi^*_{kms}(y)\phi_{k+\mathrm{q}ns}(y). \tag{4.152}$$

With a procedure similar to above, with the same substitution and completion of the square

$$\begin{aligned} J^{(2)}_{kms;k+\mathrm{q}ns}(\boldsymbol{q}) = \frac{sv_F e t_x^s}{\sqrt{\alpha}} \int \mathrm{d}\tilde{y} l_B \exp\left[-\frac{l_B^2}{4\alpha}(q_y^2 + 2i(2k'_x + q'_x)q_y + (q'_x)^2)\right] \\ \times e^{-\tilde{y}^2}\Big[a_{kms}H_{M-1}(\chi_{\boldsymbol{k}}) s a_{k+\mathrm{q}ns}H_{N-1}(\chi_{k+\mathrm{q}}) \\ - a_{kms}H_{M-1}(\chi_{\boldsymbol{k}}) t_x^s b_{k+\mathrm{q}ns}H_{N}(\chi_{k+\mathrm{q}}) \\ - b_{kms}H_{M}(\chi_{\boldsymbol{k}}) t_x^s a_{k+\mathrm{q}ns}H_{N-1}(\chi_{k+\mathrm{q}}) \\ + s b_{k+\mathrm{q}ns}H_{N}(\chi_{k+\mathrm{q}})\Big]. \end{aligned} \tag{4.153}$$

By inspection, recalling $\sqrt{1-t_x^2} = \alpha$, we see

$$\begin{aligned} J_{kms;k+\mathrm{q}ns}(\boldsymbol{q}) = sv_F e\sqrt{\alpha} \int \mathrm{d}\tilde{y}\, l_B \exp\left[-\frac{l_B^2}{4\alpha}\left(q_y^2 + 2i(2k'_x + q'_x)q_y + (q'_x)^2\right)\right] \\ \times e^{-\tilde{y}^2}\Big[a_{kms}b_{k+\mathrm{q}ns}H_{M-1}\left(\chi_{\boldsymbol{k}}\right) H_N\left(\chi_{k+\mathrm{q}}\right) \\ + b_{kms}a_{k+\mathrm{q}ns}H_M\left(\chi_{\boldsymbol{k}}\right) H_{N-1}\left(\chi_{k+\mathrm{q}}\right)\Big]. \end{aligned} \tag{4.154}$$

The diagonal elements cancel!

To perform the integration, we use the *shifted orthogonality* relation for Hermite polynomials [GZ15, Eq. (7.377)]

$$\int_{-\infty}^{\infty} \mathrm{d}x e^{-x^2} H_m(x+y)H_n(x+z) = 2^n \pi^{\frac{1}{2}} m! y^{n-m} L_m^{n-m}(-2yz), \quad m \le n, \tag{4.155}$$

where L_b^a are the *generalized Laguerre polynomial* of order b and type a. Define

the functions Ξ_1, Ξ_2 by

$$\frac{\sqrt{\alpha}\alpha_{k_z ms}\Xi_1(\boldsymbol{q}, m, n, s)}{\sqrt{\alpha_{k_z ms}^2+1}\sqrt{\alpha_{k_z+\mathrm{q}_z ns}^2+1}} = \int \mathrm{d}\tilde{y}\; e^{-\tilde{y}^2} l_B a_{\boldsymbol{k} ms} b_{\boldsymbol{k}+\mathrm{q} ns} H_{M-1}(\chi_{\boldsymbol{k}}) H_N(\chi_{\boldsymbol{k}+\mathrm{q}}), \tag{4.156}$$

$$\frac{\sqrt{\alpha}\alpha_{k_z+qns}\Xi_2(\boldsymbol{q}, m, n, s)}{\sqrt{\alpha_{k_z ms}^2+1}\sqrt{\alpha_{k_z+\mathrm{q}_z ns}^2+1}} = \int \mathrm{d}\tilde{y}\; e^{-\tilde{y}^2} l_B b_{\boldsymbol{k} ms} a_{\boldsymbol{k}+\mathrm{q} ns} H_{M}(\chi_{\boldsymbol{k}}) H_{N-1}(\chi_{\boldsymbol{k}+\mathrm{q}}). \tag{4.157}$$

Using that

$$a_{\boldsymbol{k} ms} b_{\boldsymbol{k}+\mathrm{q} ns} = \frac{\sqrt{\alpha}\alpha_{k_z ms}}{\sqrt{\alpha_{k_z ms}^2+1}\sqrt{\alpha_{k_z+\mathrm{q}_z ns}^2+1}} \left[2^{N+M-1}(M-1)!N!\pi l_B^2\right]^{-\frac{1}{2}}, \tag{4.158}$$

$$b_{\boldsymbol{k} ms} a_{\boldsymbol{k}+\mathrm{q} ns} = \frac{\sqrt{\alpha}\alpha_{k_z+\mathrm{q}_z ns}}{\sqrt{\alpha_{k_z ms}^2+1}\sqrt{\alpha_{k_z+\mathrm{q}_z ns}^2+1}} \left[2^{N+M-1}(N-1)!M!\pi l_B^2\right]^{-\frac{1}{2}}, \tag{4.159}$$

we use Eq. (4.155) to find explicit expressions

$$\Xi_1^{(1)}(\boldsymbol{q}, m, n, s) = \sqrt{\frac{2^N(M-1)!}{2^{M-1}N!}} \left(\frac{q_x' - iq_y}{2\sqrt{\alpha}} l_B\right)^{N-M+1} L_{M-1}^{N-M+1}\left(\frac{\mathrm{q}_y^2 l_B^2}{2\alpha}\right), \tag{4.160a}$$

$$\Xi_1^{(2)}(\boldsymbol{q}, m, n, s) = \sqrt{\frac{2^{M-1}N!}{2^N(M-1)!}} \left(\frac{-q_x' - iq_y}{2\sqrt{\alpha}} l_B\right)^{M-N-1} L_{N}^{M-N-1}\left(\frac{\mathrm{q}_y^2 l_B^2}{2\alpha}\right), \tag{4.160b}$$

$$\Xi_1(\boldsymbol{q}, m, n, s) = \begin{cases} \Xi_1^{(1)} & \text{if } N \geq M-1 \\ \Xi_1^{(2)} & \text{if } N \leq M-1 \end{cases} \text{ for } M > 0, N \geq 0, \tag{4.160c}$$

$$\Xi_2^{(1)}(\boldsymbol{q},m,n,s)=\sqrt{\frac{2^{N-1}M!}{2^M(N-1)!}}\left(\frac{q_x'-iq_y}{2\sqrt{\alpha}}l_B\right)^{N-1-M}L_M^{N-1-M}\left(\frac{\mathfrak{q}_y^2l_B^2}{2\alpha}\right), \tag{4.161a}$$

$$\Xi_2^{(2)}(\boldsymbol{q},m,n,s)=\sqrt{\frac{2^M(N-1)!}{2^{N-1}M!}}\left(\frac{-q_x'-iq_y}{2\sqrt{\alpha}}l_B\right)^{M-N+1}L_{N-1}^{M-N+1}\left(\frac{\mathfrak{q}_y^2l_B^2}{2\alpha}\right), \tag{4.161b}$$

$$\Xi_2(\boldsymbol{q},m,n,s)=\begin{cases}\Xi_2^{(1)} & \text{if } N-1\geq M\\ \Xi_2^{(2)} & \text{if } N-1\leq M\end{cases}\quad\text{for } M\geq 0, N>0, \tag{4.161c}$$

Here, $\mathfrak{q}_y=(q_x',q_y)$.

Thus, the current matrix element in terms of the functions Ξ_i is

$$\begin{aligned}J_{kms;k+\mathfrak{q}ns}(\boldsymbol{q})=ev_Fs\alpha^2&\frac{\exp\left[-\frac{l_B^2}{4\alpha}(q_y^2+2i(2k_x'+q_x')q_y+(q_x')^2)\right]}{\sqrt{\alpha_{k_zms}^2+1}\sqrt{\alpha_{k_z+\mathfrak{q}_zns}^2+1}}\\&\times\left[\alpha_{k_zms}\Xi_1(\boldsymbol{q},m,n,s)+\alpha_{k_z+\mathfrak{q}_zns}\Xi_2(\boldsymbol{q},m,n,s)\right].\end{aligned} \tag{4.162}$$

Energy-momentum tensor

Consider now the energy-momentum tensor matrix element, taking $t_y=0$,

$$T^{0y}_{k+\mathfrak{q}ns,kms}(\boldsymbol{q})=\frac{1}{2}\int \mathrm{d}y e^{iq_yy}\phi^*_{k+\mathfrak{q}ns}(y)s\sigma^y(E_{k_zms}+E_{k_z+\mathfrak{q}_zns}-2\mu)\phi_{kms}(y). \tag{4.163}$$

As

$$\sigma_y e^{\theta/2\sigma_x}=e^{-\theta/2\sigma_x}\sigma_y \tag{4.164}$$

we get the very fortunate result

$$\phi^*\sigma_y\phi=\frac{1}{\mathcal{N}^*\mathcal{N}}\tilde{\phi}^*\sigma_y\tilde{\phi}=\alpha\tilde{\phi}^*\sigma_y\tilde{\phi}. \tag{4.165}$$

The energy-momentum tensor thus has the exact same form as the untilted case, however with a prefactor α and using the transformed coordinates χ. We thus get

$$\begin{aligned}T^{0y}_{k+\mathfrak{q}ns,kms}(\boldsymbol{q})=\frac{is\alpha}{2}&(E_{k_zms}+E_{k_z+\mathfrak{q}_zns}-2\mu)\int \mathrm{d}y e^{iq_yy}e^{-\frac{1}{2}(\chi^2_{k+\mathfrak{q}}+\chi^2_k)}\\&\times[-a_{k+\mathfrak{q}ns}b_{kms}H_{N-1}(\chi_{k+\mathfrak{q}})H_M(\chi_k)\\&+b_{k+\mathfrak{q}ns}a_{kms}H_N(\chi_{k+\mathfrak{q}})H_{M-1}(\chi_k)].\end{aligned} \tag{4.166}$$

We will perform once again the completion of the square and substitution of y. The exponent is the same as that which we found for the current operator case, Eq. (4.146), with the change $q_y \to -q_y$. We thus make the change of variables

$$\tilde{y} = \frac{\sqrt{\alpha}}{l_B}\left(y - \frac{l_B^2}{2\alpha}(iq_y + (2k'_x + q'_x))\right), \tag{4.167}$$

giving

$$\chi_k = \tilde{y} + \frac{l_B}{2\sqrt{\alpha}}\left(q'_x + iq_y\right), \tag{4.168}$$

$$\chi_{k+\mathfrak{q}} = \tilde{y} + \frac{l_B}{2\sqrt{\alpha}}\left(-q'_x + iq_y\right). \tag{4.169}$$

Thus, after inserting and employing the defining relations for the Ξ_i functions, the matrix element reads

$$T^{0y}_{k+\mathfrak{q}ns,kms}(\boldsymbol{q}) = \frac{is\alpha}{2}\frac{E_{k_zms} + E_{k_z+\mathfrak{q}_zns} - 2\mu}{\sqrt{\alpha^2_{k_zms}+1}\sqrt{\alpha^2_{k_z+\mathfrak{q}_zns}+1}} \tag{4.170}$$

$$\exp\left[-\frac{l_B^2}{4\alpha}(q_y^2 - 2i(2k'_x + q'_x)q_y + (q'_x)^2)\right] \tag{4.171}$$

$$(-\alpha_{k_z+\mathfrak{q}_zns}\Xi_2(\bar{\boldsymbol{q}},m,n,s) + \alpha_{k_zms}\Xi_1(\bar{\boldsymbol{q}},m,n,s)), \tag{4.172}$$

where $\bar{\boldsymbol{q}} = (q_x, -q_y, q_z)$.

Summary 6

In summary, we have

$$J_{kms;k+\mathfrak{q}ns}(\boldsymbol{q}) = v_F e s\alpha^2 \Gamma^-_{k\mathfrak{q}mns}\Big[\alpha_{k_zms}\Xi_1(\boldsymbol{q},m,n,s) + \alpha_{k_z+\mathfrak{q}_zns}\Xi_2(\boldsymbol{q},m,n,s)\Big], \tag{4.173}$$

$$T^{0y}_{k+\mathfrak{q}ns,kms}(\boldsymbol{q}) = \frac{is\alpha}{2}\Gamma^+_{k\mathfrak{q}mns}(E_{k_zms} + E_{k_z+\mathfrak{q}_zns} - 2\mu) \times [-\alpha_{k_z+\mathfrak{q}_zns}\Xi_2(\bar{\boldsymbol{q}},m,n,s) + \alpha_{k_zms}\Xi_1(\bar{\boldsymbol{q}},m,n,s)], \tag{4.174}$$

with $\bar{\boldsymbol{q}} = (q_x, -q_y, q_z)$ *and*

$$\Gamma^{\pm}_{k\mathfrak{q}mns} = \frac{\exp\left[-\frac{l_B^2}{4\alpha}(q_y^2 + (q'_x)^2) \pm iq_y l_B^2(k'_x + \frac{q'_x}{2})\right]}{\left[(\alpha^2_{k_zms}+1)(\alpha^2_{k_z+\mathfrak{q}_zns}+1)\right]^{\frac{1}{2}}}.$$

4.5.2. Static limit and dimensionless form of the matrix elements

We are interested in the response in the static limit $q \to 0$. As before, we use the property of limits of products

$$\lim_{n\to a} A \cdot B = \lim_{n\to a} A \cdot \lim_{n\to a} B.$$

We may thus consider the limits of the current and energy-momentum matrix elements separately, as we did in the untilted case. Furthermore, to facilitate for more easily solving the integration later, we will use the same dimensionless energy and momentum $\epsilon_{\kappa_z ms} = v_F\sqrt{2eB}E_{k_z ms}$, $\kappa_z = \sqrt{2eB}k_z$ as before, where B is importantly still the actual magnetic field, and not the rescaled αB. Consider firstly the exponent in the $\Gamma^{\pm}$ factor from summary 6,

$$\Gamma^{\pm}_{kqmns} \propto \exp\left[-\frac{l_B^2}{4\alpha}(q_y^2 + (q_x')^2) \pm i q_y l_B^2 (k_x' + \frac{q_x'}{2})\right].$$

Define

$$P = \lim_{q\to 0} \frac{l_B q_x'}{\sqrt{2\alpha}} = \frac{t_x}{\sqrt{\alpha}}(\epsilon^0_{n,\alpha B} - \epsilon^0_{m,\alpha B}), \tag{4.175}$$

where q_x' was defined in Eq. (4.147),

$$q_x' = q_x\alpha - \frac{\beta}{v_F}(E^0_{n,\alpha B} - E^0_{m,\alpha B}).$$

In the limit, the exponent is thus

$$\lim_{q\to 0} \Gamma_{kqmns} \propto \exp\left[-\frac{\beta^2}{2\alpha}(\epsilon^0_{n,\alpha B} - \epsilon^0_{m,\alpha B})^2\right]. \tag{4.176}$$

The normalization factor $\alpha_{k_z ms}$ is independent on q, and already dimensionless. Explicitly, it is given in dimensionless quantities as

$$\alpha_{k_z ms} = -\frac{\sqrt{2e\alpha BM}}{\frac{E_{k_z ms} - t_\parallel v_F k_z}{v_F s\alpha} - k_z} = -\frac{\sqrt{\alpha M}}{s\epsilon^0_{m,\alpha B} - \kappa}. \tag{4.177}$$

When there is a non-zero tilt, the Ξ_i functions, defined in Eqs. (4.160) and (4.161), do not have a trivial form in the static limit. Expressed in the quantities introduced here, they simplify to

$$\Xi_1^{(1)}(q, m, n, s) = \sqrt{\frac{2^N(M-1)!}{2^{M-1}N!}}\left(\frac{P}{\sqrt{2}}\right)^{N-M+1} L_{M-1}^{N-M+1}\left(P^2\right), \tag{4.178a}$$

$$\Xi_1^{(2)}(q, m, n, s) = \sqrt{\frac{2^{M-1}N!}{2^N(M-1)!}}\left(-\frac{P}{\sqrt{2}}\right)^{M-N-1} L_N^{M-N-1}\left(P^2\right), \tag{4.178b}$$

$$\Xi_2^{(1)}(\boldsymbol{q},m,n,s) = \sqrt{\frac{2^{N-1}M!}{2^M(N-1)!}}\left(\frac{P}{\sqrt{2}}\right)^{N-1-M} L_M^{N-1-M}\left(P^2\right), \tag{4.179a}$$

$$\Xi_2^{(2)}(\boldsymbol{q},m,n,s) = \sqrt{\frac{2^M(N-1)!}{2^{N-1}M!}}\left(-\frac{P}{\sqrt{2}}\right)^{M-N+1} L_{N-1}^{M-N+1}\left(P^2\right), \tag{4.179b}$$

Lastly, notice that in the static limit, the entire expression of the response function is independent of k_x, and so the same procedure as was done for the untilted cone in Section 4.4.2 is valid for the tilted cone, replacing the $\boldsymbol{k}$ sum with an integral over k_z and a degeneracy factor

$$\sum_{\boldsymbol{k}} \to \frac{\mathcal{V}eB}{(2\pi)^2}\int \mathrm{d}k_z. \tag{4.180}$$

Importantly, the degeneracy factor does *not* depend on the renormalized magnetic field αB, but rather B itself.

4.5.3. Tilt perpendicular to the magnetic field

We consider here the specialized situation where $\boldsymbol{t} = t_x\hat{x}$, i.e. only tilt perpendicular to the magnetic field. The response function

$$\begin{aligned}\lim_{\omega\to 0}\lim_{\boldsymbol{q}\to 0}\chi^{xy}(\omega,\boldsymbol{q}) = \frac{eBiv_F}{(2\pi)^2}\sum_{mn}\int \mathrm{d}k_z[n_{kms}-n_{kns}] \\ \times \frac{J^x_{kms,kns}(\boldsymbol{q}\to 0)T^{y0}_{kns,kms}(\boldsymbol{q}\to 0)}{(E_{k_zms}-E_{k_zns})(E_{k_zms}-E_{k_zns})}.\end{aligned} \tag{4.181}$$

Writing out the matrix products we have

$$\begin{aligned}J^x_{kms,kns}(\boldsymbol{q}\to 0)T^{y0}_{kns,kms}(\boldsymbol{q}\to 0) = \frac{v_F ei\alpha^3}{2}e^{-P^2} \\ \times \frac{(E_{k_zms}+E_{k_zns})(\alpha^2_{k_zms}\Xi_1(0,m,n,s)^2 - \alpha^2_{k_zns}\Xi_2(0,m,n,s)^2)}{(\alpha^2_{k_zms}+1)(\alpha^2_{k_zns}+1)}.\end{aligned} \tag{4.182}$$

And so, inserting into the response function

$$\begin{aligned}\lim_{\omega\to 0}\lim_{\boldsymbol{q}\to 0}\chi^{xy}(\omega,\boldsymbol{q}) = \frac{-e^2\alpha^3 v_F B}{2(2\pi)^2}\sum_{mn}\int \mathrm{d}\kappa_z e^{-P^2}[n_{\kappa_z ms}-n_{\kappa_z ns}](\epsilon_{\kappa_z ms}+\epsilon_{\kappa_z ns}) \\ \times \frac{(\alpha^2_{\kappa_z ms}\Xi_1(0,m,n,s)^2 - \alpha^2_{\kappa_z ns}\Xi_2(0,m,n,s)^2)}{(\alpha^2_{\kappa_z ms}+1)(\alpha^2_{\kappa_z ns}+1)(\epsilon_{\kappa_z ms}-\epsilon_{\kappa_z ns})^2},\end{aligned} \tag{4.183}$$

where we also made a change of variables $k_z = \sqrt{2eB}\kappa_z$.

We make the observation that $\Xi_1(m,n) = \Xi_2(n,m)$, where it is important to note that P changes sign under interchange of m, n. The rest of the factors are invariant under the interchange $m \leftrightarrow n$, except for the step functions, which give an overall sign change. Thus, using $\Xi_1(m,n) = \Xi_2(n,m)$ and relabelling the summation indices we may consider

$$\alpha^2_{\kappa_z ms}\Xi_1^2 - \alpha^2_{\kappa_z ns}\Xi_2^2 \to 2\alpha^2_{\kappa_z ms}\Xi_1^2.$$

We may also simplify the step function expression. Physically, the step function term corresponds to only considering transitions between states with energies of opposite signs. For Type-I systems, which we are restricted to here as we consider currently only perpendicular tilt, the energy of the state with quantum number n has the same sign as n itself, excluding of course the zeroth state. For the zeroth state, the sign of the energy is $\text{sign}(-s\kappa_z)$. Using these considerations, we may make certain selection rules for the sum. In the (m,n)-plane, the first and third quadrants give no contribution, as there $mn > 0$, i.e. they have the same sign. Our sum is thus restricted to the second and fourth quadrant. It is easy to show that

$$n_{kms} - n_{k+\mathfrak{q}ns} = \begin{cases} 0 & mn > 0 \text{ or } m,n = 0, \\ -\text{sign}(m) & m,n \neq 0, \\ \text{sign}(n)\theta(\text{sign}(n)s\kappa) & m = 0, \\ -\text{sign}(m)\theta(\text{sign}(m)s\kappa) & n = 0. \end{cases} \tag{4.184}$$

Furthermore, the contributions from the second and fourth quadrants are equal, which we will now show. The mapping $(m,n,\kappa_z) \mapsto (-m,-n,-\kappa_z)$, i.e. a π rotation and κ_z inversion, transforms points from the $m < 0$ half plane to the $m > 0$ half plane, including mapping the second quadrant to the fourth quadrant. We want to consider how the integrand in question transforms under such a mapping. Recall

$$\alpha_{\kappa_z ms} = -\frac{\sqrt{\alpha M}}{s\epsilon^0_{m,\alpha B} - \kappa_z},$$
$$\epsilon^0_{m,\alpha B} = \text{sign}(m)\sqrt{\alpha M + \kappa_z^2}, \quad m \neq 0.$$

Under the above mapping, we have the following relations

$$\epsilon^0_{m,\alpha B} \mapsto -\epsilon^0_{m,\alpha B}, \tag{4.185}$$
$$\alpha_{\kappa_z ms} \mapsto -\alpha_{\kappa_z ms}, \tag{4.186}$$
$$P \mapsto -P. \tag{4.187}$$

The Ξ functions also acquires a sign for some values of m, n, however, we only consider Ξ^2. The integrand in Eq. (4.183) is thus invariant under the transformation from the second to the fourth quadrant, and so we may consider only the fourth quadrant, adding a degeneracy factor 2. The summation region is shown in Fig. 4.6.

Lastly, completely analogous to the untilted case, the integrand only depend on s and κ_z through their product $s\kappa_z$, and thus is invariant under $(s, \kappa_z) \mapsto (-s, -\kappa_z)$. As the integral spans all of κ_z, the contribution is independent of the chirality s and may be calculated for a specific choice, which is here taken to be $s = +1$.

Summary 7

The response of a perpendicularly tilted cone with chirality s is given by

$$\lim_{\omega\to 0}\lim_{q\to 0}\chi^{xy}(\omega, q) = \frac{e^2 v_F B}{2(2\pi)^2}\gamma_{\bar{N}}^{t_x}, \tag{4.188}$$

with

$$\gamma_{\bar{N}}^{t_x} = -4\alpha^3 \sum_{mn}^{\bar{N}} \int \mathrm{d}\kappa_z e^{-P^2} \frac{(\epsilon_{\kappa_z ms} + \epsilon_{\kappa_z ns})\alpha_{\kappa_z ms}^2 \Xi_1(0, m, n, s)^2}{(\alpha_{\kappa_z ms}^2 + 1)(\alpha_{\kappa_z ns}^2 + 1)(\epsilon_{\kappa_z ms} - \epsilon_{\kappa_z ns})^2}, \tag{4.189}$$

where the summation goes over $m > 0, n \leq 0$, indicated in Fig. 4.6, capped at the Landau level $\bar{N}$. The integration limits are $(-\infty, \infty)$, except for $n = 0$, where they are $[0, \infty)$.

The tilt t_x enters the expression only through its square, in α and P, and so the contribution is even in t_x.

4.5.4. Tilt parallel to the magnetic field

Even though the treatment above for a general tilt is valid for parallel tilt, the response can be found more directly from the untilted case. For $\boldsymbol{t} = t_z\hat{z}$, the energy momentum tensor T^{y0}, charge current J^x, and wave functions $\phi(\boldsymbol{r})$ are all independent of t_z, and the only difference compared to the untilted system is a change in the energies of the Landau levels. We may thus immediately use the result from the untilted case

$$\begin{aligned}\lim_{\omega\to 0}\lim_{q\to 0}\chi^{xy} = -\frac{e^2 v_F B}{2(2\pi)^2}\sum_{mn}\int \mathrm{d}\kappa_z \xi(\kappa_z, m, n)(\epsilon_{\kappa_z ms} + \epsilon_{\kappa_z ns}) \\ \times (\alpha_{\kappa_z ms}^2 \delta_{M-1,N} - \alpha_{\kappa_z ns}^2 \delta_{N-1,M}),\end{aligned} \tag{4.190}$$

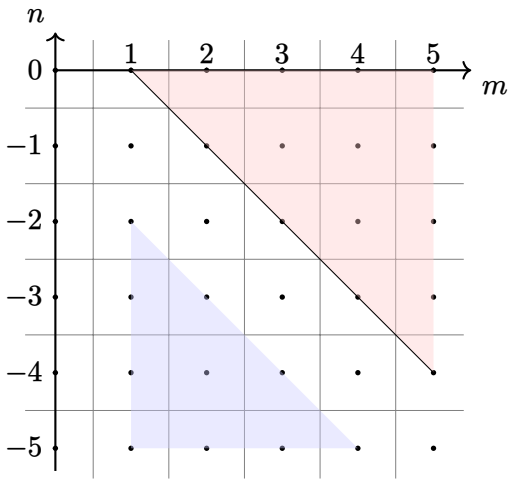

Figure 4.6.: The region of (m, n) to sum over for a Type-I perpendicularly tilted cone. The black line represents the combinations that give a finite contribution also in the untilted case. As the cone is tilted, this sharp line "diffuse" into the red and blue regions as well, where the contribution is respectively positive and negative. Note that, as Ξ_1 defined only for $M > 0$, the region with $m = 0$ gives no contribution; at $M = N$ the contribution is also zero.

with

$$\epsilon_{\kappa_z m s} = \begin{cases} t_z^s \kappa_z + \operatorname{sign} m \sqrt{M + \kappa_z^2} & m \neq 0, \\ (t_z^s - s)\kappa_z & m = 0, \end{cases} \tag{4.191}$$

$$\alpha_{\kappa_z m s} = -s \frac{\sqrt{M}}{\epsilon^0_{\kappa_z m s} - s\kappa_z}, \tag{4.192}$$

$$\lim_{\omega \to 0} \lim_{q \to 0} \xi(\kappa_z, m, n) = \frac{\left[n_{\kappa m s} - n_{\kappa n s}\right] \left[(\alpha^2_{\kappa m s} + 1)(\alpha^2_{\kappa n s} + 1)\right]^{-1}}{(\epsilon_{\kappa m s} - \epsilon_{\kappa n s})^2}. \tag{4.193}$$

In the untilted case, we made several simplifications to this expression, especially with regard to limiting the summation domain. We will here consider which of those simplifications apply also in the case of tilt t_z.

Under the transformation $(m, n, \kappa_z) \mapsto (-m, -n, -\kappa_z)$, the factors of the integrand $\xi(\kappa_z, m, n), \epsilon_{\kappa_z m s}, \alpha_{\kappa_z m s}$ are all still odd, and so the integrand is invariant under such a transformation. As the integral is over all κ_z, we may therefore consider only half the m, n plane, as was the case in the untilted case. However, in the untilted case, the sum was restricted to only one quadrant,

as at $T \to 0$ the transitions must be between states with energies of opposite signs. In the case of Type-II systems, this requirement does not restrict the sum to one quadrant. It is thus convenient to consider Type-I and Type-II separately.

In the untilted system, the contributions from the two chiralities were the same. In the case of t_z tilt, this is not the case. The proof for the response from the two chiralities being the same in the untilted case was that s and κ_z appeared only through the product $s\kappa_z$, and so the expression was invariant under $(s, \kappa_z) \mapsto (-s, -\kappa_z)$. As our integration spans all κ_z, the total response is invariant under $s \to -s$. The tilt parameter enters the expression only through $\epsilon_{\kappa_z m s} = \epsilon^0_{\kappa_z m s} + \kappa_z t_z^s$, and in the inversion symmetric case, $t_z^s = s t_z$, the argument still holds. In the case of broken inversion symmetry, however, where $t_z^s = t_z$, the argument fails. A similar argument may, however, be made for the transformation $(s, \kappa_z, t_z) \mapsto (-s, -\kappa_z, -t_z)$, for which the (inversion broken) system is invariant. The response of a cone with chirality $s = -1$ is thus equal the response with $s = +1$ and $t_z \to -t_z$. We therefore compute all responses for $s = +1$; for symmetric systems the response is equal for $s = -1$, while for broken inversion symmetry, the response is given at $t_z \to -t_z$.

Type-I

In Type-I systems, the selection rules from the step functions are independent of t_z, and the only difference from the untilted case is the term $\epsilon_{\kappa_z m s} + \epsilon_{\kappa_z n s} = \epsilon^0_{\kappa_z m s} + \epsilon^0_{\kappa_z n s} + 2\kappa_z t_z^s$. The response is therefore

$$\lim_{\omega \to 0} \lim_{q \to 0} \chi^{xy} = \frac{e^2 v_F B}{2(2\pi)^2} (\gamma^0_{\bar{N}} + \gamma_{\mathrm{div}, \bar{N}}), \tag{4.194}$$

where $\gamma^0_{\bar{N}}$ is the prefactor of the untilted case, and according to Eq. (4.139)

$$\gamma_{\mathrm{div}, \bar{N}} = -4 \sum_{i=0}^{\bar{N}} \int \mathrm{d}\kappa_z \xi(\kappa_z) 2\kappa_z t_z^s \alpha^2_{\kappa_z m s} \Big|_{\substack{m = i+1 \\ n = -i}}, \tag{4.195}$$

which has a UV divergence. Introduce the momentum cutoff Λ, in which case the integral can be solved analytically, with the result

$$\gamma_{\mathrm{div}, 0} = 2 t_z \left(\Lambda \left(\Lambda - \sqrt{\Lambda^2 + 1} \right) + \sinh^{-1}(\Lambda) \right) \tag{4.196}$$

and the contribution from each term of the sum

$$\gamma_{\mathrm{div},\bar{N}} - \gamma_{\mathrm{div},\bar{N}-1} = 2t_z \Bigg\{ \Lambda \left(\sqrt{\Lambda^2 + \bar{N}} - \sqrt{\Lambda^2 + \bar{N} + 1} \right) + (\bar{N}+1) \tanh^{-1} \left[\frac{\Lambda}{\sqrt{\Lambda^2 + \bar{N} + 1}} \right] - \bar{N} \tanh^{-1} \left[\frac{\Lambda}{\sqrt{\Lambda^2 + \bar{N}}} \right] \Bigg\}, \quad (4.197)$$

where we used the selection rule of the sum $N = M - 1$ and $m > 0, n < 0$. The contribution (4.197) is odd in t_z, and so for systems with broken inversion symmetry, the total contribution from two cones cancels.

Type-II

For Type-I semimetals, the sign of energy state $m \neq 0$ is given by the sign of m itself. For $m = 0$ the sign of the energy is given by $-s \operatorname{sign} \kappa$. Due to this, the sum is restricted to $n = M + 1, m = -M$ and $n = -M - 1, m = M$. In the case of Type-II, however, the situation is not so simple. The energy bands cross the Fermi surface, and we must also include in our sum overlap between states of the same sign, i.e. $n = M + 1, m = M$ and $n = -M - 1, m = -M$, which is non-zero for certain intervals of κ. See plot of the tilted Landau levels in Fig. 4.4 (on page 70).

In order to find explicitly the limits of integration for the Type-II case, we must find the roots of the energy levels. The zeroth Landau level always has only one root, which is in the origin. For the higher order Landau levels, we solve

$$\epsilon_{\kappa_z m s} = t_z^s \kappa_z + \operatorname{sign}(m) \sqrt{M + \kappa_z^2} = 0, \quad (4.198)$$

whose solution is

$$\kappa_z^2 = \frac{M}{t_z^2 - 1}.$$

The actual roots of the energies are

$$\kappa_z = -\operatorname{sign}(m t_x^s) \sqrt{\frac{M}{t_z^2 - 1}}. \quad (4.199)$$

The integration limit for the $0 \to 1$ transition is thus, for $t_z > 1$, $[-\sqrt{t_z^2 - 1}^{-1}, 0]$. The $1 \to 2$ transition is $[-\sqrt{2}/\sqrt{t_z^2 - 1}, -\sqrt{t_z^2 - 1}^{-1}]$, and so forth. The general $n \to m$ transition has the integration limits

$$\left[-\operatorname{sign}(t_z) \sqrt{\frac{m}{t_z^2 - 1}}, -\operatorname{sign}(t_z n) \sqrt{\frac{-n}{t_z^2 - 1}} \right].$$

The $0 \to 1$ transitions was computed analytically, and found to be

$$\gamma_0 = 2\,\mathrm{sign}(t_z)\left(|t_z|\sinh^{-1}\left(\frac{1}{\sqrt{t_z^2-1}}\right)-1\right). \tag{4.200}$$

For a general $n \to m$, $N > 0, M = N+1$ transition, the contribution $\gamma_{\bar{N}} - \gamma_{\bar{N}-1}$ was found to have very lengthy expressions. Consult Table 4.2 to find the appropriate expressions for positive and negative tilt, and interband and intraband transitions.

Table 4.2.: Decision matrix for the expression of the $m \to n; N > 0, M = N+1$ transition over different regions. Expressions given in Mathematica code format. The code listings are found in Appendix A. See main text for details.

		Tilt direction	
		$t_x > 1$	$t_x < -1$
Band type	$n < 0$	Lst. A.1	Lst. A.2
	$n > 0$	Lst. A.3	Lst. A.4

4.6. Results

In the static and local limit $\lim_{\omega\to 0}\lim_{\boldsymbol{q}\to 0}$ the transverse response function χ^{xy} of the charge current to a temperature perturbation

$$J^x = \chi^{xy}\left(\frac{-\nabla^y T}{T}\right) \tag{4.201}$$

from a single Weyl cone was found to be

$$\lim_{\omega\to 0}\lim_{\boldsymbol{q}\to 0}\chi^{xy} = \gamma_{\bar{N}}\frac{e^2 B v_F}{2(2\pi)^2\hbar}, \tag{4.202}$$

with $\gamma_{\bar{N}}$ a prefactor dependent on the chirality s, the tilt $\boldsymbol{t}$, and how many Landau levels $\bar{N}$ are included in the final evaluation of the response function. Here we have also reinserted the explicit $\hbar$.

In general, the prefactor $\gamma_{\bar{N}}$ diverges as $\bar{N} \to \infty$. However, not all Landau levels are filled, and thus the sum should not be taken to all levels. Similarly to a quantum Hall effect, the number of filled bands, the filling factor ν, is inverse proportional to the B-field strength

$$\nu \propto \frac{1}{B}. \tag{4.203}$$

Thus, we expect that the N-sum should be truncated at a Landau level, given by the filling factor ν. A detailed derivation of the exact truncation of the N-sum has not been done.

As described earlier, the contribution from the cone with chirality $s = -1$ can be found from the result of the positive chirality cone. In the case of perpendicular tilt, they are exactly the same. In the case of parallel tilt, it depends on the symmetry of the tilt. For systems with inversion symmetry, the responses from the two cones are the same. On the other hand, for broken inversion symmetry, the contribution from the cone with chirality $s = -1$ is the same as that of the $s = +1$ cone at the opposite tilt $t_z \to -t_z$. Therefore, it is useful to separate the contribution into even and odd components, for finding the total contribution from the two cones combined. Separating even and odd components also allows for presenting the data in more compact plots.

For some contribution $\gamma(t_{x/z})$, we define

$$\gamma_{\text{even}}(t_{x/z}) = \frac{\gamma(t_{x/z}) + \gamma(-t_{x/z})}{2}, \tag{4.204}$$

$$\gamma_{\text{odd}}(t_{x/z}) = \frac{\gamma(t_{x/z}) - \gamma(-t_{x/z})}{2}. \tag{4.205}$$

All results will be given in terms of these components, at $t_{x/y} > 0$. The total contribution γ_{tot} for the two cones is found by taking the appropriate combinations of Eqs. (4.204) and (4.205), as shown in Table 4.3.

4.6.1. Tilt perpendicular to the magnetic field

In the case of a tilt perpendicular to the magnetic field, we are, as previously explained, restricted to Type-I materials, as the Landau level description breaks down for Type-II perpendicular tilt. Importantly, this does not generally mean that the effect is not present for Type-II systems, but simply that the linear model Landau level description is not a good basis for the system. The collapse of the Landau levels caused Soluyanov et al. [Sol+15] to

Table 4.3.: The total contribution from two cones γ_{tot} is found by linear combinations of the even and odd components of γ, depending on the case at hand. Note that total contribution given in the table is $\gamma_{\text{tot}}/2$.

Case	Total contribution, $\gamma_{\text{tot}}/2$
Perpendicular tilt	$\gamma_{\text{even}} + \gamma_{\text{odd}} = \gamma$
Parallel tilt, broken inversion symmetry	γ_{even}
Parallel tilt, inversion symmetry	$\gamma_{\text{odd}} + \gamma_{\text{even}} = \gamma$

erroneously predict the collapse of the chiral anomaly in their now-famous paper first describing Type-II Weyl semimetals.

As explained in Section 4.5.3, the m, n summation is restricted to the fourth quadrant in the m, n plane. In the case of no tilt, only contributions from $M = N + 1$ were non-zero; we named the contribution from the $0 \to 1$ transition γ_0, the $-1 \to 2$ transition γ_1 and so forth. For perpendicular tilt, as there are contributions also away from the $M = N + 1$ line, we denote by γ_0 the contributions from inside the square of length 2 centered at the origin. The γ_1 contributions are those inside the square of length 4, and in general γ_n the square with length $2n$. This is indicated in Fig. 4.7. This definition effectively sets a ceiling on which Landau levels we consider.

The integral was computed numerically for $M, N \leq 14$ over different values of t_x with $t_z = 0$, with the individual contributions shown in Fig. 4.7. Note that the figure shows contributions for the entire m, n-plane, not only the fourth quadrant as discussed above. This is purely for illustration purposes, and only the fourth quadrant needs to be computed. The total contribution $\gamma_{\bar{N}}$ as a function of $\bar{N}$ is shown in Fig. 4.8. The contribution is even in t_x, and the two cones have the same contribution, as shown analytically in Section 4.5.3. Also shown in Fig. 4.8 is γ_0 as a function of t_x, which is seen to be strictly decreasing to zero as $t_x \to 1$. This last observation is discussed further in Section 4.6.3, under "Perpendicular tilt with only zeroth level transitions".

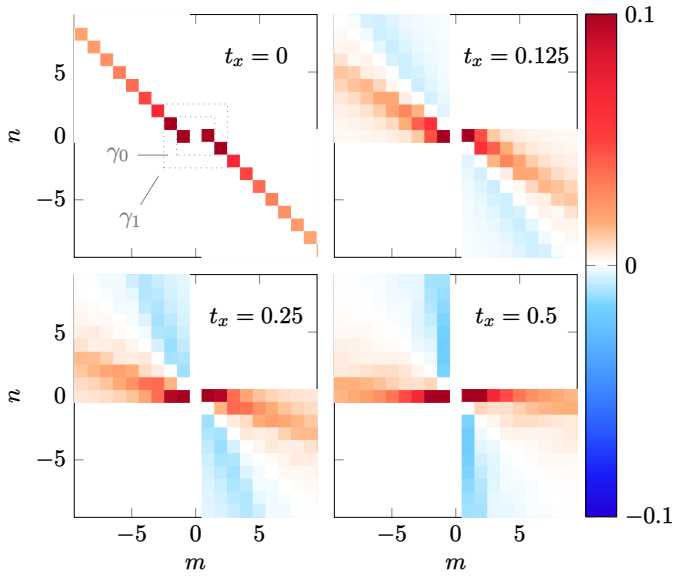

Figure 4.7.: Contributions to $\gamma_{\bar{N}}$ from $m \to n$ transitions for different values of t_x. In order to retain contrast, the color values are capped at 0.1, meaning that the γ_0 contributions are clipped. The squares indicating $\gamma_{\bar{N}}$ are drawn with sides 1 larger than their definitions, as the colored tiles have edges at half-integer values.

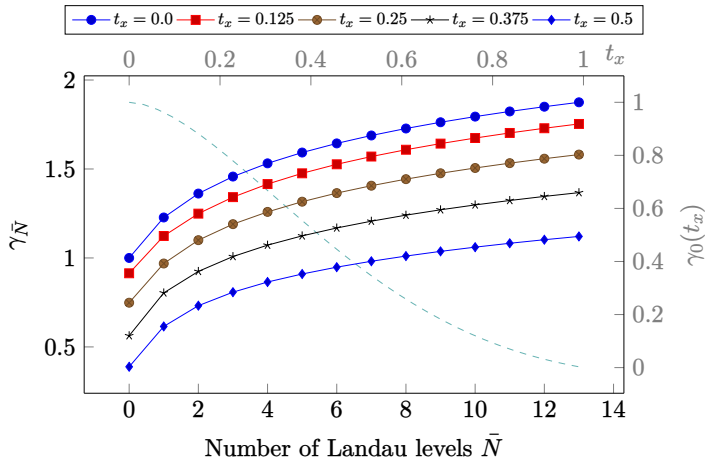

Figure 4.8.: Total contribution $\gamma_{\bar{N}}$ for a perpendicular tilt t_x, which only has an even component. See main text for details on how γ_N is defined. Shown in dashed teal on secondary axis (gray labels) is γ_0 as a function of t_x, which is strictly decreasing from 1 at $t_x = 0$ to 0 at $t_x = 1$.

4.6.2. Tilt parallel to the magnetic field

In the Type-I regime, the contributions differ from that of the untilted system by $\gamma_{\mathrm{div},\bar{N}}$, Eq. (4.195), dependent on a momentum cutoff $\Lambda = k^{\mathrm{cutoff}}/\sqrt{2eB}$, where k^{cutoff} is the physical cutoff. The explicit form of the contribution was found analytically, given in Eqs. (4.196) and (4.197). The contribution from each new Landau level, $\gamma_{\mathrm{div},\bar{N}} - \gamma_{\mathrm{div},\bar{N}}$ is shown in Fig. 4.9 for some of the lowest Landau levels. In the large cutoff limit, $\Lambda \gg 1$, expanding and dropping terms $\mathcal{O}(1/\Lambda^2)$, we find,

$$\gamma_{\mathrm{div},\bar{N}} - \gamma_{\mathrm{div},\bar{N}-1} = t_z \left(\left[-1 + \bar{N} \log\left(\frac{\bar{N}}{\bar{N}+1} \right) - \log \frac{\bar{N}+1}{4} \right] + 2 \log \Lambda \right). \tag{4.206}$$

The first term, independent of Λ, is a negative factor that decreases as $\bar{N}$ increases, and goes like $-\log \bar{N}$ for large $\bar{N}$. The contribution is proportional to t_z, i.e. there is no even component, so for systems with broken inversion symmetry, the two chiralities cancel, and the response is equal to the untilted case. In the case of inversion symmetry, the contributions from the two chiralities are equal and add up. The contribution has the same sign as the tilt, and the magnitude depends on the Landau cutoff N and momentum cutoff Λ.

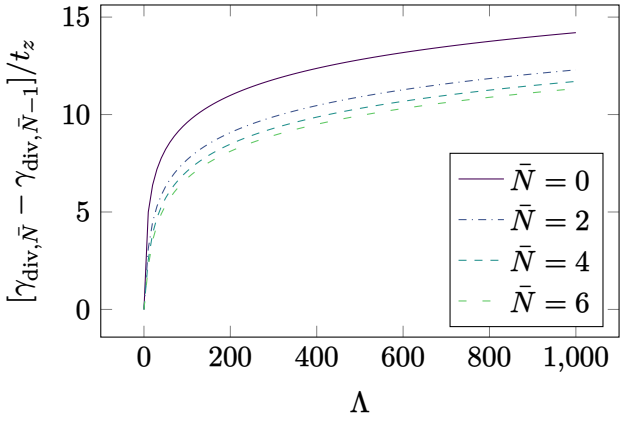

Figure 4.9.: The addition of each new Landau level to the divergent factor $\gamma_{\mathrm{div},\bar{N}}/t_z$ for the first Landau levels, as a function of the momentum cutoff Λ. Each level has the same Λ dependence; they are separated by a Λ independent factor, and the separation decreases for higher levels. See main text for details.

In the Type-II regime, the contributions have a more complicated form. Considering firstly only the lowest Landau level contribution, Eq. (4.200), which is odd in t_z, the total contribution cancels between the chiralities for broken inversion symmetry, while it adds up for inversion symmetric systems. As $|t_z| \to 1$ from above, the contribution blows up. This is to be expected as we move towards the Lifshitz transition, where we expect the linear model to perform poorly.[9] The contribution goes to zero as $t_z \to \infty$, shown in Fig. 4.10.

Considering also higher Landau level contributions, both interband and intraband transitions must be included,[10] meaning the summation is no longer restricted to a quadrant in the m, n plane, but rather to half the plane. The contributions are shown in Fig. 4.10. These contributions are not odd in t_z – they have a finite even component. Due to this, the contribution does not cancel for inversion broken systems, however, the even contribution is small in magnitude compared to the other contributions.

A schematic plot of all the contributions of a parallel tilt is shown in Fig. 4.11. In systems with broken inversion symmetry, where only the even contribution survives, we see that in the Type-I regime, the response is independent of the tilt t_z. In the Type-II regime, the response has the opposite sign, and is heavily reduced in magnitude; for a sufficiently large magnetic field, when only the zeroth Landau level is filled, the effect is non-existent. However, in inversion symmetric systems also the odd component contributes. In the Type-I regime, there is a contribution linear in t_z dependent on the momentum cutoff $\Lambda = k^{\text{cutoff}}/\sqrt{2eB}$, with the same sign as t_z. Fixing the magnitude of the term, equivalently fixing the momentum cutoff, has not been done. In the Type-II regime, close to the Lifshitz transition ($t_z = 1$), the result is divergent, which we expect is a non-physical discrepancy caused by the non-validity of the linear model. Deeper in the Type-II regime, the contribution decreases to zero but is still a significant contribution. The odd component dominates over the even component, and so the total response is of the same sign as the tilt t_z.

One disadvantage of using the Kubo formalism to find the response function, as opposed to the procedure of Chernodub, Cortijo, and Vozmediano [CCV18], who argued more directly from fundamental principles, is that the origin of the effect is less clear. Specifically, it is not clear directly from the Kubo calculation that the origin of the effect is the conformal anomaly. In the case of Type-II, it is in fact not entirely clear what is the origin of the effect.

[9] As the Fermi surface of the linear model is vastly different from the Fermi surface of the tight-binding model. See discussion on page 27 in Section 1.6.2 and van der Wurff and Stoof [vdWS19].

[10] By band, we here refer to the "conduction" band and "valence" band.

We have not been able to investigate this in-depth, but note the following important observation. When the material is tilted into Type-II, the density of states goes abruptly from vanishing to finite at the Dirac point, as mentioned earlier. As the density of states is finite, there is some finite energy related to the system as well. It is then a valid question to ask if the effect is indeed of conformal anomaly origin; the scale invariance of the system is broken by the energy scale introduced by the density of states, and so the anomaly itself is also broken. This is especially pertinent in light of the non-physical behavior seen around the Lifshitz transition; in the transition from Type-I to Type-II, the chiral anomaly is not broken, and chiral anomaly effects have been found to have analytical behavior in the transition, even for the linear model [SGT17]. This is still an open question.

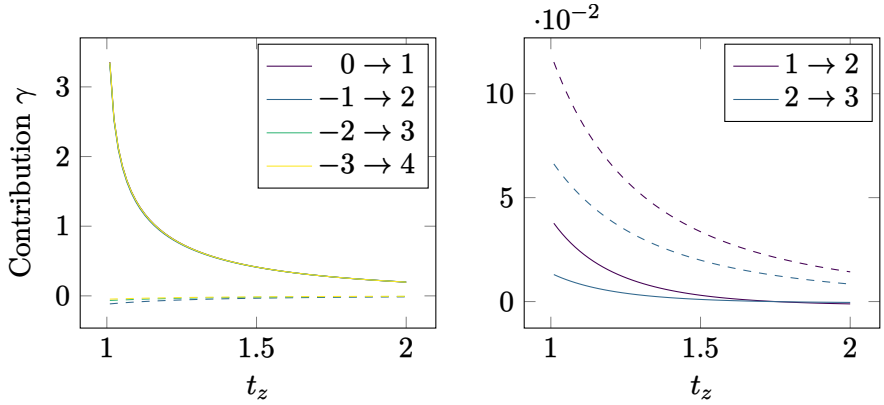

(a) Intraband, $-N \to N+1$.

(b) Interband, $N \to N+1$.

Figure 4.10.: The contribution from $n \to m$ transitions in a Type-II t_z tilted system. Solid line is the odd component γ_{odd}, dashed is even component γ_{even}.

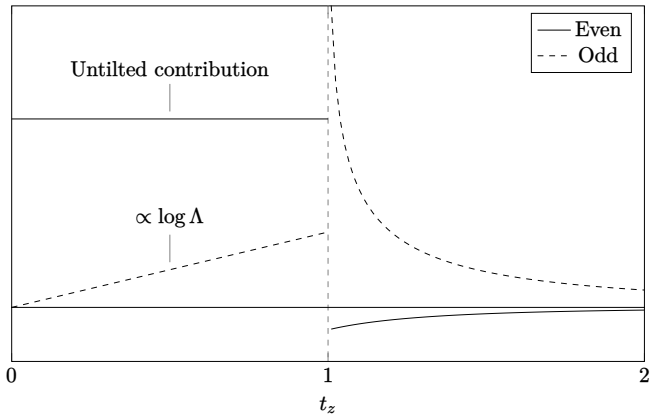

Figure 4.11.: Schematic summary of the contribution for parallel tilt t_z. Shown are the even (solid line) and odd (dashed line) parts as a function of t_z. As explained in the main text and shown in Table 4.3, the total contribution for a pair of cones is given by the sum of the components in inversion symmetric systems, and by the even component for broken inversion symmetric systems. Note that, as the contributions depend on factors such as the number of Landau levels and momentum cutoff, their relative magnitudes in the sketch are of little importance.

4.6.3. Other observations

We here present some further observations that are of interest, which we have been unable to investigate further due to time constraints. We, therefore, do not have conclusive results and do not want to present them together with the main results. However, they are of great importance and will be investigated further in future work.

Perpendicular tilt with only zeroth level transitions

Above, we defined the prefactor $\gamma_{\bar{N}}$ for perpendicular tilt as the sum of all transitions $m \to n$, $|m|, |n| < \bar{N}$; in other words, all transitions between Landau levels up to some cutoff level $\bar{N}$. However, there are other possible ways one may consider including the Landau level cutoff. In the untilted case, the *dipolar* selection rule $M = N + 1$ makes the choice obvious. With no such selection rule, the choice is however less obvious, and one other natural choice would be the following. Assuming a large magnetic field, only the lowest Landau level is occupied [Che+21], and so it would be natural to only consider $0 \to n, |n| < \bar{N}$ transitions. Doing this, the resulting response is very interesting! If we define by $\gamma_{\bar{N}}$ the sum of all $0 \to n, |n| < \bar{N}$ transitions, and compute $\gamma_{\bar{N}}$ as a function of the tilt t_x for various $\bar{N}$, we get the result shown in Fig. 4.12. When including transitions to higher Landau levels, $\gamma_{\bar{N}}$ as a function of t_x is no longer strictly decreasing – it has a maximum at $0 < t_x < 1$! This would be a very interesting experimental signature.

One pertinent question is how the cutoff level $\bar{N}$ should be found in this context. The cutoff $\bar{N}$ is not tunable in any obvious way – we have already assumed the system to be in the deep quantum limit where only the zeroth level is Landau level is filled. We do note that the effect of including ever-higher levels is diminishing; the $0 \to n$ contributions become smaller for higher n, and seem to converge as n becomes large.[11]

The procedure, however, is not rigorous. Due to time limitations, we have not been able to investigate this effect further in time for this print, however, we plan to do a more rigorous treatment in the future. In particular, this shows the importance of the choice of how one truncates the Landau level sum when there is no dipolar selection rule; with a dipolar selection rule, as is the case for no tilt and parallel tilt, the truncation yields only additional

[11] This, of course, warrants an investigation into the $0 \to n$ transition contributions shown in Fig. 4.7, to find if they are indeed decreasing faster than $1/n$.

numerical factors but does not change the behavior as a function of the tilt magnitude. Here, however, it qualitatively changes the response as a function of the tilt!

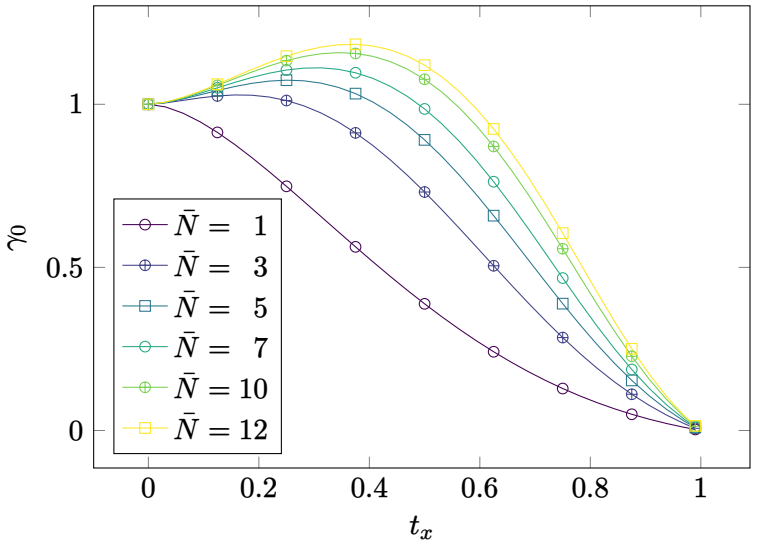

Figure 4.12.: Numerically computed values of the prefactor $\gamma_{\bar{N}}$ with only the $\bar{N}$ lowest, $0 \to n$ transitions included for perpendicular tilt t_x. The contribution is even in t_x, and vanish as $|t_x| \to 1$. For clarity, only every 4th mark is drawn.

Experimental signature at finite potential and temperature

In real materials, the Fermi level is close to, but not exactly at, the Dirac point. Arjona, Chernodub, and Vozmediano [ACV19] investigated this, which is of great interest with regard to experimental observations, by extending the computation to finite chemical potential and temperature. For a sufficiently large magnetic field, only the zeroth Landau level is filled [ACV19; Voz21], and the only transitions are the $0 \to \pm 1$ transitions. For a chemical potential μ small enough to be contained between the ± 1 Landau levels, i.e. $|\mu|/(v_F\sqrt{2eB}) < 1$, the response function was found to be invariant. Furthermore, for a finite temperature, it was found that thermally activated carriers increased the magnitude of the effect, with a stable plateau around $\mu = 0$. The width of the plateau is inversely proportional to the temperature. See Fig. 4.13.

As tilt is introduced, the energy interval in which one only has the zeroth Landau level is reduced, and as $t \to 1$ the interval vanishes. So as the system

is tilted, the width of the plateau is reduced. We reproduced the calculation for finite potential and temperature in the untilted situation,[12] but have not yet extended the computation to the tilted case. This should not present any major differences to what has been done in this work, other than including the Fermi-Dirac distribution when evaluating the k_z integral in the response function. However, both the issue of which Landau levels to include in the case of perpendicular tilt and the momentum cutoff in the case of parallel tilt has to be given extra care.

We may, however, make some conclusions without explicit calculations in the case of parallel tilt. We restrict ourselves to the Type-I case, where the aforementioned gap is finite. In the case of zero temperature, the situation is rather easy. Recall that the contribution is $\gamma^0_{\bar{N}} + \gamma_{\mathrm{div},\bar{N}}$. The first term explicitly depends on the chemical potential, but it is also independent of the tilt. The second term is tilt-dependent, and the chemical potential enters only through the Fermi-Dirac distribution; when the chemical potential is within the gap, the distribution is independent of the chemical potential, for zero temperature. Thus, the plateau is retained, with a potential independent addition $\gamma_{\mathrm{div},N}$; the width of the plateau, however, is reduced according to the width of the gap. At finite temperature, the thermal activation makes the above argument invalid, as the distribution function in the tilt-dependent term will also be affected by the chemical potential.

[12] Using the non-symmetric choice of the energy-momentum tensor, as opposed to the symmetric one used in the original calculation [ACV19].

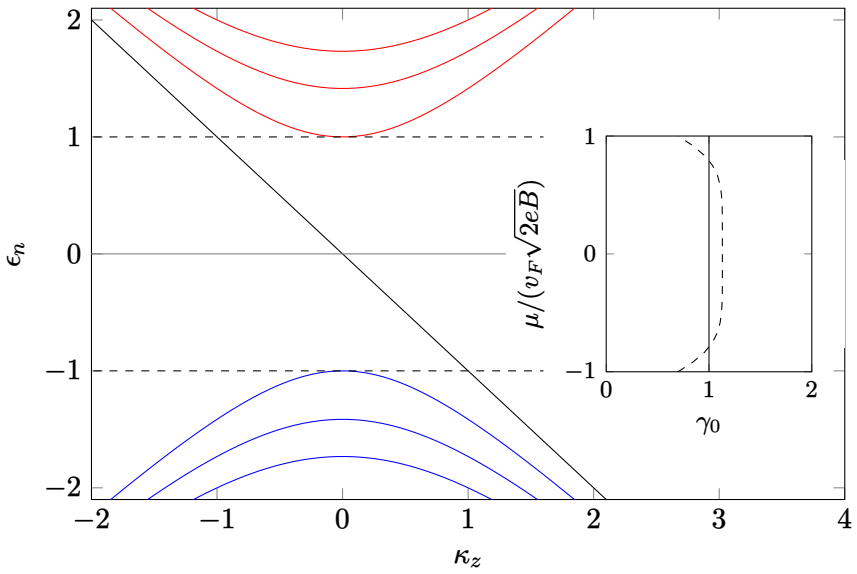

Figure 4.13.: The Landau level of an untilted Weyl cone. The inset shows the prefactor γ_0 of the response function for a small finite potential μ, within the energy interval indicated with dashed lines. In the inset, the solid line is computed at zero temperature, while the dashed line is computed at a small finite temperature. Figure inspired by Arjona, Chernodub, and Vozmediano [ACV19].

Conclusion and Outlook

We have computed a contribution to the transverse thermoelectric response function – Nernst response – of a tilted Dirac cone. The response was calculated for a single Weyl cone, and then the total response was found by summing the response of two Weyl cones of opposite chirality. The origin of the contribution is the conformal anomaly, and it is finite in the limit of no chemical potential and zero temperature. The response function was found to be tunable with the tilt vector $\boldsymbol{t}$.

In the case of tilt perpendicular to the magnetic field and parallel to the charge current, we found the response function to be even in the perpendicular tilt component $t_\perp$. The response decreases as the magnitude of the tilt is increased, and as the tilt approaches the critical tilt between Type-I and Type-II, the response is zero. In the Type-II regime with perpendicular tilt, the Landau levels collapse, and our method is no longer appropriate. In the case of tilt parallel to the magnetic field, the response function depends on the symmetry of the tilt of the Dirac cone – the effect of the two Weyl cones partially cancel when they tilt in the same direction, while for inversion symmetric tilt their contributions add up. We split the response into even and odd parts as functions of the parallel tilt component $t_\parallel$. For inversion symmetric tilt both contribute, while for broken inversion symmetry only the even component survives. The even component was found to be independent of the tilt in the Type-I regime, while it is heavily suppressed in the Type-II regime. The odd component, which only survives for inversion symmetric tilt, is proportional to the magnitude of the tilt in the Type-I regime, with its proportionality constant dependent on a momentum cutoff. In the Type-II regime, the odd component diverges to infinity close to the topological Lifshitz transition but quickly decreases as the tilt is increased. The divergence at the Lifshitz transition is believed to be an artifact of the linearized model.

This work facilitates future experimental designs and theoretical investigation into the effect and the conformal anomaly. As the direction of the tilt relative to the magnetic field is easily tunable, by simply rotating the field or sample, the dependence on the direction of the tilt, in particular, poses an interesting venue for experimental setups. We furthermore found the possibility of a distinct maximum of the response function in the case of perpendicular tilt, when considering the deep quantum where only the lowest Landau level is filled. This, however, requires further theoretical investigation.

The calculation has also demonstrated the importance of the correct treat-

ment of the energy-momentum tensor. Depending on the definition used, the resulting response is qualitatively different for tilted systems, as opposed to untilted systems.

As we conclude this thesis, there are several unanswered questions, and we believe this to be a fruitful topic for the future. Here we propose a selection of ideas and questions that are relevant, which are direct extensions of the work in this thesis.

Tilt parallel to temperature gradient Due to time constraints, we were not able to extend the calculation to tilt parallel to ∇T in time for writing the thesis. This is a natural extension, and we hope to be able to do this for a manuscript currently being written. This extension is mostly a technical matter. In particular, this situation is interesting as a t_y-component, in the geometry considered in the thesis, gives rise to a new term in the matrix element of the energy-momentum tensor.

The energy-momentum tensor The ambiguity related to the energy-momentum tensor, discussed in Section 4.1.2 is still an open question, which should be explored more. Much literature has been written on the topic, both in general [FR04] and specific to Dirac and Weyl semimetals [ACV19; vdWS19]. We have had discussions on the topic with María Vozmediano and Alberto Cortijo, and have several venues that we wish to explore further on this question.

One of our current ideas involves a fully covariant calculation, absorbing the tilt directly in the metric instead of explicitly including it in the Lagrangian. That will involve combining the curvature of the tilt and Luttinger's perturbation in a Kubo calculation. It is of interest to see if this leads to the same expressions as we found from having explicit tilt in flat space. For some initial work on this, see Appendix C.4.

Finite chemical potential and temperature As discussed in Section 4.6.3, it would be interesting to extend the calculation to finite potential and temperature. In the untilted case, the response has a stable plateau as a function of chemical potential even for finite temperature, related to the energy gap between the ± 1 Landau levels, where there is only the zeroth Landau level. As the cone is tilted, the gap is reduced and vanishes at the transition between Type-I and Type-II. An explicit calculation of this is a natural next step and requires only minor adaptions of the work done here.

Spin current response We computed the charge current response. It is also

of interest to see if there is a spin current response of the system.

Long Expressions Not Included in the Main Text

A

Listing A.1: Expression for Type-II interband transition with $t_z > 1$, given in Mathematica format.

```
(m/(-1 + tz^2) - (2*m*tz)/(-1 + tz^2) - (4*(-1 + m)*m*
    tz)/(-1 + tz^2) + (m*tz^2)/(-1 + tz^2) +
  tz*Sqrt[(m*tz^2*(1 + (-1 + m)*tz^2))/(-1 + tz^2)^2] +
     2*(-1 + m)*tz*Sqrt[(m*tz^2*(1 + (-1 + m)*tz^2))
     /(-1 + tz^2)^2] -
  Sqrt[m + (-1 + m)*m*tz^2]/(-1 + tz^2) - (2*(-1 + m)*
     Sqrt[m + (-1 + m)*m*tz^2])/(-1 + tz^2) +
  (2*tz*Sqrt[m + (-1 + m)*m*tz^2])/(-1 + tz^2) + 2*(-1
     + m)*Log[(1 - Sqrt[(1 + (-1 + m)*tz^2)/m])/(1 + tz
     )] +
  (-1 + m)*tz*Log[(1 - Sqrt[(1 + (-1 + m)*tz^2)/m])/(1
     + tz)] -
  2*(-1 + m)^2*Log[((1 + tz)*Sqrt[m/(-1 + tz^2)])/(Sqrt
     [m/(-1 + tz^2)] - Sqrt[(1 + (-1 + m)*tz^2)/(-1 +
     tz^2)])] -
  (-2*(-1 + m)^(3/2)*Sqrt[-1 + m*tz^2] + (-1 + tz)*Sqrt
     [(-1 + m)*(-1 + m*tz^2)] -
    tz*(2*m^2 - (1 + tz)*(-1 + Sqrt[(-1 + m)*(-1 + m*tz
       ^2)]) + m*(-3 + tz*(-1 + 2*Sqrt[(-1 + m)*(-1 + m
       *tz^2)])))) -
    (1 - m)*(-1 + tz)*(-1 + (1 + tz)*(2 + tz)*Log[-((-1
       + tz)*Sqrt[(-1 + m)/(-1 + tz^2)])]) -
    (-1 + tz^2)*(-2 + m*(2 + tz))*Log[(Sqrt[-1 + m] +
       Sqrt[-1 + m*tz^2])/Sqrt[-1 + tz^2]] +
    tz*Log[(-(Sqrt[-1 + m]*tz) + Sqrt[-1 + m*tz^2])/
       Sqrt[-1 + tz^2]] -
    tz^3*Log[(-(Sqrt[-1 + m]*tz) + Sqrt[-1 + m*tz^2])/
       Sqrt[-1 + tz^2]] -
    2*(-1 + m)^2*(tz + (-1 + tz^2)*Log[(-1 + m + Sqrt
       [(-1 + m)*(-1 + m*tz^2)])/(-1 + m + tz - m*tz)])
       )/(-1 + tz^2) -
```

```
tz*Log[(m*tz - Sqrt[m + (-1 + m)*m*tz^2])/(-1 + tz)])
```

Listing A.2: Expression for Type-II interband transition with $t_z < -1$, given in Mathematica format.

```
(1 + Sqrt[(-1 + m)*(-1 + m*tz^2)] - 2*m*Sqrt[(-1 + m)
    *(-1 + m*tz^2)] - Sqrt[m + (-1 + m)*m*tz^2] +
   2*m*Sqrt[m + (-1 + m)*m*tz^2] + (-1 + m)*(2 + tz)*Log
      [-((1 + tz)*Sqrt[(-1 + m)/(-1 + tz^2)])] +
   (-2 + m*(2 + tz))*Log[-((-1 + tz)*Sqrt[m/(-1 + tz^2)
      ])] + 2*Log[(Sqrt[m]*(1 - tz))/(Sqrt[m] + Sqrt[1 +
       (-1 + m)*tz^2])] -
   4*m*Log[(Sqrt[m]*(1 - tz))/(Sqrt[m] + Sqrt[1 + (-1 +
      m)*tz^2])] +
   2*m^2*Log[(Sqrt[m]*(1 - tz))/(Sqrt[m] + Sqrt[1 + (-1
      + m)*tz^2])] +
   2*Log[(Sqrt[m] + Sqrt[1 + (-1 + m)*tz^2])/Sqrt[-1 +
      tz^2]] - 2*m*Log[(Sqrt[m] + Sqrt[1 + (-1 + m)*tz
      ^2])/Sqrt[-1 + tz^2]] +
   tz*Log[(Sqrt[m] + Sqrt[1 + (-1 + m)*tz^2])/Sqrt[-1 +
      tz^2]] - m*tz*Log[(Sqrt[m] + Sqrt[1 + (-1 + m)*tz
      ^2])/Sqrt[-1 + tz^2]] +
   tz*Log[(-(Sqrt[m]*tz) + Sqrt[1 + (-1 + m)*tz^2])/Sqrt
      [-1 + tz^2]] -
   tz*Log[(-(Sqrt[-1 + m]*tz) + Sqrt[-1 + m*tz^2])/Sqrt
      [-1 + tz^2]] - 2*Log[(1 - Sqrt[(-1 + m*tz^2)/(-1 +
       m)])/(1 + tz)] +
   4*m*Log[(1 - Sqrt[(-1 + m*tz^2)/(-1 + m)])/(1 + tz)]
      - 2*m^2*Log[(1 - Sqrt[(-1 + m*tz^2)/(-1 + m)])/(1
      + tz)] +
   2*Log[-Sqrt[(-1 + m)/(-1 + tz^2)] + Sqrt[(-1 + m*tz
      ^2)/(-1 + tz^2)]] -
   2*m*Log[-Sqrt[(-1 + m)/(-1 + tz^2)] + Sqrt[(-1 + m*tz
      ^2)/(-1 + tz^2)]] -
  m*tz*Log[-Sqrt[(-1 + m)/(-1 + tz^2)] + Sqrt[(-1 + m*
      tz^2)/(-1 + tz^2)]])
```

Listing A.3: Expression for Type-II intraband transition with $t_z > 1$, given in Mathematica format.

```
(-((-1 + m)*m*tz*AppellF1[1, 1/2, 1/2, 2, (1 - tz^2)
    ^(-1), (1 - m)/(m*(-1 + tz^2))]) +
  m^2*tz*AppellF1[1, 1/2, 1/2, 2, -(m/((-1 + m)*(-1 +
      tz^2))), (1 - tz^2)^(-1)] +
  (-1 + tz^2)*(-2*Sqrt[(-1 + m)*m^3] + 2*m^2*Sqrt[(-1 +
      m)*(1 + (-1 + m)*tz^2)] - 4*m^3*Sqrt[(-1 + m)*(1
     + (-1 + m)*tz^2)] +
    2*Sqrt[m^3*(-1 + m*tz^2)] - 6*Sqrt[m^5*(-1 + m*tz
      ^2)] + 4*Sqrt[m^7*(-1 + m*tz^2)] -
    (-2*Sqrt[(-1 + m)*m^5] + 2*Sqrt[(-1 + m)*m^7] + (-
      Sqrt[(-1 + m)*m^3] + Sqrt[(-1 + m)*m^5])*tz)*Log
      [-1 + m] -
    2*Sqrt[(-1 + m)*m^5]*Log[m] + 2*Sqrt[(-1 + m)*m^7]*
      Log[m] + Sqrt[(-1 + m)*m^5]*tz*Log[m] +
    2*Sqrt[(-1 + m)*m^3]*tz*Log[1 + tz] - Sqrt[(-1 + m)
      *m^3]*tz*Log[-1 + tz^2] -
    4*Sqrt[(-1 + m)*m^5]*Log[(Sqrt[m] + Sqrt[1 + (-1 +
      m)*tz^2])/Sqrt[-1 + tz^2]] +
    4*Sqrt[(-1 + m)*m^7]*Log[(Sqrt[m] + Sqrt[1 + (-1 +
      m)*tz^2])/Sqrt[-1 + tz^2]] -
    2*Sqrt[(-1 + m)*m^3]*tz*Log[(Sqrt[m] + Sqrt[1 + (-1
       + m)*tz^2])/Sqrt[-1 + tz^2]] +
    2*Sqrt[(-1 + m)*m^5]*tz*Log[(Sqrt[m] + Sqrt[1 + (-1
       + m)*tz^2])/Sqrt[-1 + tz^2]] +
    4*Sqrt[(-1 + m)*m^5]*Log[(Sqrt[-1 + m] + Sqrt[-1 +
      m*tz^2])/Sqrt[-1 + tz^2]] -
    4*Sqrt[(-1 + m)*m^7]*Log[(Sqrt[-1 + m] + Sqrt[-1 +
      m*tz^2])/Sqrt[-1 + tz^2]] -
    2*Sqrt[(-1 + m)*m^5]*tz*Log[(Sqrt[-1 + m] + Sqrt[-1
       + m*tz^2])/Sqrt[-1 + tz^2]]))/(2*Sqrt[-1 + m]*m
    ^(3/2)*(-1 + tz^2))
```

Listing A.4: Expression for Type-II intraband transition with $t_z < -1$, given in Mathematica format.

```
(4*m*(-1 + tz)*Sqrt[(-1 + m)*(1 + (-1 + m)*tz^2)]*(-1 +
    Abs[tz]) - 4*(-1 + m)*(-1 + tz)*Sqrt[m*(-1 + m*tz
  ^2)]*(-1 + Abs[tz]) +
 8*(-1 + m)^(3/2)*m*Sqrt[1 + (-1 + m)*tz^2]*(1 + tz*
    Abs[tz]) - 8*(-1 + m)^2*Sqrt[m*(-1 + m*tz^2)]*(1 +
```

```
    tz*Abs[tz]) +
2*(-1 + m)*tz*(AppellF1[1, 1/2, 1/2, 2, (1 - tz^2)
    ^(-1), (1 - m)/(m*(-1 + tz^2))] -
   AppellF1[1, 1/2, 1/2, 2, m/(-1 + m - (-1 + m)*tz^2)
     , (1 - tz^2)^(-1)]) -
2*tz*AppellF1[1, 1/2, 1/2, 2, m/(-1 + m - (-1 + m)*tz
    ^2), (1 - tz^2)^(-1)] -
4*(-1 + m)^(5/2)*Sqrt[m]*(-1 + tz^2)*(Log[(-1 + m)/m]
     - 2*Log[(Sqrt[m] + Sqrt[1 + (-1 + m)*tz^2])/Sqrt
    [-1 + tz^2]] +
   2*Log[(Sqrt[-1 + m] + Sqrt[-1 + m*tz^2])/Sqrt[-1 +
      tz^2]]) - Sqrt[(-1 + m)*m]*(-1 + tz)*
 (-4 + 4*Abs[tz] + tz*Log[m/(-1 + tz^2)] + 4*tz*Log[(
     Sqrt[-1 + m] + Sqrt[-1 + m*tz^2])/Sqrt[-1 + tz
     ^2]] +
   4*tz^2*Log[(Sqrt[-1 + m] + Sqrt[-1 + m*tz^2])/Sqrt
     [-1 + tz^2]] + 2*tz*Log[1 + Abs[tz]] -
   6*tz*Log[Sqrt[m/(-1 + tz^2)]*(1 + Abs[tz])] - 4*tz
     ^2*Log[Sqrt[m/(-1 + tz^2)]*(1 + Abs[tz])]) +
(-1 + m)^(3/2)*Sqrt[m]*(8*tz + 8*Abs[tz] + Log[(-1 +
    m)/m] - tz^2*Log[(-1 + m)/(-1 + tz^2)] + tz^2*Log[
    m/(-1 + tz^2)] -
   8*Log[(Sqrt[m] + Sqrt[1 + (-1 + m)*tz^2])/Sqrt[-1 +
      tz^2]] - 4*tz*Log[(Sqrt[m] + Sqrt[1 + (-1 + m)*
     tz^2])/Sqrt[-1 + tz^2]] +
   8*tz^2*Log[(Sqrt[m] + Sqrt[1 + (-1 + m)*tz^2])/Sqrt
     [-1 + tz^2]] +
   4*tz^3*Log[(Sqrt[m] + Sqrt[1 + (-1 + m)*tz^2])/Sqrt
     [-1 + tz^2]] +
   8*Log[(Sqrt[-1 + m] + Sqrt[-1 + m*tz^2])/Sqrt[-1 +
     tz^2]] + 4*tz*Log[(Sqrt[-1 + m] + Sqrt[-1 + m*tz
     ^2])/Sqrt[-1 + tz^2]] -
   8*tz^2*Log[(Sqrt[-1 + m] + Sqrt[-1 + m*tz^2])/Sqrt
     [-1 + tz^2]] -
   4*tz^3*Log[(Sqrt[-1 + m] + Sqrt[-1 + m*tz^2])/Sqrt
     [-1 + tz^2]] + 6*Log[Sqrt[(-1 + m)/(-1 + tz^2)
     ]*(1 + Abs[tz])] +
   4*tz*Log[Sqrt[(-1 + m)/(-1 + tz^2)]*(1 + Abs[tz])]
     - 6*tz^2*Log[Sqrt[(-1 + m)/(-1 + tz^2)]*(1 + Abs
     [tz])] -
```

```
4*tz^3*Log[Sqrt[(-1 + m)/(-1 + tz^2)]*(1 + Abs[tz])
    ] - 6*Log[Sqrt[m/(-1 + tz^2)]*(1 + Abs[tz])] -
4*tz*Log[Sqrt[m/(-1 + tz^2)]*(1 + Abs[tz])] + 6*tz
    ^2*Log[Sqrt[m/(-1 + tz^2)]*(1 + Abs[tz])] +
4*tz^3*Log[Sqrt[m/(-1 + tz^2)]*(1 + Abs[tz])]))/(4*
    Sqrt[(-1 + m)*m]*(-1 + tz^2))
```

Contributions from the Symmetric Energy-Momentum Tensor

B

As noted in the main text, there are some subtlety in the definition of the energy-momentum tensor. The *canonical* definition, which we have used in the main text, is in general not symmetric. In the calculation by Arjona, Chernodub, and Vozmediano [ACV19], the symmetrized[1] energy-momentum tensor

$$T_S^{\mu\nu} = \frac{T^{\mu\nu} + T^{\nu\mu}}{2}$$

was used. In this appendix we show the contributions of the symmetric tensor. The contributions from $T^{\mu\nu}$ and $T^{\nu\mu}$ are shown to be equal in the non-tilted case, while they differ in the tilted case.

In the main text we have already found the contributions from the canonical tensor, and so we focus here on the contributions from $T_F^{\mu\nu} = T^{\nu\mu}$. The relevant element is $T_F^{y0} = T^{0y}$.

The tilted canonical energy-momentum tensor, Eq. (4.95),

$$T^{\mu\nu} = \frac{i}{2}(\phi^\dagger \tilde{\sigma}_s^\mu \partial_\nu \phi - \partial_\nu \phi^\dagger \tilde{\sigma}_s^\mu \phi - \eta^{\mu\nu}\mathcal{L}),$$

and so the symmetric tensor is

$$T_S^{\mu\nu} = \frac{i}{2}(\phi^\dagger \tilde{\sigma}_s^\mu \overleftrightarrow{\partial}_\nu \phi + \phi^\dagger \tilde{\sigma}_s^\nu \overleftrightarrow{\partial}_\mu \phi - \eta^{\mu\nu}\mathcal{L}), \tag{B.1}$$

where we used the notation $\phi^\dagger \overleftrightarrow{\partial} \phi = (\phi^\dagger \partial \phi - (\partial \phi^\dagger)\phi)/2$. We split T_S^{y0} into three parts; the first part corresponds to the canonical energy-momentum tensor, while the two latter correspond to the two terms of T_F^{y0}. Explicitly

$$T_S^{y0} = \underbrace{\frac{i}{2}\phi^\dagger \tilde{\sigma}_s^y \overleftrightarrow{\partial}_0 \phi}_{T^{(1)}} + \underbrace{\frac{i}{4}\phi^\dagger \partial_y \phi}_{T^{(2)}} + \underbrace{\frac{i}{4}\phi^\dagger \partial_y \phi}_{T^{(3)}}. \tag{B.2}$$

In other words, the first part is half that found in the main text, while the two latter are unique to the symmetric tensor. For convenience, we will for the rest of the appendix rename $T^{\mu\nu} = T_S^{\mu\nu}$.

[1] See Section 4.1.2 for a more precise discussion on the symmetrization of the energy-momentum tensor.

B.1. No tilt

Begin by considering the matrix elements

$$T^{0y\,(2)}_{k+\mathrm{q}ns,kms}(\boldsymbol{q}) = +\frac{1}{4}\int \mathrm{d}y e^{iq_y y} v_F \phi^*_{k+\mathrm{q}ns}(y) p_y \phi_{kms}(y), \tag{B.3}$$

$$T^{0y\,(3)}_{k+\mathrm{q}ns,kms}(\boldsymbol{q}) = -\frac{1}{4}\int \mathrm{d}y e^{iq_y y} v_F \left(p_y \phi^*_{k+\mathrm{q}ns}(y)\right) \phi_{kms}(y). \tag{B.4}$$

Recall that $\phi_{kms}(y)$, defined in Eq. (4.114), consists of two y-dependent factors: $\exp\left[-\frac{(y-k_x l_B^2)^2}{2l_B^2}\right]$ and the Hermite polynomials. The operator p_y thus produces two terms when operating on ϕ. The first term, coming from the exponent, is proportional to $y - k_x l_B^2$. The operator in Eqs. (B.3) and (B.4) acts on ϕ with the quantum number $\boldsymbol{k}$ and $\boldsymbol{k}+\mathrm{q}$, respectively; when summing the two contributions, everything thus cancels except for a term proportional to q_x, which vanishes in the local limit.

It remains to consider the result of p_y operating on the Hermite polynomials. Let $\tilde{p}_y$ indicate the p_y operator acting only on the Hermite polynomial part of ϕ, and use the property of Hermite polynomials $\partial_x H_n(x) = 2nH_{n-1}(x)$ [Olv+, Eq. 18.9.25].

$$\begin{aligned}\phi^*_{k+\mathrm{q}ns}(y)\tilde{p}_y\phi_{kms} = -i\hbar \exp\left\{-\frac{(y-k_x l_B^2)^2 + (y-(k_x+q_x)l_B^2)^2}{2l_B^2}\right\} \\ \frac{2}{l_B}\Bigg\{(M-1)a_{kms}a_{k+\mathrm{q}ns}H_{M-2}\left(\frac{y-k_x l_B^2}{l_B}\right)H_{N-1}\left(\frac{y-(k_x+q_x)l_B^2}{l_B}\right) \\ + Mb_{kms}b_{k+\mathrm{q}ns}H_{M-1}\left(\frac{y-k_x l_B^2}{l_B}\right)H_N\left(\frac{y-(k_x+q_x)l_B^2}{l_B}\right)\Bigg\}.\end{aligned} \tag{B.5}$$

Completing the square, we get

$$\begin{aligned}\int \mathrm{d}y e^{iq_y y}\phi^*_{k+\mathrm{q}ns}(y)\tilde{p}_y\phi_{kms}(y) = -i\hbar\exp\left[-\frac{l_B^2}{4}\left\{\mathrm{q}_y^2 - 2iq_y(2k_x+q_x)\right\}\right] \\ \int \mathrm{d}y \exp\left[-\left\{y + \frac{l_B^2}{2}(-iq_y - 2k_x - q_x)\right\}^2 / l_B^2\right] \\ \frac{2}{l_B}\Bigg\{(M-1)a_{kms}a_{k+\mathrm{q}ns}H_{M-2}\left(\frac{y-k_x l_B^2}{l_B}\right)H_{N-1}\left(\frac{y-(k_x+q_x)l_B^2}{l_B}\right) \\ + Mb_{kms}b_{k+\mathrm{q}ns}H_{M-1}\left(\frac{y-k_x l_B^2}{l_B}\right)H_N\left(\frac{y-(k_x+q_x)l_B^2}{l_B}\right)\Bigg\}.\end{aligned} \tag{B.6}$$

Upon introducing $\tilde{y} = \frac{y}{l_B} + l_B(-iq_y - q_x - 2k_x)/2$, as was also done in the main text, the expression reduces to

$$\int \mathrm{d}y e^{iq_y y}\phi^*_{\boldsymbol{k}+\mathrm{q}ns}(y)\tilde{p}_y\phi_{kms}(y) = -i\hbar \exp\left[-\frac{l_B^2}{4}\left\{q_x^2 + q_y^2 - 2iq_y(2k_x + q_x)\right\}\right]$$
$$\int \mathrm{d}\tilde{y} l_B \exp\left[-\tilde{y}^2\right]$$
$$\frac{2}{l_B}\Bigg\{(M-1)a_{kms}a_{k+\mathrm{q}ns}H_{M-2}\left(\tilde{y} + \frac{l_B}{2}(iq_y + q_x)\right)H_{N-1}\left(\tilde{y} + \frac{l_B}{2}(iq_y - q_x)\right)$$
$$+ Mb_{kms}b_{k+\mathrm{q}ns}H_{M-1}\left(\tilde{y} + \frac{l_B}{2}(iq_y + q_x)\right)H_N\left(\tilde{y} + \frac{l_B}{2}(iq_y - q_x)\right)\Bigg\}. \quad \text{(B.7)}$$

Considering now the local limit $\boldsymbol{q} \to 0$, the expression greatly simplifies, and we may use the orthogonality relation for the Hermite polynomials Eq. (4.120)

$$\int_{-\infty}^{\infty} \mathrm{d}x e^{-x^2} H_n(x)H_m(x) = \sqrt{\pi}2^n n!\delta_{n,m}$$

to evaulate the integral.

$$\lim_{\boldsymbol{q}\to 0}\int \mathrm{d}y e^{iq_y y}\phi^*_{\boldsymbol{k}+\mathrm{q}ns}(y)\tilde{p}_y\phi_{kms}(y) = -i\hbar\sqrt{2}\frac{\alpha_{kms}\alpha_{kns}\sqrt{M-1} + \sqrt{M}}{l_B\sqrt{\alpha_{kms}^2+1}\sqrt{\alpha_{kns}^2+1}}\delta_{N,M-1}. \quad \text{(B.8)}$$

Similarly, for $T^{0y\,(3)}_{\boldsymbol{k}+\mathrm{q}ns,kms}(\boldsymbol{q})$, one has

$$\left(\tilde{p}_y\phi^*_{\boldsymbol{k}+\mathrm{q}ns}(y)\right)\phi_{kms}(y) = -i\hbar\exp\left\{-\frac{(y - k_x l_B^2)^2 + (y - (k_x+q_x)l_B^2)^2}{2l_B^2}\right\}$$
$$\frac{2}{l_B}\Bigg\{(N-1)a_{kms}a_{k+\mathrm{q}ns}H_{M-1}\left(\frac{y-k_x l_B^2}{l_B}\right)H_{N-2}\left(\frac{y-(k_x+q_x)l_B^2}{l_B}\right)$$
$$+Nb_{kms}b_{k+\mathrm{q}ns}H_M\left(\frac{y-k_x l_B^2}{l_B}\right)H_{N-1}\left(\frac{y-(k_x+q_x)l_B^2}{l_B}\right)\Bigg\} \quad \text{(B.9)}$$

which with the same procedure as above gives

$$\lim_{\boldsymbol{q}\to 0}\int \mathrm{d}y e^{iq_y y}\left(\tilde{p}_y\phi^*_{\boldsymbol{k}+\mathrm{q}ns}(y)\right)\phi_{kms}(y) = -i\hbar\sqrt{2}\frac{\alpha_{kms}\alpha_{kns}\sqrt{N-1} + \sqrt{N}}{l_B\sqrt{\alpha_{kms}^2+1}\sqrt{\alpha_{kns}^2+1}}\delta_{M,N-1}. \quad \text{(B.10)}$$

Summary 8

In the untilted case, we have

$$\lim_{q\to 0} T^{y0\,(2)}_{kns,kms} = -\frac{i\hbar\sqrt{2}}{4}\frac{\alpha_{kms}\alpha_{kns}\sqrt{M-1}+\sqrt{M}}{l_B\sqrt{\alpha_{kms}^2+1}\sqrt{\alpha_{kns}^2+1}}\delta_{N,M-1}, \tag{B.11}$$

$$\lim_{q\to 0} T^{y0\,(3)}_{kns,kms} = \frac{i\hbar\sqrt{2}}{4}\frac{\alpha_{kms}\alpha_{kns}\sqrt{N-1}+\sqrt{N}}{l_B\sqrt{\alpha_{kms}^2+1}\sqrt{\alpha_{kns}^2+1}}\delta_{M,N-1}. \tag{B.12}$$

B.2. With tilt

In the tilted case, we have shown in the main text that

$$T^{\mu 0} = \frac{i}{2}\left[\partial_i\bar{\psi}\Gamma^j\gamma^0\Gamma^\mu\psi - \bar{\psi}\Gamma^\mu\gamma^0\Gamma^j\partial_j\psi\right].$$

Swapping the indices, we have for $\mu \neq 0$ [vdWS19]

$$T^{0i} = \frac{i}{2}[\bar{\psi}\gamma^0\partial^\mu\psi - \partial^\mu\bar{\psi}\gamma^0\psi].$$

In our work, we have considered only tilt perpendiculat to the thermal gradient, so the component of the energy-momentum tensor of interest are not affected by the tilt.

or

$$T^{0y(2)}_{k+\mathrm{q}ns,kms}(q) = +\frac{1}{4}\int \mathrm{d}y e^{iq_y y} v_F \phi^*_{k+\mathrm{q}ns}(y) p_y \phi_{kms}(y), \tag{B.13}$$

$$T^{0y(3)}_{k+\mathrm{q}ns,kms}(q) = -\frac{1}{4}\int \mathrm{d}y e^{iq_y y} v_F (p_y \phi^*_{k+\mathrm{q}ns}(y))\phi_{kms}(y). \tag{B.14}$$

Firstly, we note that

$$[p_y, e^{\theta/2\sigma_x}] = 0.$$

Furthermore, exactly as for the untilted case, the momentum operator acting on the exponential prefactor of ϕ gives contributions proportional to q_x. In the local limit $q \to 0$ this term vanishes, and we need only consider the effect of the momentum operator acting on the Hermite polynomials.

Denote by $\tilde{p}_y$ the momentum operator p_y acting only on the Hermite polynomial part of ϕ. Furthermore, we will use the property of Hermite

polynomials $\partial_x H_n(x) = 2nH_{n-1}(x)$ [Olv+, Eq. 18.9.25].

$$\tilde{p}_y \phi_{kms} = -i\hbar e^{\theta/2\sigma_x} e^{-\frac{1}{2}\chi^2} \partial_y \begin{pmatrix} a_{kms} H_{M-1}(\chi) \\ b_{kms} H_M(\chi) \end{pmatrix} \tag{B.15}$$

$$= -i\hbar e^{\theta/2\sigma_x} e^{-\frac{1}{2}\chi^2} 2\frac{\partial \chi}{\partial y} \begin{pmatrix} a_{kms}(M-1) H_{M-2}(\chi) \\ b_{kms}(M) H_{M-1}(\chi) \end{pmatrix} \tag{B.16}$$

$$= -i\hbar e^{\theta/2\sigma_x} e^{-\frac{1}{2}\chi^2} \frac{2\sqrt{\alpha}}{l_B} \begin{pmatrix} a_{kms}(M-1) H_{M-2}(\chi) \\ b_{kms}(M) H_{M-1}(\chi) \end{pmatrix}. \tag{B.17}$$

And thus, recalling that

$$e^{\theta\sigma_x} = \begin{pmatrix} 1 & -t_x \\ -t_x & 1 \end{pmatrix} \frac{1}{\sqrt{1-t_x^2}},$$

we find the product

$$\begin{aligned} \phi^*_{\boldsymbol{k}+\mathrm{q}ns}(y) \tilde{p}_y \phi_{kms} = &-\frac{i\hbar 2\sqrt{\alpha}}{l_B\sqrt{1-t_x^2}} e^{-\frac{1}{2}\chi^2_{\boldsymbol{k}} - \frac{1}{2}\chi^2_{\boldsymbol{k}+\mathrm{q}}} \\ &\Big[a_{\boldsymbol{k}+\mathrm{q}ns} H_{N-1}(\chi_{\boldsymbol{k}+\mathrm{q}}) \left\{ a_{kms}(M-1) H_{M-2}(\chi_{\boldsymbol{k}}) - t_x b_{kms} M H_{M-1}(\chi_{\boldsymbol{k}}) \right\} \\ &+ b_{\boldsymbol{k}+\mathrm{q}ns} H_N(\chi_{\boldsymbol{k}+\mathrm{q}}) \left\{ -t_x a_{kms}(M-1) H_{M-2}(\chi_{\boldsymbol{k}}) + b_{kms} M H_{M-1}(\chi_{\boldsymbol{k}}) \right\} \Big]. \end{aligned} \tag{B.18}$$

Completing the square and substituting

$$\tilde{y} = \frac{\sqrt{\alpha}}{l_B} \left(y - \frac{l_B^2}{2\alpha} (iq_y + (2k'_x + q'_x)) \right)$$

gives

$$\begin{aligned} \int \mathrm{d}y e^{iq_y} \phi^*_{\boldsymbol{k}+\mathrm{q}ns}(y) \tilde{p}_y \phi_{kms}(y) = &\exp\left[-\frac{l_B^2}{4\alpha} (q_y^2 - 2i(2k'_x + q'_x) q_y + (q'_x)^2) \right] \\ &\times \frac{-i\hbar 2\sqrt{\alpha}}{l_B\sqrt{1-t_x^2}} \int \mathrm{d}\tilde{y} \frac{l_B}{\sqrt{\alpha}} \\ \times \Big[a_{\boldsymbol{k}+\mathrm{q}ns} H_{N-1}(\chi_{\boldsymbol{k}+\mathrm{q}}) &\left\{ a_{kms}(M-1) H_{M-2}(\chi_{\boldsymbol{k}}) - t_x b_{kms} M H_{M-1}(\chi_{\boldsymbol{k}}) \right\} \\ + b_{\boldsymbol{k}+\mathrm{q}ns} H_N(\chi_{\boldsymbol{k}+\mathrm{q}}) &\left\{ -t_x a_{kms}(M-1) H_{M-2}(\chi_{\boldsymbol{k}}) + b_{kms} M H_{M-1}(\chi_{\boldsymbol{k}}) \right\} \Big]. \end{aligned} \tag{B.19}$$

We must now evaluate the integral, and express the result in the Ξ-functions, defined in Eqs. (4.160) and (4.161) of the main text.

$$\begin{pmatrix} a_{\boldsymbol{k}+\mathrm{q}ns} H_{N-1}(\chi_{\boldsymbol{k}+\mathrm{q}}) \\ b_{\boldsymbol{k}+\mathrm{q}ns} H_N(\chi_{\boldsymbol{k}+\mathrm{q}}) \end{pmatrix}^T \underbrace{\begin{pmatrix} 1 & -t_x \\ -t_x & 1 \end{pmatrix}}_{T} \begin{pmatrix} a_{\boldsymbol{k}ms}(M-1) H_{M-2}(\chi_{\boldsymbol{k}}) \\ b_{\boldsymbol{k}ms} M H_{M-1}(\chi_{\boldsymbol{k}}) \end{pmatrix}$$

For each of the entries in T, we get a product of Hermite polynomials. Where the untilted cone had two such terms, the tilt parameter t_x now gives two extra products, which we must evaluate. Let $M^{(2)}_{ij}$ be the product corresponding to T_{ij}, i.e.

$$M^{(2)}_{11} = \quad a_{\boldsymbol{k}+\mathrm{q}ns} a_{\boldsymbol{k}ms}(M-1) H_{N-1}(\chi_{\boldsymbol{k}+\mathrm{q}}) H_{M-2}(\chi_{\boldsymbol{k}}), \tag{B.20}$$

$$M^{(2)}_{12} = -t_x a_{\boldsymbol{k}+\mathrm{q}ns} b_{\boldsymbol{k}ms} M H_{N-1}(\chi_{\boldsymbol{k}+\mathrm{q}}) H_{M-1}(\chi_{\boldsymbol{k}}), \tag{B.21}$$

$$M^{(2)}_{21} = -t_x b_{\boldsymbol{k}+\mathrm{q}ns} a_{\boldsymbol{k}ms}(M-1) H_{N}(\chi_{\boldsymbol{k}+\mathrm{q}}) H_{M-2}(\chi_{\boldsymbol{k}}), \tag{B.22}$$

$$M^{(2)}_{22} = \quad b_{\boldsymbol{k}+\mathrm{q}ns} b_{\boldsymbol{k}ms} M H_{N}(\chi_{\boldsymbol{k}+\mathrm{q}}) H_{M-1}(\chi_{\boldsymbol{k}}). \tag{B.23}$$

We want to evaluate

$$F^{(2)}_{ij} = \left[(\alpha^2_{k_z ms}+1)(\alpha^2_{k_z+\mathrm{q}_z ns}+1)\right]^{\frac{1}{2}} \int \mathrm{d}\tilde{y} e^{-\tilde{y}^2} M^{(2)}_{ij}, \tag{B.24}$$

with the prefactor introduced for later convenience.

Notice that

$$F^{(2)}_{12} = -t_x \sqrt{\alpha} \sqrt{\frac{M}{2}} \alpha_{k+q,n} \Xi_2(\bar{q}, m \mp 1, n). \tag{B.25}$$

and

$$F^{(2)}_{21} = -t_x \sqrt{\alpha} \sqrt{\frac{M-1}{2}} \frac{a^2_{kms}}{l_B a_{km\mp 1 s}} \Xi_1(\bar{q}, m \mp 1, n, s). \tag{B.26}$$

$F^{(2)}_{11}$ and $F^{(2)}_{22}$ are the same as for the untilted case:

$$F^{(2)}_{11} = \sqrt{\alpha} \frac{\alpha_{k_z ms} \alpha_{k_z+\mathrm{q}_z ns} \sqrt{M-1}}{l_B \sqrt{2}} \Xi_1(\bar{q}, m \mp 1, n \mp 1, s), \tag{B.27}$$

and

$$F^{(2)}_{22} = \sqrt{\alpha} \frac{\sqrt{M}}{l_B \sqrt{2}} \Xi_1(\bar{q}, m, n, s). \tag{B.28}$$

In summary we have

$$T^{0y\ (2)}_{\boldsymbol{k}+\mathrm{q}ns,kms}(\boldsymbol{q}) = +\frac{v_F}{4}\int \mathrm{d}y e^{iq_y q}\phi^*_{\boldsymbol{k}+\mathrm{q}ns}(y)p_y\phi_{kms}(y) \tag{B.29}$$

$$= -\frac{i\hbar v_F}{2}\Gamma^+_{k\mathrm{q}mns}\sum_{i,j}F^{(2)}_{ij}, \tag{B.30}$$

where

$$\Gamma^+_{k\mathrm{q}mns} = \frac{\exp\left[-\frac{l_B^2}{4\alpha}(q_y^2 - 2i(2k'_x + q'_x)q_y + (q'_x)^2)\right]}{\left[(\alpha^2_{k_z ms}+1)(\alpha^2_{k_z+\mathrm{q}_z ns}+1)\right]^{\frac{1}{2}}\sqrt{1-t_x^2}}$$

In a similar procedure, we find $T^{0y\ (2)}_{\boldsymbol{k}+\mathrm{q}ns,kms}(\boldsymbol{q})$.

$$\tilde{p}_y\phi^*_{\boldsymbol{k}+\mathrm{q}ms} = \frac{-i\hbar\sqrt{\alpha}}{l_B}e^{-\frac{1}{2}\chi^2}\begin{pmatrix} a_{\boldsymbol{k}+\mathrm{q}ms}(M-1)H_{M-2}(\chi) \\ b_{\boldsymbol{k}+\mathrm{q}ms}(M)H_{M-1}(\chi)\end{pmatrix}. \tag{B.31}$$

And thus,

$$\left(\tilde{p}_y\phi^*_{\boldsymbol{k}+\mathrm{q}ns}(y)\right)\phi_{kms} = -\frac{i\hbar 2\sqrt{\alpha}}{l_B\sqrt{1-t_x^2}}e^{-\frac{1}{2}\chi^2_{\boldsymbol{k}}-\frac{1}{2}\chi^2_{\boldsymbol{k}+\mathrm{q}}}$$

$$\Big[a_{\boldsymbol{k}+\mathrm{q}ns}(N-1)H_{N-2}(\chi_{\boldsymbol{k}+\mathrm{q}})\left\{a_{kms}H_{M-1}(\chi_{\boldsymbol{k}}) - t_x b_{kms}H_M(\chi_{\boldsymbol{k}})\right\}$$

$$+ b_{\boldsymbol{k}+\mathrm{q}ns}NH_{N-1}(\chi_{\boldsymbol{k}+\mathrm{q}})\left\{-t_x a_{kms}H_{M-1}(\chi_{\boldsymbol{k}}) + b_{kms}H_M(\chi_{\boldsymbol{k}})\right\}\Big]. \tag{B.32}$$

With the now well-known completion of the square and substitution, we have

$$\int \mathrm{d}y e^{iq_y}\left[\tilde{p}_y\phi^*_{\boldsymbol{k}+\mathrm{q}ns}(y)\right]\phi_{kms}(y) = \exp\left[-\frac{l_B^2}{4\alpha}(q_y^2 - 2i(2k'_x+q'_x)q_y + (q'_x)^2)\right]$$

$$\times\frac{-i\hbar 2\sqrt{\alpha}}{l_B\sqrt{1-t_x^2}}\int \mathrm{d}\tilde{y}\frac{l_B}{\sqrt{\alpha}}$$

$$\times\Big[a_{\boldsymbol{k}+\mathrm{q}ns}(N-1)H_{N-2}(\chi_{\boldsymbol{k}+\mathrm{q}})\left\{a_{kms}H_{M-1}(\chi_{\boldsymbol{k}}) - t_x b_{kms}H_M(\chi_{\boldsymbol{k}})\right\}$$

$$+ b_{\boldsymbol{k}+\mathrm{q}ns}NH_{N-1}(\chi_{\boldsymbol{k}+\mathrm{q}})\left\{-t_x a_{kms}H_{M-1}(\chi_{\boldsymbol{k}}) + b_{kms}H_M(\chi_{\boldsymbol{k}})\right\}\Big]. \tag{B.33}$$

Denote the terms of the integrand by

$$M^{(3)}_{11} = \quad a_{\boldsymbol{k}+\mathrm{q}ns}a_{kms}(N-1)H_{N-2}(\chi_{\boldsymbol{k}+\mathrm{q}})H_{M-1}(\chi_{\boldsymbol{k}}), \tag{B.34}$$

$$M^{(3)}_{12} = -t_x a_{\boldsymbol{k}+\mathrm{q}ns}b_{kms}(N-1)H_{N-2}(\chi_{\boldsymbol{k}+\mathrm{q}})H_M(\chi_{\boldsymbol{k}}), \tag{B.35}$$

$$M^{(3)}_{21} = -t_x b_{\boldsymbol{k}+\mathrm{q}ns}a_{kms}NH_{N-1}(\chi_{\boldsymbol{k}+\mathrm{q}})H_{M-1}(\chi_{\boldsymbol{k}}), \tag{B.36}$$

$$M^{(3)}_{22} = \quad b_{\boldsymbol{k}+\mathrm{q}ns}b_{kms}NH_{N-1}(\chi_{\boldsymbol{k}+\mathrm{q}})H_M(\chi_{\boldsymbol{k}}). \tag{B.37}$$

We must evaluate

$$F_{ij}^{(3)} = \left[(\alpha_{k_z ms}^2 + 1)(\alpha_{k_z+\mathrm{q}_z ns}^2 + 1)\right]^{\frac{1}{2}} \int \mathrm{d}\tilde{y} e^{-\tilde{y}^2} M_{ij}^{(3)}. \tag{B.38}$$

From the untilted case we know

$$F_{11}^{(3)} = \sqrt{\frac{N-1}{2}} \frac{\alpha_{k_z ms}\alpha_{k_z+\mathrm{q}_z ns}}{l_B \alpha_{k_z+\mathrm{q}_z n \mp 1 s}} \Xi_2(\bar{q}, m \mp 1, n \mp 1, s), \tag{B.39}$$

$$F_{22}^{(3)} = \sqrt{\frac{N}{2}} \frac{1}{l_B \alpha_{k_z+\mathrm{q}_z ns}} \Xi_2(\bar{q}, m, n, s). \tag{B.40}$$

Furthermore,

$$F_{12}^{(3)} = -t_x \frac{\alpha_{k_z+\mathrm{q}_z n}}{\alpha_{k_z+\mathrm{q}_z n \mp 1} l_B} \sqrt{\frac{N-1}{2}} \Xi_2(\bar{q}, m, n \mp 1, s), \tag{B.41}$$

$$F_{21}^{(3)} = -\frac{t_x}{l_B} \sqrt{\frac{N}{2}} \frac{\alpha_{k_z m}}{\alpha_{k_z+\mathrm{q}_z n}} \Xi_2(\bar{q}, m \mp 1, n, s). \tag{B.42}$$

We thus have

$$T^{0y\ (3)}_{k+\mathrm{q}ns,kms}(q) = -\frac{v_F}{4} \int \mathrm{d}y e^{iq_y y} \left(p_y \phi^*_{k+\mathrm{q}ns}(y)\right) \phi_{kms}(y) \tag{B.43}$$

$$= \frac{i\hbar v_F}{2} \Gamma^+_{k\mathrm{q}mns} \sum_{ij} F_{ij}^{(3)}. \tag{B.44}$$

Summary 9

The non-canonical part of the energy-momentum tensor $T_F^{\mu\nu} = T^{\nu\mu}$ in a tilted system have the matrix elements

$$T^{0y\ (2)}_{k+\mathrm{q}ns,kms}(q) = -\frac{i\hbar v_F}{2} \Gamma^+_{k\mathrm{q}mns} \sum_{i,j} F_{ij}^{(2)}, \tag{B.45}$$

$$T^{0y\ (3)}_{k+\mathrm{q}ns,kms}(q) = \frac{i\hbar v_F}{2} \Gamma^+_{k\mathrm{q}mns} \sum_{ij} F_{ij}^{(3)}. \tag{B.46}$$

with

$$\Gamma^+_{k\mathrm{q}mns} = \frac{\exp\left[-\frac{l_B^2}{4\alpha}(q_y^2 + (q_x')^2) + iq_y l_B^2 (k_x' + \frac{q_x'}{2}))\right]}{\left[(\alpha_{k_z ms}^2 + 1)(\alpha_{k_z+\mathrm{q}_z ns}^2 + 1)\right]^{\frac{1}{2}}}$$

and where the factors $F_{ij}^{(n)}$ where found to be

$$F_{12}^{(2)} = -t_x\sqrt{\alpha}\sqrt{\frac{M}{2}}\alpha_{k+q,n}\Xi_2(\bar{q}, m\mp 1, n), \tag{B.47}$$

$$F_{21}^{(2)} = -t_x\sqrt{\alpha}\sqrt{\frac{M-1}{2}}\frac{a_{kms}^2}{l_B a_{km\mp 1s}}\Xi_1(\bar{q}, m\mp 1, n, s), \tag{B.48}$$

$$F_{11}^{(2)} = \sqrt{\alpha}\frac{\alpha_{k_z ms}\alpha_{k_z+\mathrm{q}_z ns}\sqrt{M-1}}{l_B\sqrt{2}}\Xi_1(\bar{q}, m\mp 1, n\mp 1, s), \tag{B.49}$$

$$F_{22}^{(2)} = \sqrt{\alpha}\frac{\sqrt{M}}{l_B\sqrt{2}}\Xi_1(\bar{q}, m, n, s), \tag{B.50}$$

$$F_{11}^{(3)} = \sqrt{\frac{N-1}{2}}\frac{\alpha_{k_z ms}\alpha_{k_z+\mathrm{q}_z ns}}{l_B\alpha_{k_z+\mathrm{q}_z n\mp 1s}}\Xi_2(\bar{q}, m\mp 1, n\mp 1, s), \tag{B.51}$$

$$F_{22}^{(3)} = \sqrt{\frac{N}{2}}\frac{1}{l_B\alpha_{k_z+\mathrm{q}_z ns}}\Xi_2(\bar{q}, m, n, s), \tag{B.52}$$

$$F_{12}^{(3)} = -t_x\frac{\alpha_{k_z+\mathrm{q}_z n}}{\alpha_{k_z+\mathrm{q}_z n\mp 1}l_B}\sqrt{\frac{N-1}{2}}\Xi_2(\bar{q}, m, n\mp 1, s), \tag{B.53}$$

$$F_{21}^{(3)} = -\frac{t_x}{l_B}\sqrt{\frac{N}{2}}\frac{\alpha_{k_z m}}{\alpha_{k_z+\mathrm{q}_z n}}\Xi_2(\bar{q}, m\mp 1, n, s). \tag{B.54}$$

B.2.1. Simplifications for tilt parallel to the magnetic field

The procedure greatly simplifies in the case of parallel tilt. As noted in the main text, parallel tilt only rescales the energies Landau levels, while the wave functions and operators stay invariant. The procedure for the untilted cone, done in Appendix B.1, is thus relevant here as well, with an interchange of the energy levels where relevant.

The $T^{(2)}$ and $T^{(3)}$ parts of the energy-momentum tensor for parallel tilt is therefore the same as the result without tilt, found in summary 8. In the main text we showed a simplification procedure for terms of the form

$$\alpha_{\kappa_z ms}^2\delta_{M-1,N} - \alpha_{\kappa_z ns}^2\delta_{N-1,M} \tag{B.55}$$

in the total response function. The outline of the idea was to note that we sum over all m, n, and by certain symmetries of the terms under interchange

of $m \leftrightarrow n$, we could rename summation indices and replace

$$\alpha^2_{\kappa_z ms}\delta_{M-1,N} - \alpha^2_{\kappa_z ns}\delta_{N-1,M} \to 2\alpha^2_{\kappa_z ms}\delta_{M-1,N}. \tag{B.56}$$

For details on the procedure see Section 4.4.2 of the main text. By simply inserting $T^{(2)}, T^{(3)}$ in the response function, one may easily show that the resulting term is on the form Eq. (B.55), with the first term corresponding to $T^{(3)}$ and the second to $T^{(2)}$. The response from $T^{(2)}$ and $T^{(3)}$ is thus equal.

By the procedure explained in Section 4.1.2, the response of $T^{(2)} + T^{(3)}$ may be rewritten as the response of $T^{(1)}$, which contains the factor $E_{k_z ms} + E_{k_z ns}$, with the energies replaced with the untilted energies. In other words, using the energy momentum tensor $T_F^{\mu\nu}$, the response is the same as the response found for parallel tilt in the main text, Eq. (4.190),

$$\lim_{\omega\to 0}\lim_{q\to 0}\chi^{xy} = -\frac{e^2 v_F B}{2(2\pi)^2}\sum_{mn}\int \mathrm{d}\kappa_z \xi(\kappa_z)(\epsilon_{\kappa_z ms} + \epsilon_{\kappa_z ns}) \times (\alpha^2_{\kappa_z ms}\delta_{M-1,N} - \alpha^2_{\kappa_z ns}\delta_{N-1,M}),$$

with the term $\epsilon_{\kappa_z ms} + \epsilon_{\kappa_z ns}$ replaced with the untilted energies $\epsilon^0_{\kappa_z ms} + \epsilon^0_{\kappa_z ms}$. The response from the $T_F^{\mu\nu}$ tensor is therefore the exact same as that of the untilted cone, as long as one stays in Type-I. It differs from the response found in the main text by the divergent prefactor $\gamma_{\mathrm{div},N}$.

C Auxiliary Results

C.1. Conformal symmetry of a tilted system

The origin of the term *conformal anomaly* is the *conformal symmetry*. Under the conformal transformation, the massless QED Lagrangian is invariant, as shown in the main text. Specifically, the QED Lagrangian

$$\mathcal{L} = -\frac{1}{4}F^{\mu\nu}F_{\mu\nu} + i\bar{\psi}\not{D}\psi,$$

with the usual $\bar{\psi} = \psi^\dagger\gamma^0, \not{D} = \gamma^\mu D_\mu, D_\mu = \partial_{\mu - ieA_\mu}$ transforms under the scaling

$$x \to \lambda^{-1},\ A_\mu \to \lambda A_\mu,\ \psi \to \lambda^{\frac{3}{2}}\psi,$$

as

$$\mathcal{L} \to \lambda^4\mathcal{L}.$$

The action $S = \int \mathrm{d}^4x\mathcal{L}$ is thus invariant (as $\mathrm{d}^4x \to \lambda^{-4}\mathrm{d}^4x$), and the theory is classically manifestly scale invariant.

Consider now the tilted Dirac Lagrangian considered in our work,

$$\mathcal{L}ki\bar{\psi}\Gamma^\mu\partial_\mu\psi, \tag{C.1}$$

with $\Gamma^\mu = \gamma^\mu + t^\mu\gamma_P\gamma^0$, where $\gamma_P = I_4$ when inversion summery is broken and $\gamma_P = \gamma^5$ for inversion symmetric systems. The tilt parameter $t^\mu = (0, \boldsymbol{t})$ is invariant under scaling, and thus also this theory is classically scale invariant.

C.2. Spin states of the Dirac cone

Similar to the discussion in Section 1.5 on the spin structure of a system with Rashba coupling, we here consider the spin structure of the Weyl cone. We begin by finding the eigenstates of the Weyl Hamlitonian $H = v_F\boldsymbol{\sigma}\boldsymbol{p}$. Assume plane wave states, and some arbitrary linear combination of spin up and spin down,

$$\psi_\pm = e^{i\boldsymbol{k}\boldsymbol{r}}\alpha\begin{pmatrix}1\\ b\end{pmatrix},$$

where α is some normalization. Solving the time independent Schrodinger equation

$$H\psi = E\psi,$$

we find

$$b = -\frac{k_z \pm k}{k_x - ik_y}. \tag{C.2}$$

Requiring normalized states $\langle\psi|\psi\rangle = 1$ gives the normalization

$$|\alpha|^2 = \frac{1}{1+|b|^2}.$$

Having found the states, we find the spin expectation value

$$\boldsymbol{S} = \langle\psi|\hat{S}|\psi\rangle\,, \tag{C.3}$$

where $\boldsymbol{S}$ is the spin expectation value and $\hat{S} = \frac{\sigma}{2}$ is the spin operator, where $\hbar$ was set to 1. Simply evaluating Eq. (C.3), yields

$$\boldsymbol{S} = \pm\frac{\boldsymbol{k}}{2k}. \tag{C.4}$$

The spin structure is that of a hedgehog. This gives a nice intuitive explanation of the symmetries of a Dirac cone. Recall that under an inversion transformation, momentum is flipped while spin is invariant. Under time-reversal both momentum and spin change direction. When all symmetries are present, the Dirac cone consists of two superimposed Weyl cones. Breaking inversion symmetry separates the cones in momentum while breaking time-reversal symmetry separates the cones in energy.[1] The three cases are shown schematically in Fig. C.1. By inspection, one sees that when the cones are separated in momentum, the spin at the opposite momentum has the same direction, and so time-reversal symmetry is broken. Similarly, when the cones are separated in energy, the spin at the opposite momentum has the opposite direction, and so inversion symmetry is broken.

[1] Giving a nodal loop.

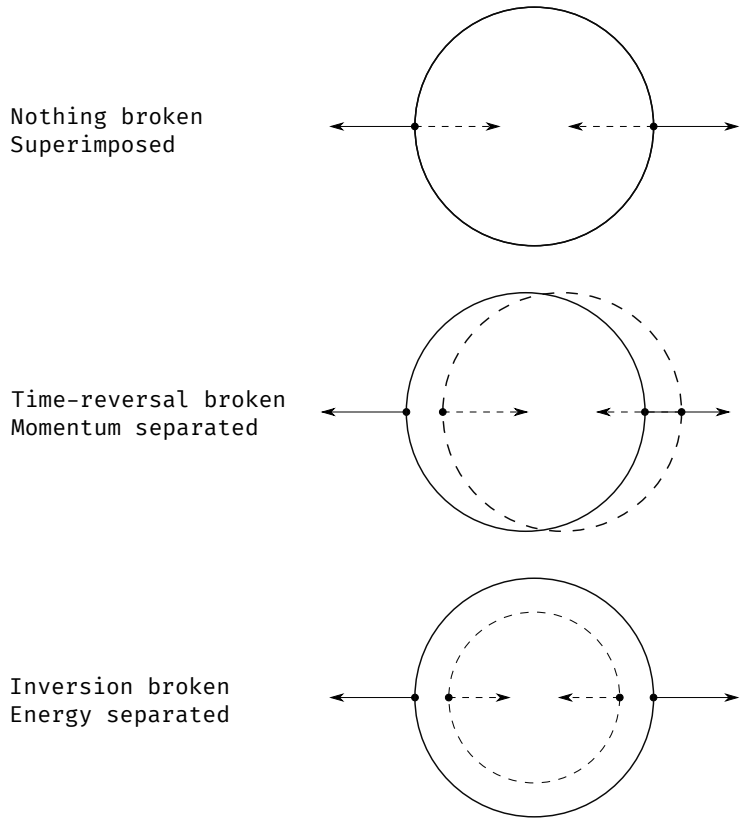

Figure C.1.: Schematic overview of symmetry properties of a Dirac cone. Drawn is the energy contour of a Dirac cone for some non-zero energy; in other words, the intersection of a Dirac cone with a plane at some energy $E \neq 0$. The arrows indicate the spin direction. From top to bottom, there is a Dirac cone with two superimposed Weyl cones, momentum separated Weyl cones, and energy separated Weyl cones. The solid and dashed lines corresponds to the two chiralities.

C.3. Only translationally invariant systems have conservation of momentum in correlators

Theorem 2. *If the momentum space correlator is $\langle A(p)B(-p)\rangle$, the real space correlator is translationally invariant.*

Proof: Consider the correlator

$$\langle A(x)B(y)\rangle\,. \tag{C.5}$$

If its momentum space equivalent is

$$\langle A(q)B(-q)\rangle = \langle A(q)B(p)\rangle\,\delta(p+q), \tag{C.6}$$

then the real space correlator is given by

$$\int \mathrm{d}p\mathrm{d}q\,\langle A(p)B(q)\rangle\,\delta(p+q)e^{ipx+iqy} = \int \mathrm{d}p\,\langle A(p)B(-p)\rangle\,e^{ip(x-y)}. \tag{C.7}$$

This function is only dependent on $x-y$, and thus translationally invariant. Therefore, the only way to get a correlator on the form $\langle A(p)B(-p)\rangle$ is to assume trnaslational invariance. □

C.4. Removing the explicit tilt from the Lagrangian by a non-flat metric

In the main text, we have used the Lagrangian

$$L_s = i\phi^\dagger\tilde{\sigma}^\mu\partial_\mu\phi, \tag{C.8}$$

where we defined the *modified* Pauli matrices $\tilde{\sigma}^\mu = \sigma^\mu + t^\mu$, $t^\mu = (0,\boldsymbol{t})$. We here present an alternative, where we instead consider moving the tilting into the metric, i.e. considering a non-tilted cone in curved spacetime. In essence, we want

$$g^{\mu\nu}\sigma_\nu p_\mu$$

to give $(\sigma^\mu + t^\mu)p_\mu$. We see that this involves putting t^μ on the 0-components of the metric.

Consider the metric

$$g^{\mu\nu} = \eta^{\mu\nu} + t^\mu(\delta^\mu_0 + \delta^\nu_0) = \begin{pmatrix} 1 & t^x & t^y & t^z \\ t^x & -1 & 0 & 0 \\ t^y & 0 & -1 & 0 \\ t^z & 0 & 0 & -1 \end{pmatrix}. \tag{C.9}$$

The top row is however problematic, as it gives an unwanted

$$g^{0\nu}\sigma_\nu = \sigma^0 - \boldsymbol{t}\boldsymbol{\sigma}.$$

Interestingly, the metric thus *cannot* be symmetric! We conclude that the appropriate choice is

$$g^{\mu\nu} = \eta^{\mu\nu} + t^\mu \delta_0^\nu = \begin{pmatrix} 1 & 0 & 0 & 0 \\ t^x & -1 & 0 & 0 \\ t^y & 0 & -1 & 0 \\ t^z & 0 & 0 & -1 \end{pmatrix}. \tag{C.10}$$

Consider therefore the Lagrangian

$$\mathcal{L} = \phi^\dagger g^{\mu\sigma}\sigma_\sigma \partial_\mu \phi. \tag{C.11}$$

Using once again the canoncial defintion

$$T^{\mu\nu} = \frac{\partial \mathcal{L}}{\partial(\partial_\mu \phi)}\partial^\nu \phi \tag{C.12}$$

$$= \phi^\dagger g^{\mu\sigma}\sigma_\sigma \partial^\nu \phi, \tag{C.13}$$

we find the component of the energy-momentum tensor

$$T^{y0} = \phi^\dagger g^{y\sigma}\sigma_\sigma \partial^0 \phi = \phi^\dagger (t^y \sigma_0 + \sigma_y)\partial^0 \phi. \tag{C.14}$$

Remark 1. The four-Pauli matrices are defined as

$$\sigma^\mu = (\sigma^0, \sigma^1, \sigma^2, \sigma^3) = (\sigma^0, \sigma_x, \sigma_y, \sigma_z), \tag{C.15}$$

where the matrices with lower roman indices are the well-known Pauli matrices. Thus, the four-matrices with lowered inddex are

$$\sigma_\mu = g_{\mu\nu}\sigma^\mu = (\sigma^0, -\sigma^1, -\sigma^2, -\sigma^3). \tag{C.16}$$

Bibliography

[ACV19] V. Arjona, M. N. Chernodub, and M. A. H. Vozmediano. "Fingerprints of the Conformal Anomaly on the Thermoelectric Transport in Dirac and Weyl Semimetals: Result from a Kubo Formula". In: *Physical Review B* 99.23 (June 10, 2019), p. 235123. DOI: 10.1103/PhysRevB.99.235123. — 1, 53, 54, 59, 75, 78, 108–110, 112, 121

[Adl69] S. L. Adler. "Axial-Vector Vertex in Spinor Electrodynamics". In: *Physical Review* 177.5 (Jan. 25, 1969), pp. 2426–2438. DOI: 10.1103/PhysRev.177.2426. — 44

[AMV18] N. P. Armitage, E. J. Mele, and A. Vishwanath. "Weyl and Dirac Semimetals in Three-Dimensional Solids". In: *Reviews of Modern Physics* 90.1 (Jan. 22, 2018), p. 015001. DOI: 10.1103/RevModPhys.90.015001. — 1, 15, 18

[Arj19] V. Arjona Romano. "Novel Thermoelectric and Elastic Responses in Dirac Matter". PhD thesis. Madrid, Spain: Autonomous University of Madrid, Dec. 13, 2019. URL: https://repositorio.uam.es/handle/10486/690486 (visited on 04/26/2022). — 1

[Ber84] M. Berry. "Quantal Phase Factors Accompanying Adiabatic Changes". In: *Proceedings of the Royal Society of London. A. Mathematical and Physical Sciences* (1984). DOI: 10.1098/rspa.1984.0023. — 19, 21

[BH13] B. A. Bernevig and T. L. Hughes. *Topological Insulators and Topological Superconductors*. Princeton: Princeton University Press, 2013. 247 pp. ISBN: 978-0-691-15175-5. — 1, 8

[BJ69] J. S. Bell and R. Jackiw. "A PCAC puzzle: $\pi^0 \to \gamma\gamma$ in the σ-Model". In: *Il Nuovo Cimento A (1965-1970)* 60.1 (Mar. 1, 1969), pp. 47–61. DOI: 10.1007/BF02823296. — 44

[Bur15] A. A. Burkov. "Chiral Anomaly and Transport in Weyl Metals". In: *Journal of Physics: Condensed Matter* 27.11 (Feb. 2015), p. 113201. DOI: 10.1088/0953-8984/27/11/113201. — 1

[Bur16] A. A. Burkov. "Topological Semimetals". In: *Nature Materials* 15.11 (11 Nov. 2016), pp. 1145–1148. DOI: 10.1038/nmat4788. — 1, 28

[CCV18] M. N. Chernodub, A. Cortijo, and M. A. H. Vozmediano. "Generation of a Nernst Current from the Conformal Anomaly in Dirac and Weyl Semimetals". In: *Physical Review Letters* 120.20 (May 14, 2018), p. 206601. DOI: 10.1103/PhysRevLett.120.206601. 1, 53, 104

[Cha18] M.-C. Chang. *Lecture Notes for Manybody Physics I*. Jan. 3, 2018. URL: https://phy.ntnu.edu.tw/~changmc/Teach/Manybody/ch03.pdf (visited on 10/21/2021). 55

[Che+21] M. N. Chernodub et al. "Thermal Transport, Geometry, and Anomalies". Oct. 11, 2021. DOI: 10.48550/ARXIV.2110.05471. 15, 16, 39, 57, 58, 107

[Che16] M. N. Chernodub. "Anomalous Transport Due to the Conformal Anomaly". In: *Physical Review Letters* 117.14 (Sept. 28, 2016), p. 141601. DOI: 10.1103/PhysRevLett.117.141601. 1, 51, 53

[Ell17] J. Ellis. "TikZ-Feynman: Feynman Diagrams with TikZ". In: *Computer Physics Communications* 210 (Jan. 2017), pp. 103–123. DOI: 10.1016/j.cpc.2016.08.019.

[ERH07] H.-A. Engel, E. I. Rashba, and B. I. Halperin. "Theory of Spin Hall Effects in Semiconductors". May 23, 2007. DOI: 10.48550/ARXIV.COND-MAT/0603306. Repr. from. Ed. by H. Kronmüller and S. S. P. Parkin. Hoboken, NJ: John Wiley & Sons, 2007. 12

[FC13] M. Fruchart and D. Carpentier. "An Introduction to Topological Insulators". In: *Comptes Rendus Physique* 14.9-10 (Nov. 2013), pp. 779–815. DOI: 10.1016/j.crhy.2013.09.013. 1

[FR04] M. Forger and H. Römer. "Currents and the Energy-Momentum Tensor in Classical Field Theory: A Fresh Look at an Old Problem". In: *Annals of Physics* 309.2 (Feb. 2004), pp. 306–389. DOI: 10.1016/j.aop.2003.08.011. 57, 112

[FZB17] Y. Ferreiros, A. A. Zyuzin, and J. H. Bardarson. "Anomalous Nernst and Thermal Hall Effects in Tilted Weyl Semimetals". In: *Physical Review B* 96.11 (Sept. 8, 2017), p. 115202. DOI: 10.1103/PhysRevB.96.115202. 25, 28

[GV05] G. Giuliani and G. Vignale. *Quantum Theory of the Electron Liquid*. Cambridge: Cambridge University Press, 2005. ISBN: 978-0-521-52796-5. DOI: 10.1017/CBO9780511619915. 33

[GZ15] I. S. Gradshteĭn and D. Zwillinger. *Table of Integrals, Series, and Products*. Eighth edition. Amsterdam and Boston: Elsevier, Academic Press is an imprint of Elsevier, 2015. 1133 pp. ISBN: 978-0-12-384933-5. 88

[Hol89] B. R. Holstein. "The Adiabatic Theorem and Berry's Phase". In: *American Journal of Physics* 57.12 (Dec. 1, 1989), pp. 1079–1084. DOI: 10.1119/1.15793. 21

[Inc] W. R. Inc. *Mathematica, Version 13.0.0*. URL: https://www.wolfram.com/mathematica.

[IZ80] C. Itzykson and J. B. Zuber. *Quantum Field Theory*. International Series in Pure and Applied Physics. New York: McGraw-Hill International Book Co, 1980. 705 pp. ISBN: 978-0-07-032071-0. 74

[JXH16] S. Jia, S.-Y. Xu, and M. Z. Hasan. "Weyl Semimetals, Fermi Arcs and Chiral Anomalies". In: *Nature Materials* 15.11 (11 Nov. 2016), pp. 1140–1144. DOI: 10.1038/nmat4787. 15

[Kac18] M. Kachelriess. *Quantum Fields: From the Hubble to the Planck Scale*. First edition. Oxford Graduate Texts. Oxford: Oxford University Press, 2018. 528 pp. ISBN: 978-0-19-880287-7. 41, 43, 45, 47, 51, 57, 74

[KDP80] K. v. Klitzing, G. Dorda, and M. Pepper. "New Method for High-Accuracy Determination of the Fine-Structure Constant Based on Quantized Hall Resistance". In: *Physical Review Letters* 45.6 (Aug. 11, 1980), pp. 494–497. DOI: 10.1103/PhysRevLett.45.494. 1

[Lan56] L. D. Landau. "The Theory of a Fermi Liquid". In: *Zh. Eksp. Teor. Fiz.* 30.6 (1956), p. 1058. [Sov. Phys. JETP 5 101 (1957)]. 15

[Lin17] J. Linder. *Intermediate Quantum Mechanics*. 1st. Bookboon, 2017. ISBN: 978-87-403-1783-1. 82

[LLF14] R. Lundgren, P. Laurell, and G. A. Fiete. "Thermoelectric Properties of Weyl and Dirac Semimetals". In: *Physical Review B* 90.16 (Oct. 13, 2014), p. 165115. DOI: 10.1103/PhysRevB.90.165115. 39

[Lut64] J. M. Luttinger. "Theory of Thermal Transport Coefficients". In: *Physical Review* 135 (6A Sept. 14, 1964), A1505–A1514. DOI: 10.1103/PhysRev.135.A1505. 38

[Mah00] G. D. Mahan. *Many-Particle Physics*. 3rd ed. Physics of Solids and Liquids. New York: Kluwer Academic/Plenum Publishers, 2000. 785 pp. ISBN: 978-0-306-46338-9. 33, 35, 38, 39

[Man+15] A. Manchon et al. “New Perspectives for Rashba Spin–Orbit Coupling”. In: *Nature Materials* 14.9 (9 Sept. 2015), pp. 871–882. DOI: 10.1038/nmat4360. 13

[MKT17] T. M. McCormick, I. Kimchi, and N. Trivedi. “Minimal Models for Topological Weyl Semimetals”. In: *Physical Review B* 95.7 (Feb. 21, 2017), p. 075133. DOI: 10.1103/PhysRevB.95.075133. 26, 27

[Olv+] F. W. J. Olver et al. *NIST Digital Library of Mathematical Functions*. Release 1.1.3 of 2021-09-15. URL: http://dlmf.nist.gov/. 62, 80, 122, 125

[Ram19] R. Ramazashvili. “Zeeman Spin-Orbit Coupling in Antiferromagnetic Conductors”. In: *Journal of Physics and Chemistry of Solids*. Spin-Orbit Coupled Materials 128 (May 1, 2019), pp. 65–74. DOI: 10.1016/j.jpcs.2018.09.033. 7

[Rot95] K. Rottmann. *Matematisk formelsamling*. Oslo: Bracan forl., 1995. ISBN: 978-82-7822-005-4. 35, 55

[Sci16] R. S. A. of Sciences. *The Nobel Prize in Physics 2016*. Press release. Oct. 4, 2016. URL: https://www.nobelprize.org/prizes/physics/2016/press-release/ (visited on 12/12/2021). 1

[SGT17] G. Sharma, P. Goswami, and S. Tewari. “Chiral Anomaly and Longitudinal Magnetotransport in Type-II Weyl Semimetals”. In: *Physical Review B* 96.4 (July 13, 2017), p. 045112. DOI: 10.1103/PhysRevB.96.045112. 25, 28, 63, 105

[SN17] J. J. Sakurai and J. Napolitano. *Modern Quantum Mechanics*. 2nd ed. Cambridge: Cambridge university press, 2017. ISBN: 978-1-108-42241-3. 5, 7, 73

[Sol+15] A. A. Soluyanov et al. “Type-II Weyl Semimetals”. In: *Nature* 527.7579 (7579 Nov. 2015), pp. 495–498. DOI: 10.1038/nature15768. 25, 29, 63, 100

[Tat15] G. Tatara. “Thermal Vector Potential Theory of Transport Induced by a Temperature Gradient”. In: *Physical Review Letters* 114.19 (May 14, 2015), p. 196601. DOI: 10.1103/PhysRevLett.114.196601. 38

[TCG16] S. Tchoumakov, M. Civelli, and M. O. Goerbig. “Magnetic-Field-Induced Relativistic Properties in Type-I and Type-II Weyl Semimetals”. In: *Physical Review Letters* 117.8 (Aug. 16, 2016), p. 086402. DOI: 10.1103/PhysRevLett.117.086402. 25, 60, 64, 67, 83

[Ton] D. Tong. *Gauge Theory Lecture Notes*. URL: https://www.damtp.cam.ac.uk/user/tong/gaugetheory.html (visited on 11/03/2021). 43, 44, 82

[vdWS19] E. C. I. van der Wurff and H. T. C. Stoof. "Magnetovortical and Thermoelectric Transport in Tilted Weyl Metals". In: *Physical Review B* 100.4 (July 11, 2019), p. 045114. DOI: 10.1103/PhysRevB.100.045114. 28, 57, 59, 75, 104, 112, 124

[Vol17] G. E. Volovik. "Topological Lifshitz Transitions". In: *Low Temperature Physics* 43.1 (Jan. 2017), pp. 47–55. DOI: 10.1063/1.4974185. 25

[Voz21] M. A. H. Vozmediano. "Theoretical Physics Colloquium : Geometry and Anomalies in Dirac Matter". Sept. 22, 2021. URL: https://www.youtube.com/watch?v=Zu2Rzd6rkVQ (visited on 06/06/2022). 15, 28, 108

[WBB14] T. Wehling, A. Black-Schaffer, and A. Balatsky. "Dirac Materials". In: *Advances in Physics* 63.1 (Jan. 2, 2014), pp. 1–76. DOI: 10.1080/00018732.2014.927109. 1, 43, 61

[Wu+20] K. Wu et al. "Two-Dimensional Giant Tunable Rashba Semiconductors with Two-Atom-Thick Buckled Honeycomb Structure". In: *Nano Letters* 21 (Dec. 24, 2020). DOI: 10.1021/acs.nanolett.0c04429. 13

[YYY16] Z.-M. Yu, Y. Yao, and S. A. Yang. "Predicted Unusual Magnetoresponse in Type-II Weyl Semimetals". In: *Physical Review Letters* 117.7 (Aug. 11, 2016), p. 077202. DOI: 10.1103/PhysRevLett.117.077202. 25, 60, 68

[Zee10] A. Zee. *Quantum Field Theory in a Nutshell*. 2nd ed. In a Nutshell. Princeton, N.J: Princeton University Press, 2010. 576 pp. ISBN: 978-0-691-14034-6. 1, 41, 43–45, 47–49